
Masters

Science

2004-04-01

Optimisation of Organic Materials for Laser Applications

Kieran P. Henderson
Technological University Dublin

Follow this and additional works at: <https://arrow.tudublin.ie/scienmas>



Part of the [Physics Commons](#)

Recommended Citation

Henderson, K. (2004). *Optimisation of organic materials for laser applications*. Masters dissertation. Technological University Dublin. doi:10.21427/D73K7N

This Theses, Masters is brought to you for free and open access by the Science at ARROW@TU Dublin. It has been accepted for inclusion in Masters by an authorized administrator of ARROW@TU Dublin. For more information, please contact arrow.admin@tudublin.ie, aisling.coyne@tudublin.ie, vera.kilshaw@tudublin.ie.

Optimisation of Organic Materials for Laser applications.

By

Kieran P.J. Henderson

**A thesis submitted to the Dublin Institute of Technology,
for the award of Master of Philosophy
(MPhil)**

**Focas/ School of Physics,
Dublin Institute of Technology,
Kevin Street,
Dublin 8**

April 2004

Declaration

I certify that this thesis, which I now submit for examination for the award of the degree of Master of Philosophy (MPhil) is entirely my own work and has not been taken from the work of others unless cited and acknowledged within the text of my work.

This thesis was prepared according to the regulations for postgraduate studies by research of the Dublin Institute of technology and has not been submitted in whole or in part for an award in any other Institute or University.

Signature: 
Kieran P. J. Henderson

Date 27-01-24

To my Family

*All I can say about life is,
Oh God, enjoy it!
Bob Newhart*

Index:

| | |
|---|-----|
| 1.0 Introduction: | 3 |
| 1.1 References: | 9 |
| 2.0 Theory: | 10 |
| 2.1 Introduction: | 11 |
| 2.2 Photophysics: | 22 |
| 2.3 Absorption: | 23 |
| 2.4 Luminescence: | 26 |
| 2.5 Radiationless Transitions: | 27 |
| 2.6 Vibrational Transitions: | 29 |
| 2.6.1 Infra-red Spectroscopy: | 29 |
| 2.7 Raman Spectroscopy: | 31 |
| 2.8 Transition probability: | 34 |
| 2.9 Einstein coefficients: | 36 |
| 2.10: Nature of conjugated Polymers: | 44 |
| 2.11: Aggregation: | 48 |
| 2.12: Summary: | 48 |
| 2.13: References: | 50 |
| 3.0: | 51 |
| 3.1: Solvatochromism: | 52 |
| 3.2: Solvation Energies: | 53 |
| 3.3: Onsager Field Model: | 57 |
| 3.4: Onsager examples: | 58 |
| 3.5: Summary: | 62 |
| 3.6: References: | 64 |
| 4.1 Materials and Experimental: | 65 |
| 4.1.2 Synthesis: | 66 |
| 4.2 Electronic Spectroscopy: | 71 |
| 4.2.1 Introduction: | 71 |
| 4.2.2 Instrumentation: | 72 |
| 4.2.3 Experimental: | 74 |
| 4.3 Fluorescence Spectrometer: | 75 |
| 4.3.1 Introduction: | 75 |
| 4.3.2 Instrumentation: | 76 |
| 4.3.3 Experimental: | 77 |
| 4.4 I.R. Spectroscopy: | 78 |
| 4.4.1. Introduction: | 78 |
| 4.4.2. Instrumentation ¹⁸ : | 78 |
| 4.4.3 Experimental: | 79 |
| 4.5 Raman Spectroscopy: | 81 |
| 4.5.1 Introduction: | 81 |
| 4.5.2. Instrumental: | 82 |
| 4.5.3. Experimental: | 82 |
| 4.7. Summary: | 85 |
| 4.8. References: | 86 |
| 5.0. Molecular Environment-Vibronic Coupling: | 88 |
| 5.1. Introduction: | 88 |
| 5.2. Solvatochromism: | 91 |
| 5.3. Vibronic coupling: | 93 |
| 5.4. Lifetime measurements: | 95 |
| 5.5. Instrumental: | 96 |
| 5.5 Experimental: | 98 |
| 5.6. Summary: | 102 |
| 5.7. Reference: | 103 |

| | |
|--|-----|
| 6.0 Intermolecular Coupling: | 105 |
| 6.1 Concentration dependent absorption of the PmPV trimer | 105 |
| 6.2 Concentration dependent photoluminescence of the PmPV trimer | 107 |
| 6.3 Concentration dependent absorption of the PmPV polymer..... | 108 |
| 6.4 Concentration dependent photoluminescence of the PmPV polymer: | 112 |
| 6.5 Concentration dependent Photoluminescence lifetime measurements..... | 115 |
| 6.6 Summary: | 116 |
| 6.7 Reference | 117 |

Abstract:

This project sets out to investigate the variations of the optical properties of organic conjugated polymers with a view towards understanding the transition from isolated molecule (solution) to the solid state. The polymer poly(p-phenylene vinylene-co-2,5-dioctyloxy-m-phenylene vinylene) (PmPV) is chosen as it is of interest for both light emitting and nanotube composite applications. As a model compound, 2,5-dioctyloxy-p-distyrylbenzene, termed the trimer, is employed for comparison. The objectives are to characterize the effect of the environment, using solvent and concentration dependent studies, on the optical properties of the polymer and to compare the results for the more complex polymeric system to the more definable molecular trimer. Low concentration UV/vis absorption and fluorescence studies indicate that the trimer well represents the electronic properties of the polymer.

Solvent dependent studies of the trimer indicate that although the absorption and fluorescence spectra are relatively solvent independent, the relative fluorescence yield is strongly dependent on the solvent environment of the trimer. The variation does not correlate with traditional solvatochromic parameters, but rather can be correlated with the integrated overlap of the Raman spectra of the trimer and the solvent. The variation of the fluorescence lifetime with solvent is similarly related to this vibrational overlap parameter. This indicates that the primary effect of the changing environment is on the vibrational coupling and thus the nonradiative decay mechanisms.

No such clear correlation is seen for the polymer. However, it is seen that the fluorescence lifetime of the trimer and to a greater extent the polymer is strongly dependent on concentration, implying aggregation effects. The absorption and fluorescence spectra of the polymer are seen to be strongly concentration dependent, and the results indicate that the polymer has a strong tendency to aggregate. Moreover, the degree of concentration dependence is seen to be different for polymers made by different routes. Raman studies of the trimer made via the Wittig condensation and the Horner Emmons condensation routes in both toluene and DMF, indicated that different reaction schemes produce different degrees of isomerisation along the conjugated backbone. The cis/trans ratio was quantified by comparison to known mixtures of cis/trans

stilbene characterized by $H^1 - NMR$. The variation was seen to yield a 5:1 ratio of Trans to Cis ratio for the trimer. The variation of the cis/trans ratio was also investigated utilizing Raman spectroscopy, for the trimer the synthetic route proved massively important in the degree of isomerisation. Cis/trans ratio ranging from 17 – 51%.

Similar variations in degree of isomerisation in the polymer were observed and quantified. The % Cis in the polymer varied between 8 – 55%, depending on synthetic route. As the Wittig DMF polymer is that in which the strongest aggregation is seen, the degree of aggregation can be correlated with the cis content of the backbone. The effect of the cis isomerisation on the backbone conformation can be visualized using HyperChem. Whereas the all trans backbone forms a regular helix due to the meta linkage, the introduction of cis linkages disrupts this regular coiling. In the tightly coiled trans form the π electrons of the successive coils can interact giving a well defined intramolecular. Disruption of the coiling opens up the π backbone to intermolecular interactions which can have considerable effect on the optical properties. It is concluded that engineering the intramolecular interactions in this fashion may be a route towards controlling and limiting the detrimental effect of the less definable intermolecular interactions.

Acknowledgements

I would like to thank Dr Hugh Byrne for all his help and supervision and for giving me the opportunity to undertake this research with the Physics of Molecular Materials group (POMM). I would also like to thank Dr. Vincent Toal for allowing me to work within the school of Physics. I would like to extend my warmest thanks to all members of POMM particular Dr. Alan Dalton for his support and advice during the project. I am also very grateful for the help I received from the physics, chemistry and FOCAS technicians.

Many thanks also to the school of Chemistry for use of their facilities. I would also like to thank my fellow postgraduates both in Physics and Chemistry for support and playful distraction.

I would also like to thank Prof. Werner Blau (TCD) and his research group for all their help. by Stephie Maier and Anna Drury for the synthesis of the polymers and trimer. Dr Andy Davey for the molecular modelling of the trimer and polymer. Would also like to thank Dr Alan Dalton for his help and assistance in performing the Raman measurements and helpful discussion in their interpretation.

Finally, I would like to thank my Family and friends for all their support. The production of this thesis has been a long and arduous process and I know without the support and encouragement of Family and friends, it would have been substantially harder.

Thank you

Publications:

1:

“Electronic Properties of Structurally Modified C₆₀ Films”,
K. Henderson, G. Chambers and H.J. Byrne, in Proceedings of ICSM98,
Montpellier, Synthetic Metals vol 101-103, 2360 (1999)

2:

“Correlation of Molecular Vibrational Structure with Luminescent Quantum Yields”, K. Henderson; K.P. Kretsch; A. Drury, S. Maier, A.P. Davey; W. Blau and H.J. Byrne, Proceedings of ICEL2, Sheffield, Synthetic Metals (1999)

3:

“Correlation of molecular vibrational structure and luminescent quantum yields“, K. Henderson, K.P. Kretsch, A. Drury, S. Maier, A.P. Davey, W. Blau and H.J. Byrne, Synth. Metals, 111-112, 559, (2000)

4:

“Solvent effects on the luminescent properties of conjugated polymers”
K. Henderson, A.B. Dalton, G. Chambers, A. Dury, S. Maier, A.G. Ryder, W.J. Blau and H.J. Byrne, Synthetic Metals, 119, 555-556 (2001)

5:

“Isomerisation and inter-chain effects in a semi-conjugated co-polymer poly(m-phenylenevinylene-co-2,5dioctyloxy-p-phenylenevinylene”
A.B. Dalton, G. Chambers, K. Henderson, B. Paci, B. Mc Carthy, A. Dury, J.N. Coleman, C. Fiorini, J-M. Nunzi, W.J. Blau and H.J. Byrne,
Synthetic Metals, 119, 557-558 (2001)

6:

“Spectroscopic characterisation of the C₆₀ photo-polymer produced from solution” G. Chambers, K. Henderson, A.B. Dalton, B. Mc Carthy and H.J. Byrne,
Synthetic Metals, 121, 1111-1112 (2001)

7:

“Spectroscopic and structural analysis of precursors to hexagonal close packed phases in C₆₀ thin films” G. Chambers, D. Fenton, J.R. Lawrence, K. Henderson, A.B. Dalton and H.J. Byrne, Synthetic Metals, 121, 1145-1146 (2001)

8:

“A functional conjugated polymer to process, purify and selectively interact with single wall carbon nanotubes”, A.B. Dalton, K. Henderson, G. Chambers, J.N. Coleman, W.J. Blau, C. Stephan, S. Lefrant, B. Mc Carthy and H.J. Byrne,
Synthetic Metals, 121, 1217-1218 (2001)

Chapter 1

Introduction

| | |
|--------------------------------|----------|
| <u>1.0 Introduction:</u> | <u>2</u> |
| <u>1.1 References:</u> | <u>8</u> |

1.0 Introduction:

The concept of light emission from organic materials is by no means a new one, it has been widely studied since the 1960's. For example, electroluminescence (EL) observed in anthracene was studied as early as 1963 by Pope, Kallmann and Magante.¹

The electroluminescence was generated by radiative carrier recombination, i.e. where the recombination of holes and electrons occurs producing light. To make these holes and electrons combine, high field injection, utilising high voltages must be used. Practical device applications of such a discovery were limited due to the high voltages need, in excess of 1000V's. However the experiment did provide much information on the bandgap of anthracene exceeding that of the singlet state².

The other area of interest at that time was the area of Laser Dyes. Few could have anticipated at the time of these discoveries in the 1960's, how successful and versatile a laser source, organic dyes would become. The prospect of a broadly tunable source was immediately attractive, but much remained to be understood about these materials. Early studies on laser dyes correctly speculated on the role of the vibronic levels in the relaxation of electronically excited molecules.⁴ The first experimental work carried out was done by Stockman⁵, who using a high powered flashlamp to excite a solution of perylene, which showed some gain, but suffered from high triplet-triplet absorption losses.

In 1966, Sorokin and Lankard⁶ from IBM's Thomas J. Watson Research Center, Yorktown Heights were the first to obtain stimulated emission from an organic compound, namely chloro-aluminium-phthalocyanine. The enormous amount of research being carried out in this area at the time is shown by the large amount of publication, that appear in the period 1966-72 in the Journal of Dye Lasers, some 454 references being published.

But why was there so much interest in this area? It was sort of a fulfilment of a scientist's dream, to have a laser capable of lasing over a wide range of frequencies and wavelengths. Dye lasers offer this possibility. They offered scientists the ability to operate over the spectrum from near-UV to near IR, i.e. they would be tuneable.

Although tunability was a major factor at the time there are several other as important factors:

- 1: Stable⁷ continuous single mode operation.
- 2: High pulse energies⁸.
- 3: Ultrashort pulses ca. 27fs⁹
- 4: High average powers.¹⁰

Dyes could also be used in different physical states: solid, liquid and gases and their concentration and thus absorption and gain are easily controllable. A liquid dye laser offers advantages over other states, such as it is self-repairing, and convection currents protect any one point from over heating. They therefore have one major advantage over solid state in that, without sample destruction they have similar power outputs. Finally and one of the most important reasons is that they are relatively cheap.

But if Dye Lasers were a scientist's dream why are they not in more wide spread use today. The answer to this lies in the fact that all the exceptional properties highlighted above are in effect only observed in the liquid state. The properties above are significantly reduced when one studies the solid state. The reason for this is that, dyes are usually small molecules and so crystallise to produce poor optical quality films. Furthermore, the properties of the individual dye molecules, often the result of careful chemical tuning, are lost in the solid state due to the interaction of the π electron system with that of neighbouring molecules in π -stacked aggregates. Luminescence is particularly sensitive to the local environment and is often effectively quenched in the solid state.

The issue of poor quality films meant that dye lasers application to solid state devices was severely curtailed and so research in this area continued without much success till the 1980's. The answer to the scientists dilemma came on the form of polymeric materials. These polymeric materials do not suffer the problems associated with dye lasers and the strong electroluminescence¹¹ and stimulated emission¹² observed from organic polymers has revitalised interest in this area, as organic polymers have as broad a range as dye lasers. The first polymer to show some promise was PVK (poly - (

N - carbazole). Although it was first studied in the 1950's¹³, it was not until the 1980's that it came to the forefront of research.

In 1983, in the National Physical Laboratory, United Kingdom, a young scientist named Robert Partridge demonstrated electroluminescence from a device utilising PVK. This stimulated interest in the area but due to the low efficiency of the device, the intensity of the research dwindled, until the 1990's.

Research into polymeric materials resurfaced intensified, when in 1990 an article appeared in Nature magazine¹⁴. It was published by two Cambridge Researchers, Bradley and Friend, reporting electroluminescence from a polymeric device utilising poly (phenylene vinylene) PPV. The efficiencies quoted in this article were up to this point unheard of in a polymeric device, and subsequently research in this area flourished. Like dye lasers which were tunable over the entire spectra intense research went into developing polymers that would emit over the entire spectrum.

However, as is the case for the organic laser dyes, π -conjugated polymers are also subject to aggregation which can significantly quench the luminescence emission in the solid state. Studying and optimising the molecule in solution is futile if the properties do not hold through to the solid state. The majority of the uses for such devices are in the solid state. To identify and control such variation in the deviation of effects from solid/solution state, a study of the environment and control of such is undertaken. This project sets out to investigate the environmental effects on the optical properties of the material.

The material employed is a relative the original PPV, but has alternating *meta* ring linkages which disrupts the conjugation and shifts the absorption and emission spectra to the blue. As will become apparent in the course of the study, the *meta* linkage also has a significant impact on the polymer morphology. A model trimer is also employed in the photophysical study, whereby the absence of complex polymeric morphology simplifies the physics of the system. The effect of several solvent environments is investigated to determine whether the vast differences in the absorption and fluorescence can be attributes to the solvent. The solvent effect on the lifetime of the excited state is also investigated in terms of environment and isomerism. The isomerism of both the PmPV trimer and polymer are investigated in relation to a well studied ideal compound.

The aim of the project is to seek an explanation for the vast differences in the solvent effects on the material and thus optimise the environmental impact to increase the efficiency of the material for industrial applications.

The body of this work is presented as follows;

Chapter 2, deals with the development of materials for optoelectronic applications. It looks at the principles behind such development, key to which is an understanding of the electronic configuration and photophysics of the materials. Understanding of the electronic configuration allows for the properties of organic systems to be tailored via chemical structure. The principles from the simple Bohr equations based on semiclassical physics right through to Einstein's Coefficients are dealt with and explained. Photophysics is presented in a general format utilising a Jablonski diagram for unimolecular processes, illustrating absorption, fluorescence and non-radiative processes. Relative contributions can be quantified and parameterised through the Einstein Rate equation approach. These processes are extremely important as in designing materials for use in the optoelectronic area, non-radiative processes and different forms of quenching need to be minimised to increase the fluorescence efficiency.

In this project UV-vis, fluorescence, Raman and I.R. are used as probes of the photophysics of a select polymer and model oligomers. In dilute solution molecular processes utilising a range of solvents to explore how the environment effects non-radiative decay and thus how it can be minimised. A concentration study is also undertaken to access the effect of aggregation on the system. The effect of chemical structure or backbone conformation on the aggregation is also studied in an effort to curtail the inter-molecular interactions to optimise the performance of the material.

Chapter 3, deals with "Solvatochromism". As the environment within which a molecule is situated in, can have a profound effect on the optical properties of the molecule. The solvatochromic shift is discussed in terms of solvation energies and relating the Schrödinger equation to microscopic properties of the medium such as dielectric constant and refractive index. The relationship between that of solvation energies, dipole-dipole interaction and ion-dipole interaction is developed through the Born and Onsager equations. In exploring the dependence of coupling to an environment

it is important to consider whether the environment is having a significant effect on the molecule and so a solvatochromic study is needed.

Solvent choice is very important to keep the solvatochromic effect to a minimum. Various solvents are used in the investigation, whose effect on the optical properties is investigated. Optical probing through, UV and Fluorescence spectra for PmPV are used to show some very interesting effects.

Chapter 4, deals with the most important aspect of the project, the Materials. Although the synthesis is not part of this project the synthetic route is shown. It is a complex process, which can have numerous permutations dependant on reaction conditions and solvent. All these possible permutations lead to various products, intermediates and side reactions. The electronic absorption spectrum is investigated and explained and associated instrumentation is documented and described.

Chapter 5, deals with the effects of environment on the photophysics of the molecule and specifically the vibronic coupling that takes place between molecule and it's environment. Solvent effects on the optical properties of both the Trimer and the polymer are described. Utilising the results trends are developed and discussed for both the trimer and the polymer within the chapter.

Chapter 6, deals exclusively with the concentration effects. The concentration affects were discussed earlier with respect to aggregation and its profound effect luminescence efficiency. Both the trimer and polymer concentrations are investigated and trends developed and discussed. The effect on molecular lifetimes is also investigated for concentration.

Chapter 7, deals with isomerism, the relationship between two or more different chemical compounds that have the same molecular formula but different configurations. The concept of isomerism is investigated and explained through modelling of an "Ideal compound" – Stilbene's. This Cis/Trans relationship is developed and explained through both theoretical modelling and visualisation.

The thesis has presented some interesting results. The environment has been shown to have a profound effect on the molecule, in terms of optical characteristic's, species formed and conformation of the molecule in differing solvents. Differing methods of preparing the material can lead to vastly different properties. To understand these is

exceptionally important, as if there is to be an optical efficient solid state material to be developed, firstly one must understand how it acts in the solution state. If all the efficiency's are lost from going from solution to solid state, then the material will be worthless.

1.1 References:

- 1: Pope M., Kallmann H. and Magnante P., (1963). *J Chem. Phys.* **38**, 2042.
- 2: Sano M, Pope M., Kallmann H. (1965). *J Chem. Phys.* **43**. 2920.
- 3: Hwang, H., Kao K. C. (1973). *J Chem. Phys.* **58**. 3521.
- 4: Raunti S. G. Sobel'mann I.I. (1961). *Opt. Spectrosc.* **10**, 65.
- 5: Stockmann D.L., Mallory W. R., Tikkel F.K. (1964) *Proc IEEE* **52**, 318.
- 6: Sorokin P.P., Lankard J.R., (1966) *IBM J Res. Dev.* **10**, 162.
- 7: Hough J., Hils D., Rayman M.D., Ma L.S., Hollberg L., and Hall J.L. (1984) *Appl. Phys. B.* **33** 179-185.
- 8: Balatkov, F.N., Barikhin, B.A., and Sukhanov, L.V. (1974) *JETP Lett* **19**. 174-175.
- 9: Valdmanis, J.A, Fork, R.L. and Gordon J.P. (1985) *Opt. Lett*, **10**. 131-133.
- 10: Duarte, F.J. and Piper, J.A. (1984) *Appl. Lett.* **23**. 1391-1394.
- 11: Gettinger C.J., Heeger A.J., (1994) *Jour of Chem. Phys.*, **101**. 1673-1678.
- 12: Henari FZ, Manaa H, Kretsch KP, Blau WJ, Rost H, Pfeiffer S, Teuschel A, Tillmann H, Horhold HH; *CHEM. PHYS. LETT*, **307** (3-4): 163-166 JUL 2 1999
- 13: Hogel, H, Sus, O. and Neugebauer, W. (1957). German Patent 1068115.
- 14: Burroughes JH, Bradley Y DDC, Brown AR, Marks RN, M^{AC} Kay K, Friend RH, Burns PL, Holmes AB, *Nature* (1990) **363**. 756-758

Chapter 2 Theory

| | |
|---|----|
| 2.1. Introduction:..... | 11 |
| 2.2. Photophysics:..... | 22 |
| 2.3. Absorption:..... | 23 |
| 2.4. Luminescence:..... | 25 |
| 2.5. Radiationless Transitions:..... | 26 |
| 2.6. Vibrational spectroscopy:..... | 28 |
| 2.6.1. Infra-red Spectroscopy:..... | 28 |
| 2.7. Raman Spectroscopy:..... | 30 |
| 2.8. Transition probability:..... | 38 |
| 2.9. Einstein Coefficients:..... | 35 |
| 2.10. Nature of Conjugated Polymers:..... | 42 |
| 2.11. Aggregation:..... | 46 |
| 2.12. Summary:..... | 47 |
| 2.13. References:..... | 48 |

2.1. Theory:

In researching conjugated molecules and polymers, one must look at their fundamental constituent, carbon. Carbon, element number 6, holds great significance for all lifeforms, since everything living is carbon based. Carbon was the basis for the development of organic chemistry, a field of immense importance to technology. It is the chemistry of dyes, drugs, paper, ink, paints, plastics and the chemistry of the food we eat. But, why would a physicist be interested in it? To understand this, one must look at its electrical make up, one that gives it unusual yet highly interesting and useful properties.

The question of what is matter made of has pushed scientists to the limit since the time of the Greeks. However until the early 1900's it still remained a mystery. Max Planck's quanta or packet of energy proposal for light, Einstein's explanation of the photoelectric effect (light being made up of the photons of energy) and Rutherford scattering, all culminated in the Neils Bohr proposal for a model of the atomic structure. Rutherford proposed that the positive charge was contained in the nucleus of the atom, electrons circling similar to orbiting planets. This being the case then each orbiting electron must have a well-defined energy associated with it. Rutherford proposed levels with an associated energy of E_n , is the associated energy, where h is Planck's constant, c is the speed of light and n is the energy level given in equation 2.1.1

$$E_n = \frac{hcR}{n^2} \qquad \text{Eqn. 2.1.1.}$$

However Rutherford's theory clashed with classical electromagnetic theory, which stated that any accelerating charge emits radiation. Bohr overcame this obstacle by making the following postulates: (i) the energy of electronic orbitals is constant, (ii) an electron in any of these states does not emit radiation, (iii) an electron can make a transition from one level to another by making an abrupt transition, (iv) this transition is associated with an energy difference ΔE , ($\Delta E =$ the photon), (v) the orbitals are characterised by quantised values of the orbital angular momentum, L , which has a value $nh/2\pi$. The basis for the Bohr model is the concept of Wave-Particle Duality. Based on the conclusions of the photoelectric effect, that electromagnetic radiation

could have a particulate nature as well as a wave-like nature, de Broglie proposed that particles, such as electrons, have a wave like nature. He proposed that the wavelength, λ is given by equation 2.1.2

$$\lambda = \frac{h}{p} \quad \text{Eqn. 2.1.2.}$$

where p is the particle momentum

In the Bohr model, for an orbital to be stable, its circumference must be exactly equal in length to an integer number of electronic wavelengths. Thus:

$$n\lambda = 2\pi r \quad \text{Eqn. 2.1.3.}$$

but,

$$\lambda = \frac{h}{p} = \frac{h}{mv} \quad \text{Eqn. 2.1.4.}$$

Where

h is Planck's constant

v is the velocity of the electron

m is the mass

thus,

$$\frac{nh}{2p} = mvr \quad \text{Eqn. 2.1.5.}$$

which is Bohr's postulate.

The result is a set of quantised orbitals of radius,

$$r = \epsilon_0 \frac{n^2 h^2}{\pi m e^2} \quad \text{Eqn. 2.1.6}$$

and energy

$$E = \frac{1}{\epsilon_0^2} \frac{m e^4}{8 n^2 h^2} \quad \text{Eqn. 2.1.7.}$$

It was recognised that the Bohr model based on semiclassical physics, or extensions of it was constrained by classical concepts. Schrödinger developed a novel approach to describe the true wavelike motion of an electron. The simplest illustration of Schrödinger's approach is the particle in a one-dimensional box, with a fixed constant potential. Schrödinger's particle in a box is described by a wave function, ψ , whose energy can be expressed utilising the de Broglie function as equation 2.1.8¹.

$$E_n = \frac{p^2 n}{2m} = \frac{n^2 h^2}{8mL^2} \quad \text{Eqn. 2.1.8.}$$

where p is the momentum of the particle within the box, m is the mass of the particle, h is Planck's constant n is the energy level and L is the width of the box in which the particle is situated. The above equation represents the possible energy levels for a particle in a box, which most importantly are quantised in terms of the integer, n . Each of the energy levels corresponds to a wave function is given by equation 2.1.9 and the distribution and energies are determined by the shape and magnitude of the potential and are a function of both space and time, $\psi(r,t)$.

$$\psi_n(x) = A \sin \frac{n\pi x}{L} \quad \text{Eqn. 2.1.9.}$$

The solution to the Schrödinger's equation, the wavefunction, determines the probability of distribution of the electron in the potential. The probability of finding the particle in all space is represented in equation 2.1.10, where, ψ^* , represents the complex conjugate of the wavefunction. This is the so-called normalisation condition².

$$\int \psi \psi^* dx = 1 \quad \text{Eqn. 2.1.10.}$$

In the case of an atom the potential is radially symmetric and inversely proportional to distance squared. Solutions to the Schrödinger equation for the Hydrogen atom yield quantised wavefunctions, which are inversely proportional to the Principal quantum number, n , in agreement with the Bohr model set out in

equation 2.1.4. While the Bohr model and the Schrödinger wavefunctions are consistent with each other in that they predict a spherical symmetric orbital for $n=1$, the probability distributions for the higher orbitals are more complex. One must consider quantised orbital angular momentum, magnetic moment and electron spin. The result is the well known s,p,d,f subshells of each level.

Carbon, atomic number 6, has electronic configuration $1s^2, 2s^2, 2p^2$. The orbital at the lowest energy is the $1s$ orbital as shown in Figure 2.1.1; where X, Y, Z represent the 3 geometric planes. The s orbital is spherical in structure, the $2s$ being the next highest, having a similar shape.

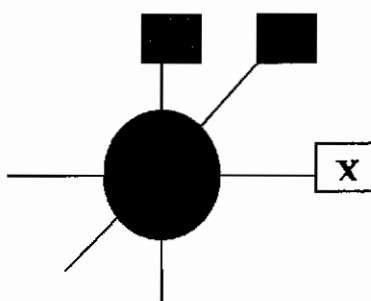


Figure 2.1.1. Illustrates the shape of the s orbital.

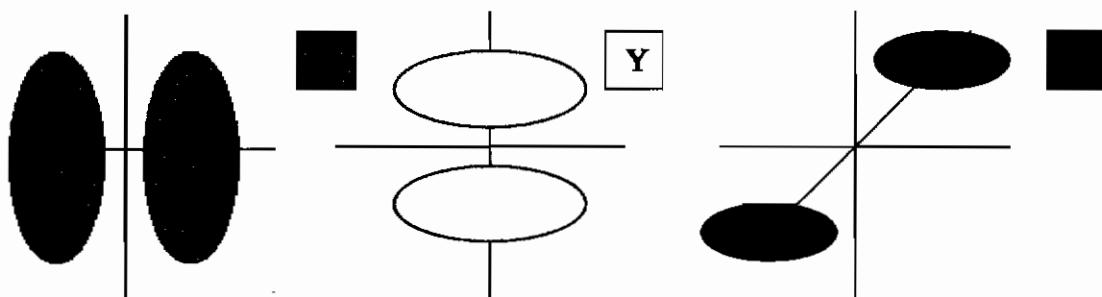


Figure 2.1.2. Illustrates the shape of the 3 different p orbitals.

The next highest is the $2p$ orbital. The $2p$ orbital is in fact 3 orbitals of equal energy in the absence of external magnetic field and neglecting spin orbit coupling. Each of the three $2p$ orbitals is dumb-bell shaped. The three orbitals point along different axes as illustrated in Figure 2.1.2. There are a number of rules, which determine the electronic configuration of an atom, the most fundamental of these being Pauli's exclusion principle and Hund's rule of maximum multiplicity.

Pauli's Rule states that only two electrons can occupy any atomic orbital and to do so they must have opposite spins.

Hund's rule states that When the electrons occupy the orbitals of equal multiplicity they do so singularly.

The electrons of opposite spin are termed paired electrons. Electrons of like spin prefer to be as far away from each other as possible. This is one of the most important of all factors that determine the shape and properties of molecules. Hund's rule describes the process where by the electron will fill orbitals singularly, the p orbital being a good example. The p orbitals p_x, p_y, p_z , will be filled by one electron each before they fill with a second electron, as is the case in nitrogen.

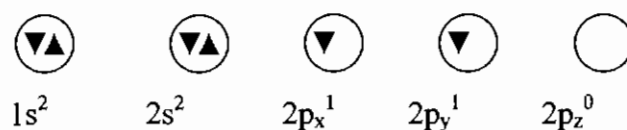


Figure 2.1.3. Electronic configuration for carbon.

This would suggest that Carbon has only a valence of 2, and would form CH_2 , which is highly reactive as shown in Figure 2.1.3³. Carbon does not however stably form this compound. It is energetically favourable for one electron to be promoted from 2s to 2p orbital, as illustrated in Figure 2.1.4; whence a mixing of the 2s and 2p orbitals occurs to form hybrid orbitals, giving a variety of valences depending on the degree of hybridisation occurring.

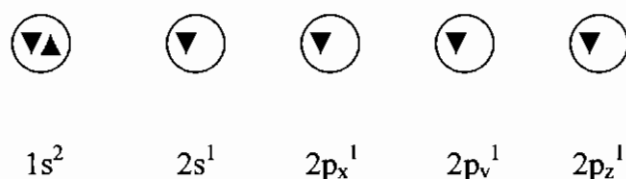


Figure 2.1.4. Electronic configuration for carbon in molecular bonding.

The easiest form of hybridisation to understand is sp^3 hybridisation, of which methane and diamond are examples. sp^3 hybridisation involves a combination of the 2s and all the 2p orbitals to form four sp hybrid orbitals, yielding a valence of four. Figure 2.1.5. illustrates the molecular structure of methane.



Figure 2.1.5. Structure of methane in which carbon is sp^3 hybridised.

In overlapping the sp wavefunctions to form strong sigma bonds (σ) as in ethane, they can combine to give constructive or destructive interference. This gives rise to two possible molecular states, bonding or anti-bonding. These two different states each have an individual energy associated with them, as illustrated in Figure 2.1.6. In the ground state the bonding orbital is doubly occupied whereas the anti-bonding is empty which leads to the nomenclature of highest occupied molecular orbital (HOMO) and lowest unoccupied molecular orbital (LUMO). In a diatomic molecule, the difference between the HOMO –LUMO corresponds to the bond energy. Energies associated with σ bonds in carbon based materials are typically ~ 5 - 10eV .

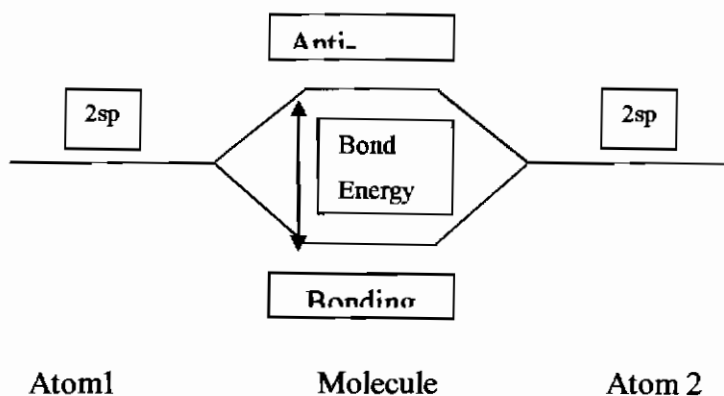


Figure 2.1.6. Illustrates the mixing of wavefunctions.

An example of sp^2 hybridisation is ethene or graphite. Three hybrid orbitals are formed by the combination of $2s$ and two of the $2p$ orbitals. The three sp^2 orbitals yield a valence of three and form strong sigma bonds (σ). In the bonding configuration of ethene as illustrated in Figure 2.1.7 there remains a singularly

occupied 2p orbital per carbon. These electrons are not principally responsible for the bonding of the molecule, but overlap to form a weak pi bond, (π), as shown in Figure 2.1.8. The difference arises due to the orientation of the overlap, whether the orbitals overlap head on or overlap sideways. The combination of the strong σ and the weaker π bond is commonly referred to as a double bond. π electrons are reactive and in bonding terms an sp^2 hybridised carbon is said to be unsaturated.

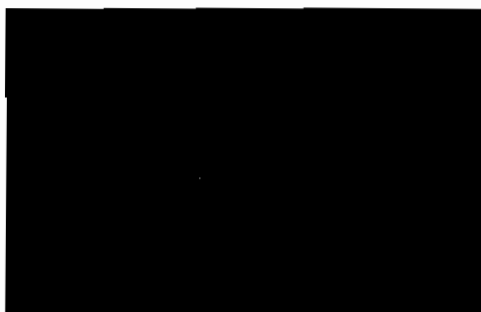


Figure 2.1.7. Structure of ethene, in which carbon is sp^2 hybridised.

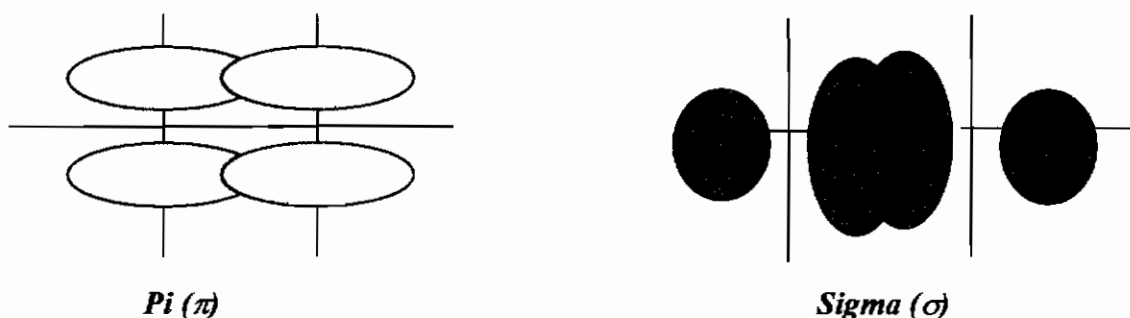


Figure 2.1.8. Schematic illustration of, pi (π) and sigma (σ) bonding between sp hybridised carbon orbitals

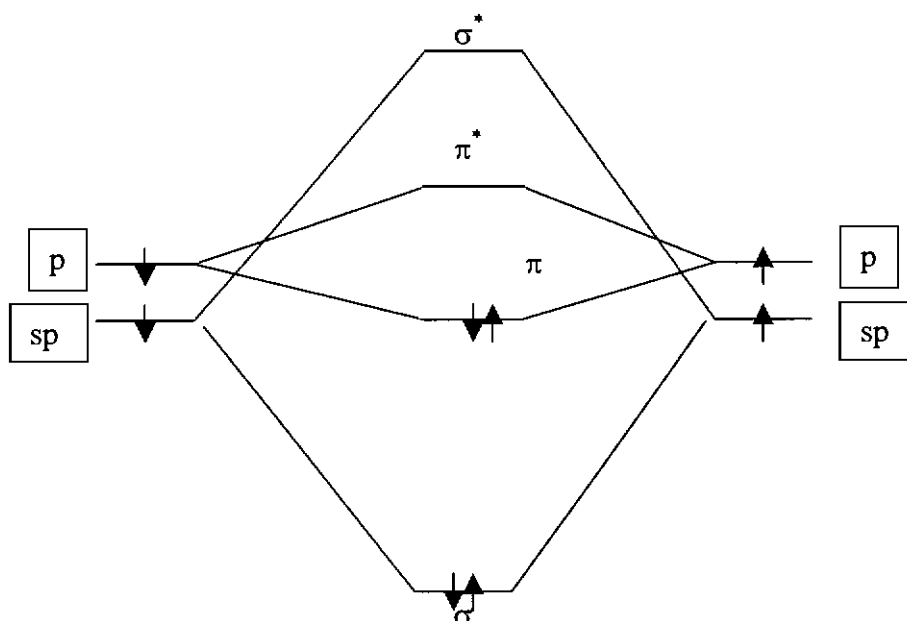


Figure 2.1.9. Energy level diagram for the overlap of s and p orbitals for ethylene.

The energetics associated with the system is illustrated in Figure 2.1.9. As before, the overlap of the sp hybrid orbitals results in bonding σ and anti bonding σ^* orbitals separated typically by 5-10eV. The p orbitals overlap considerably less. The bonding energy and the antibonding energy separation are correspondingly lower. In π bonded systems, the HOMO is thus the π orbital whereas the LUMO is the π^* . Typically, π bond energies are in the region of 3-5eV.

In the case of sp -hybridised carbon, the $2s$ orbital combines with one of the $2p$ orbitals, forming two sp hybrid orbitals, which form strong σ bonds. The remaining two p orbitals are orthogonal and can independently form π bonds, contributing to an overall triple bond as in the case of acetylene as shown in Figure 2.1.10. or carbynes. As the two π bonds are mutually orthogonal the energetics of the system are not changed from those of a doubly bonded molecule, except that the second π bond, fortifies the bond reducing bond distance and increasing the overall bond energy.

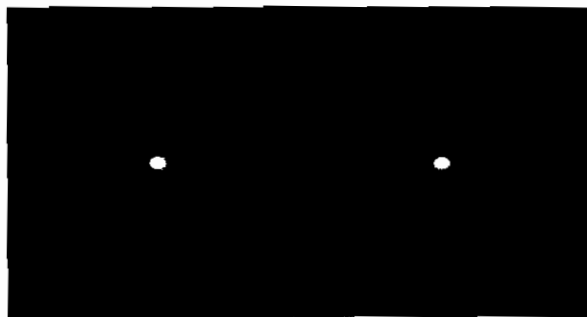


Figure 2.1.10. Structure of acteylene, in which orbitals are sp hybridised.

Molecules with more than one carbon atom are easily synthesised, the most familiar being saturated polymers e.g. polythene. In extended molecules with alternating double or triple bonds, the weakly bound π electrons can extend over more than one bonded pair of atoms. The system becomes conjugated and the π electrons can become delocalised to a first approximation over the extent of the molecule. As the extent of the conjugation increases, the π wavefunction overlap reduces the energy difference between the π and π^* orbitals and as more electrons contribute to the wavefunction, the levels broaden into bands, (Figure 2.1.11. red lines denote π^* and blue lines represents π). The π electrons are considered to be mobile along the backbone of such a conjugated system, with the promise of semiconducting or metallic properties. As shown in Figure 2.1.11, with increasing conjugation, the molecular orbitals band together and the band gap, ΔE_g , decreases.

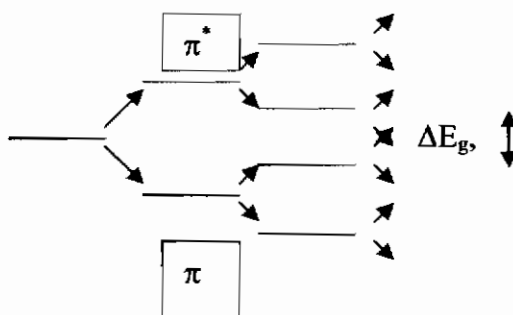


Figure 2.1.11. Evolution of ΔE_g , between the π and π^* levels as conjugation increases.

Exact theoretical calculation of such systems is complex, although molecular modelling has advanced significantly in recent years. The simplest description of one-dimensional conjugated organic molecules is that of the free electron model proposed by Kuhn for carbocyanine dyes⁴. In one description of this model by Rustagi and Ducuing⁵ the molecule is treated as a one-dimensional box of length $2L$, being the so-called conjugation length. For a molecule with j multiple bonds of length l , the conjugation length is given by equation 2.1.11

$$L = l(j + \delta) \quad \text{Eqn. 2.1.11.}$$

where δl describes an additional length contribution from the end groups and δ accommodates a dependence of the conjugation on the polarisability of the end groups and is generally of the order of unity. Within this box are $2N$ degenerate electrons, where, N is described by equation 2.1.12

$$N = (j + 1) \quad \text{Eqn.2.1.12.}$$

assuming an additional contribution of one conjugate electron to the backbone by each of the end groups. It should be noted that this assumes the proposition of Baughman and Chance⁶ that the additional two π electrons of triple bonds, located in orbitals, which are normal to the plane of the conjugated system, do not significantly contribute to the electronic properties of the material.

In an attempt to account for the alternating bond structure of a conjugated molecule, a periodic potential function as described by equation 2.1.13

$$V(\xi) = (-1)^j V_0 \cos\left(\frac{\pi\xi}{L_0}\right) \quad \text{Eqn. 2.1.13.}$$

may be superimposed on the square well potential, where V_0 is the amplitude, ξ is the co-ordinate along the chain and L_0 is the average length of one conjugation (one multiple plus one single bond).

$$E = V_0 + \left(\frac{h^2}{4mL_0^2} - \frac{V_0}{4}\right) \frac{1}{N} + 0.5 \quad \text{Eqn. 2.1.14.}$$

This model predicts⁷ therefore a systematic decrease in the band separation (E_0) with increasing conjugation as illustrated in Figure 2.1.11. A plot of E_0 against $1/N$, where N is the degree of conjugation i.e. effective conjugation length yields a straight line for the case of Enyne oligomers as shown in graph below. This simple quasi-free electron model demonstrates that the energy levels of materials can be controlled by backbone conjugation. The conjugation can be further controlled by the variation of endgroups and sidegroups⁸. Thus if the manipulate the conjugation then one can to an extent control the electronic properties.

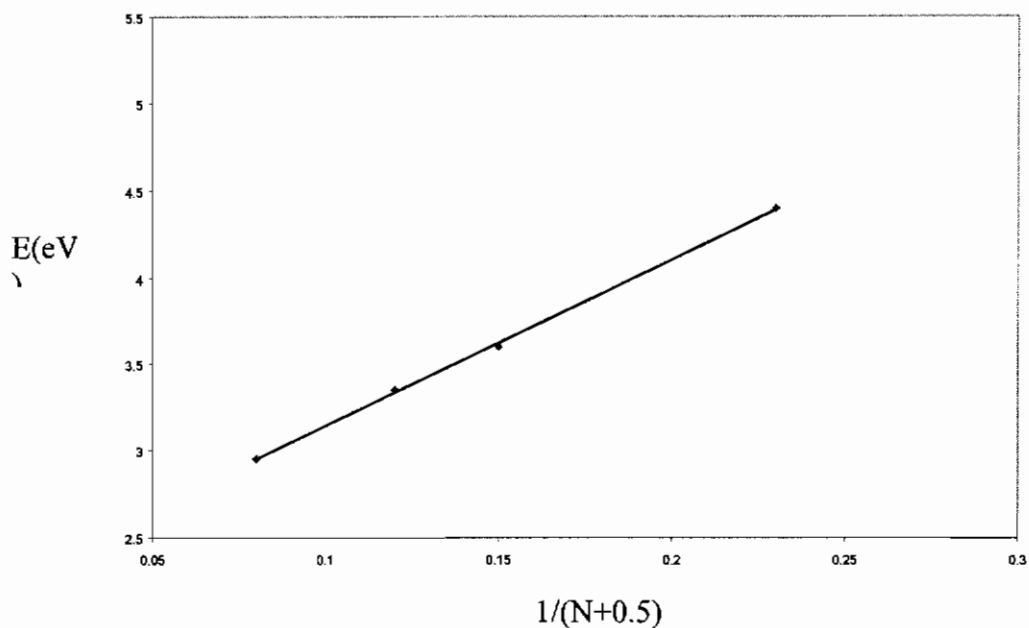


Figure 2.1.12 Oligomer Band Gap as a function of $1/(N+0.5)$.

It should be noted these models characterise the materials purely in terms of potential energy. In molecules at finite temperatures the atoms are free to move relative to each other, giving rise to vibrations and rotations. These motions are similarly quantised and are characteristic of a given material. In the next section the use of electronic and vibrational spectroscopy for characterisation of materials and processes is described.

2.2. Photophysics:

In the previous section the energy levels or states associated with different organic compounds has been outlined. Spectroscopy is a method of probing transitions of electrons between different energy states⁹. The type of transition, and the associated energy determines the type of spectroscopy involved; electronic transitions are associated with UV-vis and/or luminescence spectroscopy, vibrational/rotational transition with I.R. and/or rotational with Raman spectroscopy. In general spectroscopy is a technique to view the photophysics and hence the energetics of the material.

“A photophysical process is defined as a physical process resulting from the electronic excitation of a molecule or system of molecules by non-ionising electromagnetic radiation (photon)”¹⁰.

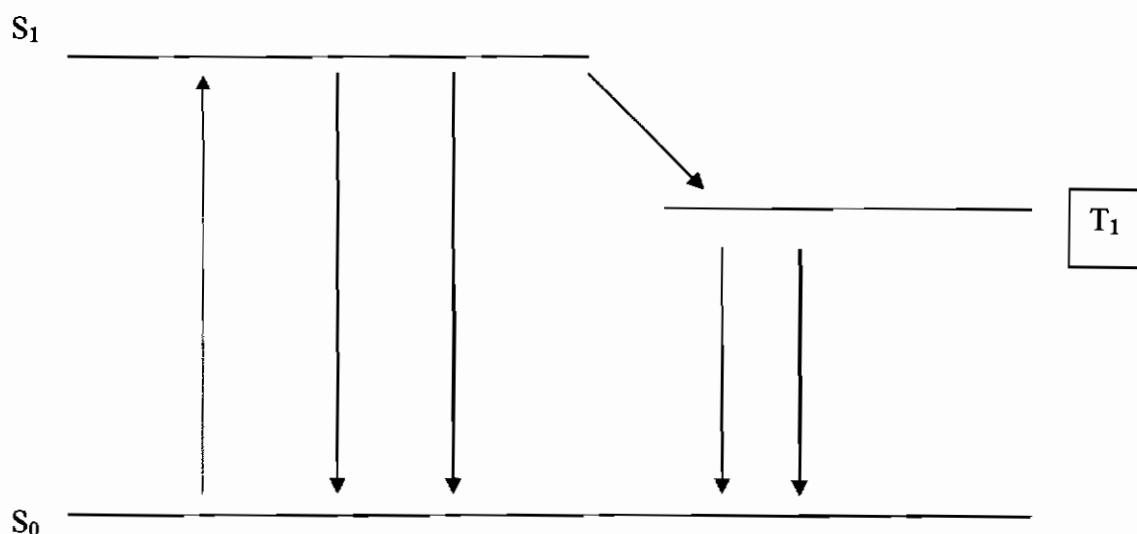


Figure 2.2.1. Unimolecular Photophysical Process.

Figure 2.2.1. graphically shows a Jablonski diagram outlining unimolecular photophysical processes that can occur, which can be divided into the following categories:

- (i) Absorption: (Red line)
- (ii) Luminescence: (Blue Lines)
- (iii) Radiationless Transitions: (Black Lines)

These processes are described in the following sections.

2.3. Absorption:

As outlined in the section 2.1, potential energy determined by that of constituent atoms and bonding overlap dictate molecular energies. At finite temperatures, atoms of molecules can vibrate about their equilibrium positions and in a gas, molecules can rotate and the motion associated with both have quantised kinetic energies. The total energy (E_T) of a molecule in its electronic ground state, excluding translational and internal nuclear energy is the sum of three components, the electronic energy (E_e), the vibrational energy (E_v), and the rotational energy (E_r) as described in equation 2.3.1.

$$E_T = E_e + E_v + E_r \quad \text{Eqn. 2.3.1.}$$

$$E_e \gg E_v \gg E_r \quad \text{Eqn. 2.3.2.}$$

These effects and the fact that organic molecules can have vibrational and rotational degrees of freedom can make the electronic structure appear structureless. The energy associated with the electronic and vibrational contributions outweighs those from the rotational, equation 2.3.2. shows the energy relationship. Rotational effects can be ignored in most media, due to restricted freedom of movement and thus low energy associated with them, however in the gaseous state this is not so. A molecule as complex as, for example, an aromatic hydrocarbon, possesses many alternative vibrational modes. At low temperatures detailed vibronic structure is resolvable, but at normal temperatures thermal broadening and solvent interaction effects smear the detail out and only a few modes such as C-C are normally dominant in the room temperature electronic absorption spectra.

As the total energy of the ground state vibronic states has been described as the sum of electronic and vibrational energies, the wavefunction (ψ) of a state can be expressed as the product of the electronic (θ) and vibrational (ϕ) wavefunction. This is the Born-Oppenheimer approximation¹¹.

Equation 2.3.3. describes the wavefunction of a lower electronic state.

$$\psi = \theta_x \phi_{lm}$$

Eqn. 2.3.3.

Equation 2.3.3. describes the wavefunction of a lower electronic state. The electronic component θ_x , can be separated from the nuclear component ϕ_{lm} , since the electronic mass is three orders of magnitude lower than the nuclear, and consequently the speed of response to a radiation field (or photon) is significantly faster.

These wavefunctions form the basis for the quantum-mechanical theory of radiative and radiationless processes in a molecule.

The potential energy diagram of a diatomic molecule plots the total electronic and vibrational energy of the molecule as a function of the nuclear separation, r , and the wavefunction, ϕ_{lm} , of the vibrational modes approximate to those of a harmonic oscillator as shown in Figure 2.3.1. An important concept related to absorption is the Franck-Condon Principle¹².

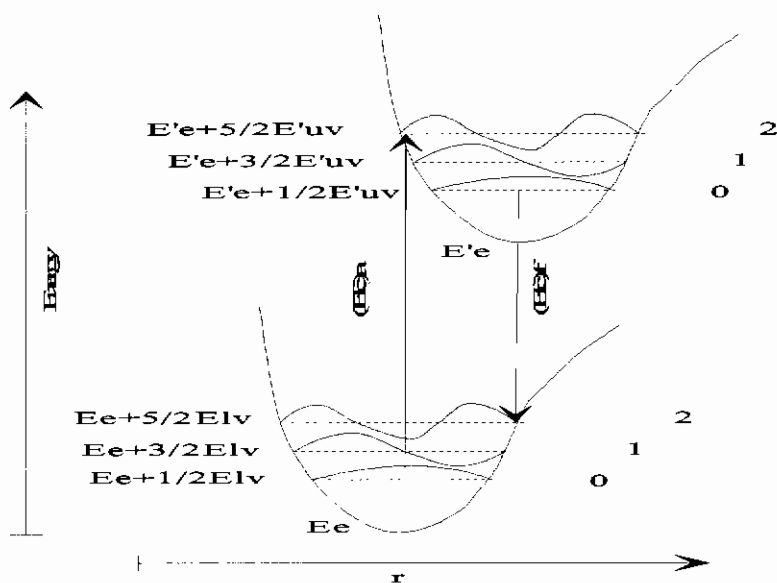


Figure 2.3.1. Shows the wavefunctions of ground and excited electronic states.

The Franck-Condon principle states that because the time required for an electronic transition is negligible compared with that of nuclear motion, the most probable vibronic transition is the one, which involves no change in the nuclear coordinates. This transition or Franck-Condon maximum represents a vertical transition on the potential energy diagram. In other words the Franck-Condon maximum

corresponds to the maximum overlap between ground state vibrational wavefunction, ϕ , and the excited state vibrational wavefunction, ϕ^* .

The Born-Oppenheimer and the Franck-Condon principle are invariably linked. As the Franck-Condon principle states that the electronic transition is extremely fast compared to nuclear motion, there exists an intermediate Born-Oppenheimer approximation¹³. As the electrical transition occurs first, the Born-Oppenheimer can be written as described by equation 2.3.4.

$$\psi_e^* = \theta_x^* \phi_{lm}^* \quad \text{Eqn. 2.3.4.}$$

After the electronic transition the nuclear relaxation occurs, yielding ϕ_{lm}^* . This will yield the final excited state wavefunction as given by equation 2.3.5.

$$\psi_e^{**} = \theta_x^* \phi_{lm}^* \quad \text{Eqn. 2.3.5.}$$

On interaction with a photon of appropriate energy, the electron undergoes a transition from the initial state, ψ_g , to the intermediate state ψ_e^* . The transition process can be probed by Absorption spectroscopy. The energy difference between the levels is determined by the electronic structure. Typically it falls within the Ultraviolet or Visible region, highlighting the importance of UV-vis spectroscopy¹³.

2.4. Luminescence:

Luminescence emission is the return to equilibrium by which the excited molecule loses energy by emission of a photon whereby it reaches a lower excited state or ground state. As discussed in the previous section, whereas absorption of a photon results in a transition to ψ_e^* , the state evolves (~ 1 psec) by nuclear relaxation to the state ψ_e^{**} . This state is metastable and can relax by the emission of a photon to the ground state. As is the case with absorption the Born-Oppenheimer approximation and the Franck-Condon Principle also apply to this transition. Thus the system initially relaxes to ψ_g^* , before reaching its ground state ψ_g . The emission spectrum is thus a mirror image of the absorption spectrum as illustrated in Figure 2.4.1, for the example of the polymer Pomp as discussed in Chapter 4. The spectra are shifted by an energy which corresponds to the sum of the energy differences between ψ_e^* and ψ_e^{**} , and ψ_g^* and ψ_g . This shift is called the Stokes shift.

Luminescence spectroscopy is a measure of radiative relaxation in materials. A distinction is made between fluorescence and phosphorescence according to the change in the spin quantum number between the initial and final states. When the quantum numbers stay the same, $\Delta S=0$ and the transition is spin allowed, the emission is defined as fluorescence. If there is a change in spin quantum number, $\Delta S \neq 0$, the transition is spin-forbidden and is termed phosphorescence. In the excited state, an electron can spin flip, a process referred to as intersystem crossing, resulting in a singlet, (S) to triplet, (T) transition. A material can thus exhibit both fluorescence and phosphorescence. The main difference between these two types is to do with lifetimes. Fluorescence is short lived with emission lifetimes in the range 1ns to 1 μ s, Phosphorescence lifetimes vary from 1ms to many seconds or even minutes.

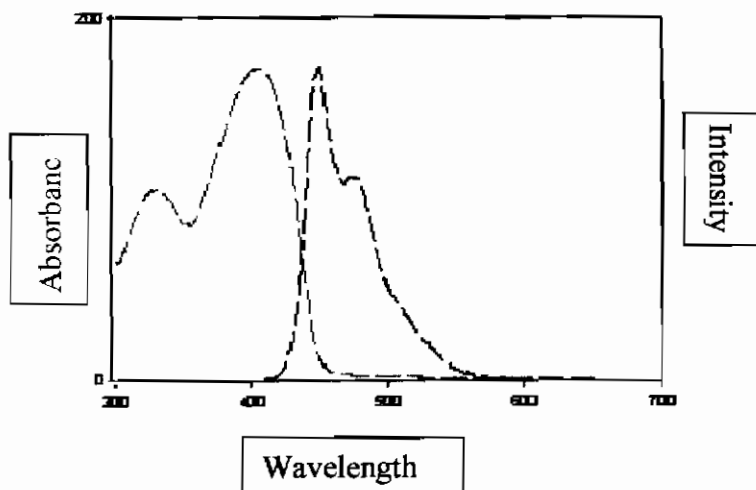


Figure 2.4.1. UV-vis absorption and emission spectra of PmPV.

2.5. Radiationless Transitions:

An alternative to the return to equilibrium by emission of radiation, is a coupling of the excess energy to the molecular structure through vibrations, resulting in a nonradiative transition. In materials for optoelectronic devices, radiationless transitions can be a problem as they generate heat. They reduce fluorescence intensity and quantum yield and thus reduce applicability of the material.

Common nonradiative relaxation processes are internal conversion and intersystem crossing.

Internal conversion can be defined as “an isoenergetic radiationless electronic transition between states of the same multiplicity”¹². If a molecule is excited into an excited singlet state S_x of total energy as described by equation 2.5.1.

$$E_{xt} = E_e + \frac{1}{2}E_v + mE_{nv} \tag{Eqn. 2.5.1}$$

where E_{xt} is the total energy of the system, E_e is the electronic energy, $1/2E_v$ is the zero point vibrational energy and $m E_{nv}$ is the vibrational excitation, it can lose the additional vibrational energy and relax to the lowest vibrational level of the state or

subsequently relax to a lower vibrational state. The energy is lost through vibronic coupling within the lattice structure or to the environment.

In a condensed medium a molecule which is excited by photon absorption rapidly can dissipate its vibrational excitation energy $m E_v$ to the surrounding medium thermally yielding a total energy as illustrated in equation 2.5.2. The so-called “hot” molecule distributes its excess phonons to its environment and comes to thermal equilibrium. The reason that rotational energy is not included in equation 2.5.1. is that the rotational energy is extremely small in comparison to both the vibrational and electronic.

$$(E_t)_0 = E_e + \frac{1}{2} E_{uv} \quad \text{Eqn. 2.5.2.}$$

As an alternative to the emission of a photon the system may now undergo a radiationless transition to the highest vibrational level of S_1 with energy E_t

$$E_t = E_{xt} = E_{xe} + \frac{1}{2} E_{xu} + mE_{xu} \quad \text{Eqn. 2.5.3.}$$

The excess energy mE_{xu} maybe rapidly dissipated to the environment and the system is returned to the ground state. Dissipation of energy within a state is called internal conversion. Due to the typical speeds of internal conversion (~ 1 psec), fluorescence usually only occurs from the S_1 level leading to the so called Kasha’s rule. Furthermore internal conversion between S_1 and S_0 , which often diminishes fluorescence quantum yields to negligible values.

The observation of T_1 - S_0 phosphorescence from molecules initially excited into S_1 is clear evidence for a radiationless transition, or intersystem crossing, from S_1 to the triplet state, T_1 . Singlet-Triplet intersystem crossing can either occur from the zero-point of S_1 or thermally populated levels of S_1 . The probability of a transition is from the S_1 level to either a vibronically excited level of T_1 . The reverse transition of Triplet to Singlet can also be seen. Triplet-Singlet radiative transitions are usually spin-forbidden. Their occurrence is due to the coupling between the wavefunction of the triplet and singlet states by for example spin-orbit coupling. The magnitude of the

and transitions between vibrational levels occur by the absorption or emission of radiation of energy $h\omega$.

The I.R. spectrum gets complicated when one considers polyatomic molecules. In understanding such a spectrum one must consider a number of fundamental frequencies and their symmetry, the possibility of overtones and combination bands and finally but equally important is the influence of rotation on the spectrum. Considering only fundamental vibrations, a molecule with N atoms in space has three-reference points, x , y , z -axis. Therefore the total number of co-ordinate values is $3N$ i.e. it has $3N$ degrees of freedom. However in a linear molecule it has $3N-5$ degrees of freedom but $3N-6$ in a non-linear¹⁵. This is due to the fact that in a linear molecule if the molecule is moved to the side then the molecule is not altered, however if a non-linear molecule is moved then the entire co-ordinate system is distorted. Each different mode will have a characteristic vibrational frequency, and different peaks will be seen in the I.R. spectra associated with these vibrations. Figure 2.6.1 illustrates the different regions, which associate the characteristic bands associated with different vibrations^{15a}. The majority of molecules possess an IR fingerprint, for which they can be identified.

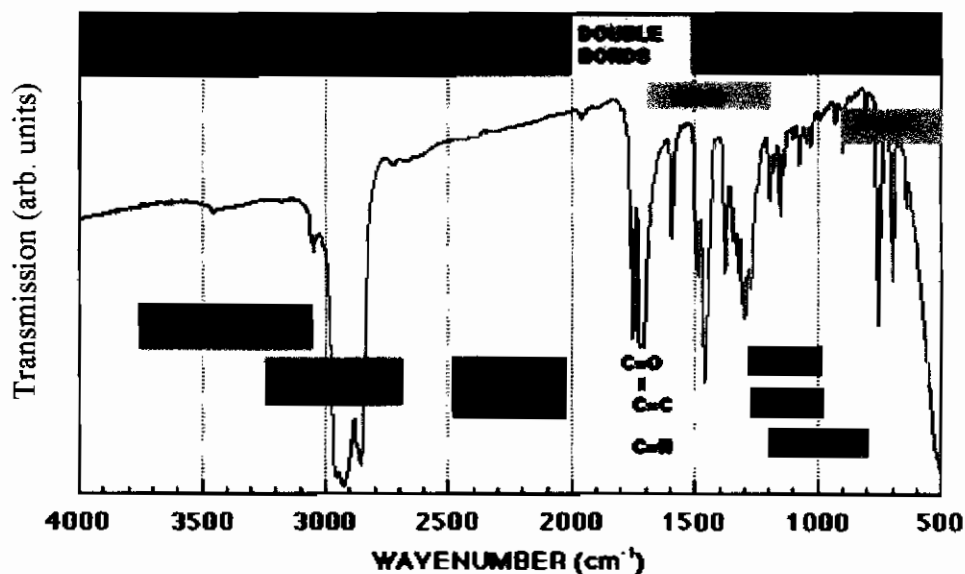


Figure 2.6.1. Typical I.R. transmission spectrum indicating bands associated with molecular vibrations.

2.7. Raman Spectroscopy:

In 1928, Sir C.V. Raman documented the phenomenon of inelastic light scattering¹⁶. Radiation scattered by molecules contains photons with the same frequency as the incident radiation, but may also contain photons with changed or shifted frequency. This effect is very weak – less than one photon out of a million (0.0001%) will scatter from that sample at a wavelength slightly shifted from the original wavelengths. The process was later named after him, with the shifting of frequency referred to as the Raman effect and the frequent-shifted light as Raman radiation. By the end of the 1930's, Raman spectroscopy had become a principle method of non-destructive chemical analysis, with Raman winning the Nobel Prize in Chemistry for his efforts¹⁷.

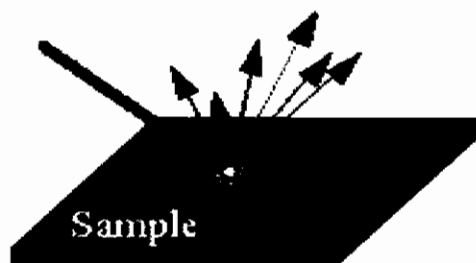


Figure 2.7.1 illustrates the Raman Effect.

To understand the Raman effect shown in Figure 2.7.1 one must look at the energy difference (E_v) between the incident light (E_i) and the Raman scattered light (E_s). The difference is equal to the energy involved in changing the molecule's vibrational state (i.e. getting the molecule to vibrate at energy, E_v). This energy difference is called the Raman shift, as described by equation 2.7.1

$$E_v = E_i - E_s \qquad \text{Eqn. 2.7.1.}$$

Several different Raman shifted signals will often be observed, each being associated with different vibrational or rotational motions of molecules in the sample.

These Raman lines will have either a higher or lower frequency corresponding to either the loss or gain of energy by the molecule. The frequency shifts are independent of the frequency of the exciting radiation.

The Raman effect arises from the coupling of induced polarisation of scattering molecules that is caused by the electric vector of the electromagnetic radiation with the molecular vibrational modes, light of frequency, ω_L produces a polarisation in a material is given by

$$P_{(\omega_i)} = \chi_{(\omega_i)} E_0 \cos \omega t \quad \text{Eqn. 2.7.2.}$$

Where

P, is the Polarisation ω_L is the frequency of incident light,

E is the Electric Field and finally $\chi_{(\omega)}$ is the Polarisability.

Oscillating polarisation represents accelerating charge, which will reradiate at the frequency of oscillation. $\chi_{(\omega_L)}$ is considered to be a constant of a material associated with its electronic properties. However at a finite temperature a material is not at equilibrium and atoms will vibrate about equilibrium position, R, along normal co-ordinates, with frequency ω_K in accordance with a simple harmonic oscillator approximation, as given in equation 2.6.1. The displacement from equilibrium can be represented by equation 2.7.3

$$\Delta R(t) = \Delta R \cos(\omega_k t) \quad \text{Eqn. 2.7.3.}$$

The susceptibility to polarisation, χ_k , thus varies through a cycle and can be represented by equation 2.7.4.

$$\chi_k(t) = \chi_0 + \Delta \chi_k \cos(\omega_k t) \quad \text{Eqn. 2.7.4.}$$

The polarisation now has the form as illustrated in equation in equation 2.7.5.

$$P(\omega_L, \omega_k) = \chi_0(\omega_L) E_0 \cos \omega_L t + \Delta \chi_k E_0 \cos(\omega_L) t \cos(\omega_k t - \delta_k) \quad \text{Eqn. 2.7.5.}$$

Where δ_k takes into account any phase difference between the molecular vibration and the electric field oscillation. This may be written as:

$$P(\omega_L, \omega_k) = \chi_0(\omega_L) E_0 \cos \omega_L t + \frac{1}{2} \Delta \chi_k E_0 (\cos((\omega_L - \omega_k) t - \delta_k) + \cos((\omega_L + \omega_k) t + \delta_k)) \quad \text{Eqn. 2.7.6.}$$

Thus the polarisation is given by equation 2.7.7:

$$P = P(\omega_0) + P(\omega_0 - \omega_k) + P(\omega_0 + \omega_k) \quad \text{Eqn. 2.7.7.}$$

Where

$P(\omega_0)$ corresponds to Rayleigh Scattering,

$P(\omega_0 - \omega_k)$: corresponds to the subtraction of a vibrational quantum from the photon energy resulting in the creation of a vibration - termed Stokes.

$P(\omega_0 + \omega_k)$: corresponds to the addition of a vibrational quantum to the photon by the annihilation of a vibration - termed Anti-Stokes.

In Raman spectroscopy, each vibration can couple to the laser generating a vibrational spectrum on both the Stokes and Anti-Stokes sides. The Stokes shift is normally measured, as at room temperatures it is easier to create a phonon than to annihilate one, in accordance with the Boltzman¹³ distribution.

2.8. Transition probability:

In absorption spectroscopy the interaction of light with material is described by the Beer-Lambert Law as shown in Eqn:2.8.1.

$$I_{out} = I_{in}^* \exp^{-\alpha l} \quad \text{Eqn 2.8.1.}$$

α = Absorption coefficient depending on the frequency, ν of the light.

I_{out} = light intensity out. L = sample path length.

I_{in} = light intensity in.

α is a property of the bulk material describing the strength of the absorption per unit length. If the bulk is made up of identifiable building blocks, a property called the absorption cross section is described by equation 2.8.2

$$\alpha(\nu) = N\sigma(\nu) \quad \text{Eqn 2.8.2.}$$

N = number of individual atoms or species per unit volume.

σ = absorption cross-section area.

The absorption cross-section describes the probability of absorption of a photon of frequency

(i): $h\nu = (E_f - E_i)$, this means that the photon energy must be equal to the difference between the final and initial energy.

(ii) : Initial state must have an oscillating dipole moment. As light is an oscillating electromagnetic field, the field interprets the lack of dipole moment as neutral and has no effect. Moment can be described by equation 2.8.3.

$$\underline{M} = \sum_i e_i \underline{r}_i \quad \text{Eqn. 2.8.3.}$$

Where \underline{r}_i is the displacement of the i^{th} charge from its neutral position. It is a vector quantity, and its interaction with the electric field is a vectorial quantity, equation 2.8.4.

$$\underline{I} = \underline{M} \times \underline{E} \qquad \text{Eqn. 2.8.4.}$$

Therefore it is not sufficient to have an oscillating dipole to interact with the light, but the dipole must be aligned with the polarisation of the light.

(iii): Absorption or Emission of a photon results in a change in dipole moment. The initial dipole is further distorted by the action of the electric field. This more or less polar state has characteristics of the final wavefunction

(iv) : The Overlap integral must be non zero, as shown in equation 2.8.5

$$\int \phi_f(er) \phi_i dr \neq 0 \qquad \text{Eqn. 2.8.5.}$$

Quantum mechanically the overlap integral describes the probability of a transition from the initial state, ϕ_i , to the final state, ϕ_f through the action of the dipole operator. It incorporates all of the conditions above and can be calculated if the wavefunctions are known. The probability of a transition is given by equation 2.8.6:

$$P_{IF} = \left| \int \phi_f(er) \phi_i \right|^2 \qquad \text{Eqn. 2.8.6.}$$

A consequence of the contribution of equation 2.8.6 is that during a transition the parity of a wavefunction (symmetry in the case of molecules) must change. UV-vis and fluorescence are electric dipole transitions and are governed by these selection rules. Raman is a scattering process and is therefore governed by a different set of rules, highlighting the fundamental difference between the two methods. In I.R. the dipole, μ , needs to change as the molecule vibrates about its equilibrium position:

$$\left. \frac{d\mu}{dR} \right|_0 \neq 0 \qquad \text{Eqn. 2.8.7.}$$

In Raman the polarisability, χ , needs to change as the molecule vibrates about the equilibrium position as described in equation 2.8.8

$$\left. \frac{d\chi}{dR} \right|_0 \neq 0 \qquad \text{Eqn. 2.8.8.}$$

In many cases these conditions are mutually exclusive and thus I.R. and Raman are complementary. By performing both an I.R. and Raman investigation on a material a complete picture of backbone and sidechain interaction is determined.

2.9. Einstein Coefficients:

The energetics of a material are determined by the interaction of the constituent atoms or molecules and govern where in the spectrum it will absorb or emit radiation. The strength of the interaction with the radiation field is a complex function of the nature of the ground and excited wavefunctions. To date the quantum approach has been described which utilises the overlap integral and wavefunction to portray what is happening during absorption, fluorescence and overlapping of orbitals. The system can only be described if a precise definition of the wavefunctions is available. The Einstein model, on the other hand, is a phenomenological model, which considers an ensemble of species in the presence of a radiation field. A series of rate equations, with transition probabilities described by Einstein coefficients, determine the state of a system at any time.

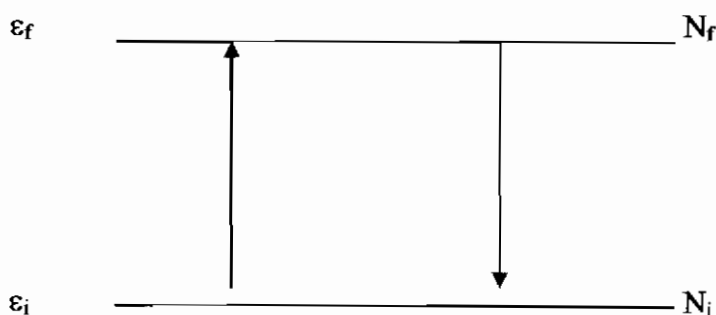


Figure 2.9.1. Represents a two-level system.

Figure 2.9.1. illustrates a two level atomic system showing absorption (black line) and luminescence (red line). A rate equation can be written to describe the evolution of the populations of the two levels. Einstein proposed, that under the action of a radiation field, $\rho(\nu)$, a transition from the initial state to the final state in a system of N_i initial states could occur with a probability P_{if} depending on the Co-efficient for stimulated absorption as shown in equation 2.9.1

$$P_{if} = N_i B_{if} \rho(\nu) \quad \text{Eqn. 2.9.1.}$$

He also argued that the probability of inducing a transition in the inverse direction should be equal and opposite (ignoring differing spectroscopic weights). Thus he proposed the relationship shown in equation 2.9.2 and in doing so predicted the phenomenon of stimulated emission of radiation.

$$B_{if} = B_{fi} \quad \text{Eqn.2.9.2.}$$

With only these two mechanisms, however, a return to equilibrium in the absence of the radiation field would be impossible. Thus he introduced the Einstein co-efficient for spontaneous emission, A_{fi} . The probability for spontaneous emission is independent of radiation field, as described by equation 2.9.3

$$P_{fi} = N_f A_{fi} \quad \text{Eqn.2.9.3.}$$

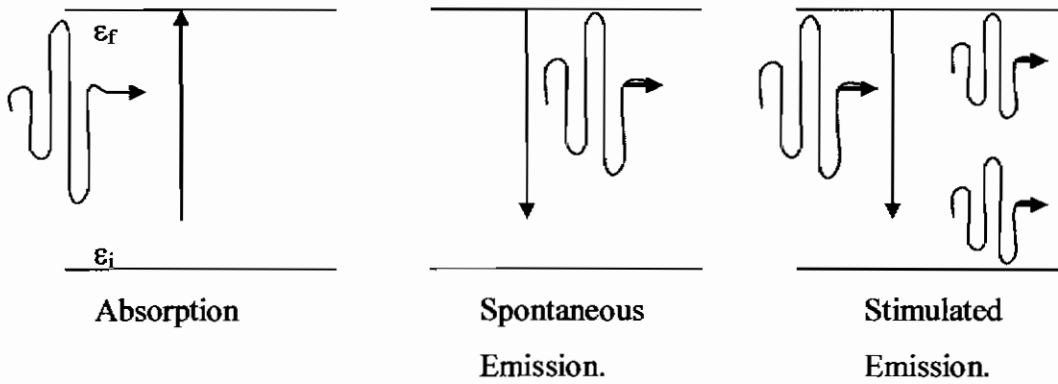


Figure 2.9.2. Illustrates the different types of processes observed.

Under this formalism, the system can be described by the rate equations, given in equation 2.9.4

$$\left(\frac{dN_i}{dt}\right) = -N_i B_{if} \rho(\nu) + N_f B_{fi} \rho(\nu) + N_f A_{fi}$$

$$\left(\frac{dN_f}{dt}\right) = N_i B_{if} \rho(\nu) - N_f B_{fi} \rho(\nu) - N_f A_{fi}$$

$$\left(\frac{dN_i}{dt}\right) = -\left(\frac{dN_f}{dt}\right)$$

Eqn. 2.9.4.

This is a simple example of a 2 level system applying to isolated atoms. The Einstein rate equations can be used to give an indication of the lifetime of the states as the population of each level of the system can be calculated and thus the change in these populations can be determined. It is of interest to solve the system of equations under two extreme experimental conditions.

- (i) **Steady State:** Under continuous illumination, the system comes to equilibrium and the rate of change of any level is zero, equation 2.9.5

$$\left(\frac{dN_i}{dt}\right) = -\left(\frac{dN_f}{dt}\right) = 0 \quad \text{Eqn.2.9.5.}$$

thus,

$$N_i B_{if} \rho(\nu) - N_f B_{fi} \rho(\nu) - N_f A_{fi} = 0 \quad \text{Eqn.2.9.6.}$$

or

$$\frac{N_f}{N_i} = \frac{B_{if} \rho(\nu)}{B_{fi} \rho(\nu) + A_{fi}} \quad \text{Eqn.2.9.7.}$$

Thus, if the co-efficients of the system are known, the population distribution is a function of the intensity only and can be determined.

Equation 2.9.7 can also be written as equation 2.9.8

$$\rho(\nu) = \frac{\frac{A_{fi}}{B_{fi}}}{\left(\frac{N_i B_{if}}{N_f B_{fi}}\right) - 1} \quad \text{Eqn.2.9.8.}$$

It should be noted, however, that the Boltzman distribution is determined by (where g_i and g_f are spectroscopic weight factors, the incorporation of these weighting factors is shown in equation 2.9.8a

$$\frac{N_i}{N_f} = \frac{g_i}{g_f} \exp\left(\frac{E_f - E_i}{kT}\right) \quad \text{Eqn.2.9.8a.}$$

Therefore,

$$\rho(\nu) = \frac{\frac{A_{fi}}{B_{fi}}}{\left(\frac{g_i B_{if}}{g_f B_{fi}}\right) \exp\left(\frac{h\nu}{kT}\right) - 1} \quad \text{Eqn.2.9.9.}$$

This is exactly the form of equation for a Black body radiator, leading to the conclusion that atoms and radiation in thermal equilibrium constitute a Black body radiator. Planck's formula states itself through equation 2.9.10

$$\rho(\nu) = \frac{\frac{8\pi h}{\lambda^3}}{\exp \frac{h\nu}{kT} - 1} \quad \text{Eqn.2.9.10.}$$

and it is also know that,

$$B_{if} = B_{fi} \quad \text{Eqn.2.9.2.}$$

Therefore,

$$A_{fi} = \frac{8\pi h}{\lambda^3} B_{fi} \quad \text{Eqn.2.9.11.}$$

and also,

$$A_{fi} = \frac{8\pi h}{\lambda^3} B_{fi} \quad \text{Eqn.2.9.12.}$$

All of the Einstein Coefficients can now be interrelated and moreover can be related to the overlap integral, through equation 2.9.13

$$B_{if} \propto B_{fi} \propto A_{fi} \propto \int \Psi_f(er) \Psi_i \quad \text{Eqn. 2.9.13.}$$

(ii) Delta-function conditions.

Rate Equations also simplify under delta function illumination conditions (i.e) when the radiation field lasts for a small fraction of time compared to all of the relaxation rates. The initial pulse generates a nonequilibrium population distribution and subsequent evolution of the system only occurs through spontaneous emission (in atomic systems).

$$\left(\frac{dN_f}{dt}\right) = -N_f A_{fi} \quad \text{Eqn.2.9.14.}$$

or

$$N_f(t) = N_f(0)\exp(-A_{fi}t) \quad \text{Eqn.2.9.15.}$$

This is the familiar exponential decay, characterised by the radiative lifetime,

$$\tau = \frac{1}{A_{fi}} \quad \text{Eqn.2.9.16.}$$

The two level system is an idealisation which really only applies to isolated atoms. In molecules, the Stokes shift should be included, giving rise to a three level system. This shift, $\Delta\nu$, now means that the emission frequency is $\nu-\Delta\nu$, and radiation of frequency (ν) can no longer give rise to stimulated emission this is expressed in equation 2.9.17.

$$\frac{dN_i}{dt} = -N_i B_{if} \rho(\nu) + N_f A_{fi} \quad \text{Eqn. 2.9.17.}$$

If $N_f A_{fi}$, or the number of photons (of frequency $\nu-\Delta\nu$) emitted per second is high enough, then they can stimulate the emission.

$$\frac{dN_i}{dt} = -N_i B_{if}(\nu) + N_f A_{fi} + N_f B_{if} (N_f A_{fi}) \quad \text{Eqn. 2.9.18.}$$

If we can couple energy to molecular (or lattice) vibrations, however, then we have an alternate route towards dissipating the energy from the excited state to return to the ground state, introducing non-radiative relaxation (Internal Conversion) to the system.

$$\frac{dN_i}{dt} = -N_i B_{if} \rho(\nu) + N_f k_{nr} + N_f A_{fi} + N_f B_{if} (N_f A_{fi}) \quad \text{Eqn. 2.9.19.}$$

Where k_{nr} is the non-radiative relaxation rate. In terms of the nomenclature of rates, rather than Einstein co-efficients, equation 2.8.5 can be written in the form of equation 2.9.20

$$\frac{dN_f}{dt} = -N_f \sigma_{if} \frac{I}{h\nu} + N_f k_{nr} + N_f k_{rad} + N_f \sigma_{stim} (N_f k_{rad}) \quad \text{Eqn. 2.9.20.}$$

σ_{if} = absorption cross-sectional area, σ_{stim} = stimulated emission cross-sectional area.

k_{rad} = spontaneous emission rate $I/h\nu$ = Incident photon density.

Under Delta function illumination conditions, the decay of the system is exponential as before, but the lifetime of the system is no longer exclusively determined by the radiative decay rate.

$$\frac{dN_f}{dt} = N_f (k_{nr} + k_{rad}) \quad \text{Eqn. 2.9.21.}$$

$$\tau_{fl} = \frac{1}{(k_{nr} + k_{rad})} = \frac{1}{\frac{1}{\tau_{nr}} + \frac{1}{\tau_{rad}}} = \frac{\tau_{rad} \tau_{nr}}{\tau_{rad} + \tau_{nr}} \quad \text{Eqn. 2.9.22.}$$

The fluorescence lifetime τ_{fl} is dictated by the more rapid process and the rate equations highlight the fact that there are two possible potential routes for the decay, which compete with each other. The Quantum Yield for radiative decay can be defined as the ratio of photons out/photons in and is given by equation 2.9.23.

$$\phi = \frac{N_f k_{rad}}{N_f k_{nr} + N_f k_{rad}} = \frac{k_{rad}}{k_{nr} + k_{rad}} \quad \text{Eqn. 2.9.23.}$$

There exists another process, which must be looked at when considering rate equation. Inter-system crossing adds an extra term for N_f , equation 2.9.24.

$$\frac{dN_f}{dt} = N_f (k_{nr} + k_{rad} + k_{isc}) \quad \text{Eqn. 2.9.24.}$$

This will yield a similar lifetime equation as above in equation 2.9.23; with just one extra term for the intersystem crossing shown in equation 2.9.25.

$$\tau_f = \frac{1}{(k_{nr} + k_{rad} + k_{isc})} = \frac{1}{\left(\frac{1}{\tau_{nr}} + \frac{1}{\tau_{rad}} + \frac{1}{\tau_{isc}}\right)} = \frac{\tau_{nr} \tau_{rad} \tau_{isc}}{(\tau_{nr} + \tau_{rad} + \tau_{isc})} \quad \text{Eqn. 2.9.25.}$$

Intersystem crossing accounts for any transitions from the singlet state to the triplet state, from which a triplet yield can be determined. Intersystem crossing being a percentage of all decay processes as described in equation 2.9.26.

$$\phi_T = \frac{k_{isc}}{(k_{nr} + k_{rad} + k_{isc})} \quad \text{Eqn. 2.9.26.}$$

Studying the photophysics of the system, processes can be identified with measurable parameters as shown in the Einstein coefficients. In particular, in fluorescence, competing factors can be identified with a view to optimising the material response. These competing non - radiative processes should be minimised in order to optimise the luminescence efficiency of a material.

2.10. Nature of Conjugated Polymers:

Section 2.1 outlines the chemical structure of organic materials and, in particular, highlights the chemical tailorability of the electronic and optical properties of conjugated molecules. Section 2.2 describes the photophysics of such molecular systems and describes a phenomenological rate equation approach to quantify the state of a system under illumination. Extending the idealised linear molecule modelled in Section 2.1 by the Free Electron Model, to trans-polyacetylene as shown in Figure 2.10.1, one can anticipate many of the intrinsic properties of a delocalised π electron polymer¹⁸:

- (I): electronic band gap E_g is only $\cong 1.4\text{eV}$, this would allow low energy electronic excitations.
- (II): polymer chain can be rather easily oxidised or reduced through charge transfer.
- (III): carrier mobilities are large enough that high electrical conductivities are realised in doped states.

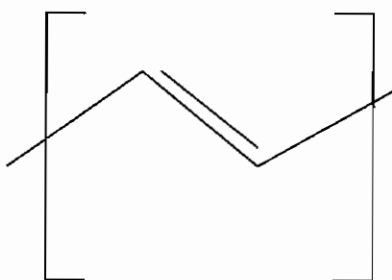


Figure 2.10.1. Repeating unit of trans-polyacetylene.

The molecular orbital description outlined above assumes however that the excited state extends over the molecule and that, upon excitation, nuclear relaxation is similarly distributed over the molecule. In conjugated molecules that extend to the lengths of polymers this is not always the case. A significant consequence of this is that:

(IV): excited states or charge carrying species are not excitons or free electrons/holes, but quasi-particles determined by electron-lattice coupling which may move freely.¹⁸

To investigate these species one must distinguish between degenerate and non-degenerate conjugated polymers. Trans-polyacetylene is unique among conjugated polymers in that it possesses a degenerate ground state²⁰, i.e. it possesses two distinct ground state structures as shown in Figure 2.10.2 which differ from each other through the exchange of carbon-carbon single/double bonds. Both structures have alternating double and single bonds and the degree of bond length (Δr) alternation, being the difference between length of a single and double bond, has been shown to be $\cong .08$ angstroms in both²¹ as shown in Figure 2.10.3. For this reason the two structures are degenerate.

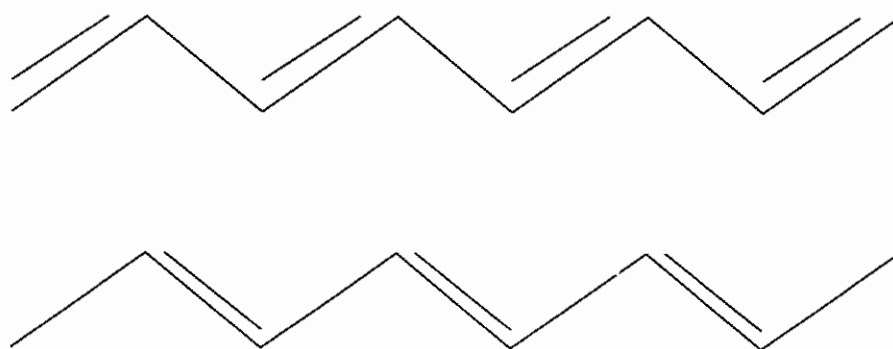


Figure 2.10.2. Two distinct ground states structures of trans - polyacetylene.

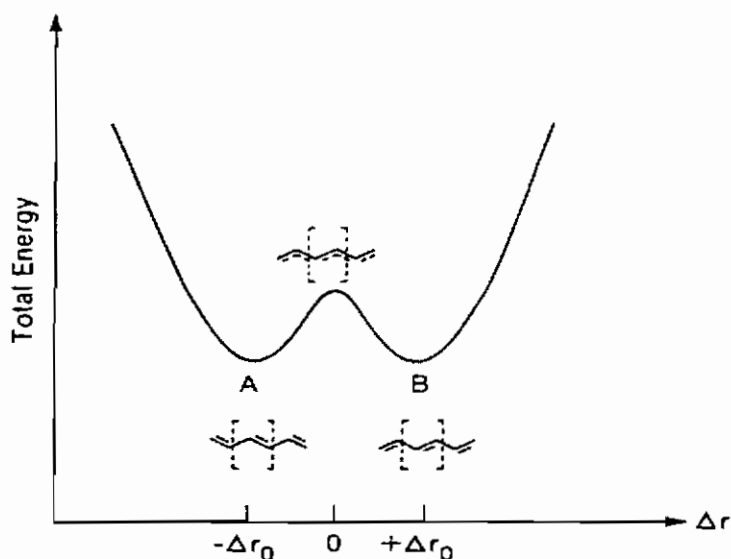


Figure 2.10.3. Total Energy curve for trans - polyacetylene chain as a function of the degree of bond length alternation.

Upon photoexcitation, the electron associated with one of the double bonds is localised, and the bond becomes antibonding.

Locally the bond alteration is lost and thus non-equilibrium state is free to move along the chain. This freedom to move led to the nomenclature of solitons.

Most conjugated polymers are, however, nondegenerate. This means they have a preferred sense of bond alteration and for a change in that alternation as a result of a photoexcitation to propagate, energy is required. PPV is an example of such a non-degenerate conjugated polymer and the different structures of PPV are shown in Figure 2.10.4. In the ground state PPV is benzenoid in form. Upon photoexcitation, it locally takes on a quinoidal form but the energy difference between the two forms limits the extent to which the quinoidal form can extend. The result is a polaron pair or bipolaron⁹. In polymers with large degree of bond alternation or nondegeneracy, the excitation can be locally confined resembling an exciton in a 3-d semiconductor, or indeed an excitation in a smaller organic moiety. The photophysics of PPV and its derivatives have been the subject of much study and indeed debate over the past decade. The debate has raged over whether an electron – lattice coupled or an excitonic interpretation of the excited states is most appropriate¹⁹. In this study, PmPV as discussed in Chapter 4 is employed. It is anticipated that this polymer, which is more nondegenerate than PPV, the latter approach, is more appropriate. The

interpretation will be substantiated by comparison of the optical properties of the polymer to model short chain oligomers.

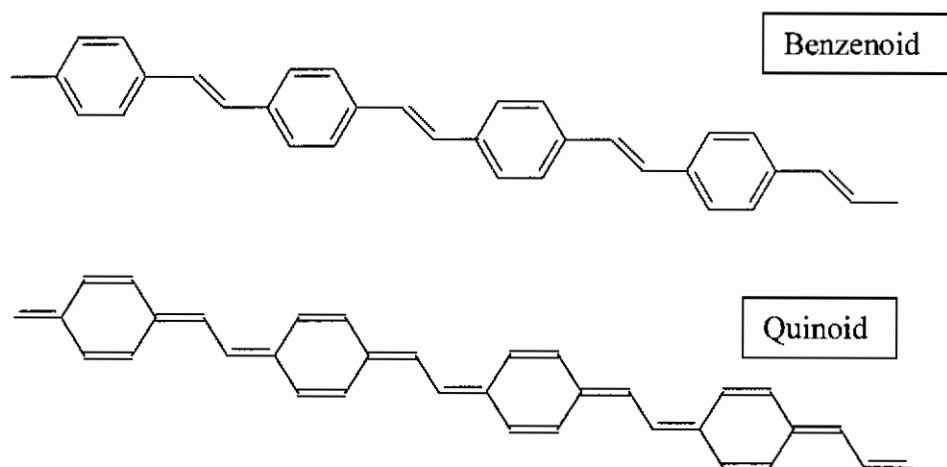


Figure 2.10.4. Two resonant structures of PPV.

2.11: Aggregation:

In the preceding sections the energetics and photophysics described is that of unimolecular systems. In reality the system is often not unimolecular due to the presence of excimers, exiplexes and aggregates. The close proximity of molecules can have significant influence on the photophysics of the system. With aggregate formation the major spectral changes that have been observed are:

- (I); displacement of emission and absorption bands relative to gaseous state bands.
- (II): splitting of spectral lines with a corresponding change in polarisation properties.
- (III): variation of selection rules and oscillator strength.
- (IV): changes in molecular vibrational frequencies and introducing intermolecular lattice modes.
- (V): appearance of totally new states.
- (VI) Significant decrease in luminescence quantum yield.

All of these effects imply that the photophysics of the system can differ significantly from that of the individual molecules. Application of simple theory becomes even more difficult, within the context of this work, (VI) is of particular relevance as it detracts from the luminescence properties of the material. This work tries to understand and control such effects, as it is futile to design molecules with desired properties if these properties are lost in solid state.

2.12. Summary:

In developing materials for optoelectronic applications an important area to understand is the electronic configuration and photophysics of materials. Understanding of the electronic configuration allows for the properties of organic systems to be tailored via chemical structure. The photophysics can be represented in a general format utilising a Jablonski diagram for unimolecular processes, illustrating absorption, fluorescence and non-radiative process. Relative contributions can be quantified and parameterised through the Einstein Rate equation approach. These processes are extremely important as in designing materials for use in the

optoelectronic area, non-radiative processes and different forms of quenching need to be minimised to increase the fluorescence efficiency.

Whereas Unimolecular processes are well understood and structural property relations are well developed, many characteristics of molecules are lost in their condensed phase. In the development of optoelectronics devices it is essential that these phenomena be understood.

In this project UV-vis, fluorescence, Raman and I.R. are used as probes of the photophysics of a select polymer and model oligomers. In dilute solution molecular processes utilising a range of solvents to explore how the environment affects non-radiative decay and thus how it can be minimised. A concentration study is also undertaken to access the effect of aggregation on the system. The effect of chemical structure or backbone conformation on the aggregation is also studied in an effort to curtail the inter-molecular interactions to optimise the performance of the material.

2.13. References:

- 1: Eisberg R; Resnick R; Quantum Physics of Atoms, Molecules, Solids, Nuclei and Particles 2nd Interscience, Wiley, New York 1985.
- 2: Cantwell Dr T. Final Year, Quantum Mechanics course, B.Sc Degree.
- 3: Morrison and Boyd Organic Chemistry 8th Wiley 1989.
- 4: Kuhn H, Forsch. Chem. Org. Naturstoffe, **16**, (1958)
- 5: Rustagi K.C; Opt. Comm. **10**, 258 (1974)
- 6: Chance R.R; *J. Polym. Sci Polym. Phys. Ed*, **14**, 2037 (1976)
- 7: Wenz G. *et al Macromol*, **17**, 837 (1984)
- 8: Byrne H.J., PhD Thesis, Trinity College Dublin 1989.
- 9: Birks J.B. Organic Molecular Photophysics, Vol 2, Wiley, New York 1973.
- 10: Birks J.B. Organic Molecular Photophysics, Vol 1, Wiley, New York 1973.
- 11: Young, University Physics, 8th Addison – Wesley 1992.
- 12: Byrne Dr. H. J.; Final year Notes Dublin Institute of Technology, Dublin.
- 13: Kittel C, Introduction to solid state physics, 6th ed, New York Chichester : Wiley, 1986
- 14: Mc Glynn S.P; Azumi T; Kinoshita M; *Molecular Spectroscopy of the Triplet state*, Ch. 8 and the references therein.
- 15: Banwell C.N. Fundamentals of molecular spectroscopy, McGraw Hill, 1994.
- 16: Raman C.V; Kristnan K.S; Nature; **121 (3048)**, 501, 1928.
- 18: Skotheim T.A.; Elsenbaumer R; Rynolds J; Handbook of Conducting Polymers, Marcel and Dekker, 1998.
- 19: Bredas J.L., Street G. B., *Acc. Chem Res.* 1985, **18**, 309-315.
- 20: Su W.P' Schrieffer J.R, Heeger A.J, *Phys. Rev. Lett.* **42**, 1698, 1979.
- 21: Fincher C.R. *et al, Phys. Rev. Lett;* **51**; 1191, 1983.

Chapter 3 *Solvatochromism*

| | |
|--------------------------------|----|
| 3.1 Solvatochromism | 51 |
| 3.2 Solvation Energies | 53 |
| 3.3. Onsager Field Model | 56 |
| 3.4 Onsager examples:..... | 57 |
| 3.5 Summary | 61 |
| 3.6. References | 63 |

3.1 Solvatochromism

The previous chapter discussed the photophysics of an ideal system. However various deviations from such a system exist, depending on environment and the presence of solvent or intermolecular effects. "Solvatochromic shifts result from the difference of solvation energies between the two electronic states involved in the observable absorption or emission transition"¹. Considering an ensemble of molecules as a solution, then the century old proverb 'Similia similibus solvuntur' or 'like dissolves like' has been used in choosing suitable solvents. The presence of a similar functional group was usually sufficient. The proverb has however limited applicability as one must look to the intermolecular interaction between solvent and solute molecules, which determine mutual solubility. A compound, "a" dissolves in a solvent "b" only when the intermolecular forces of attraction, k_{aa} and k_{bb} for the pure compound can be overcome by the forces of k_{ab} in solution. Table 3.1.1. Illustrates the type of interactions between solvent and solute. The sum of the interaction forces between the molecules of solvent and solute can be used to determine the solvation energies. The degree of interaction, be it between solvent and solute or solute and solvent determines the deviation from single molecular behaviour.

| <i>Solute a</i> | <i>Solute b</i> | <i>a---a</i> | <i>b---b</i> | <i>a---b</i> | <i>Solubility of a in b</i> |
|-----------------|-----------------|--------------|--------------|--------------|-----------------------------|
| Non Polar | Non Polar | Weak | Weak | Weak | Possibly High |
| Non Polar | Polar | Weak | Strong | Weak | Probably Low |
| Polar | Non Polar | Strong | Weak | Weak | Probably Low |
| Polar | Polar | Strong | Strong | Strong | Possibly High |

Table 3.1.1. Summary of interactions between the solute and solvent.

3.2 Solvation Energies

Solvatochromic shift¹ is defined as the displacement of an electronic spectrum (absorption or emission) from one solvent to another. The solvent effects on electronic spectra can be quite complex and may result in 1 or more of the following effects:

- (i) Broadening of a spectral line.
- (ii) A change in intensity (hypochromism or hyperchromism).
- (iii) Change in shape of an absorption or emission band, reflecting intensities in vibrational sub-bands.

Solvatochromic shifts are very important in describing the relative energies of electronic states of molecules and for determining some physical properties such as dipole moment.

Atoms and molecules all have discrete energy states, which represent rotational, vibrational and electronic excitations in order of increasing energy. Atoms or molecules, are an assembly of nuclei and electrons and the energy levels and the spatial distribution of electrons largely determine the properties of matter. The Schrödinger equation (equation 3.2.1.) allows the description of the energies and spatial distribution of electrons.

$$E\psi = H(\Psi) \qquad \text{Eqn. 3.2.1.}$$

Where

E is the energy,

ψ is the spacial distribution,

H is the Hamiltonian operator.

The spatial distribution is given in three dimensions, $\psi_{x,y,z}$ and therefore the probability particle existing in any space at a specific period in time = $\psi^2_{(x,y,z)}$. In relation to solvatochromic shift, the total energy is only important, since the absorption or enission spectrum is then basically the energy difference between two orbitals labelled, ϕ_i (lower) and ϕ_f (final), as illustrated in Figure 3.2.1.

The Schrödinger equation applies to an isolated molecule and it does not take into account the interaction of the solvent, which is described by classical electrostatic equations.

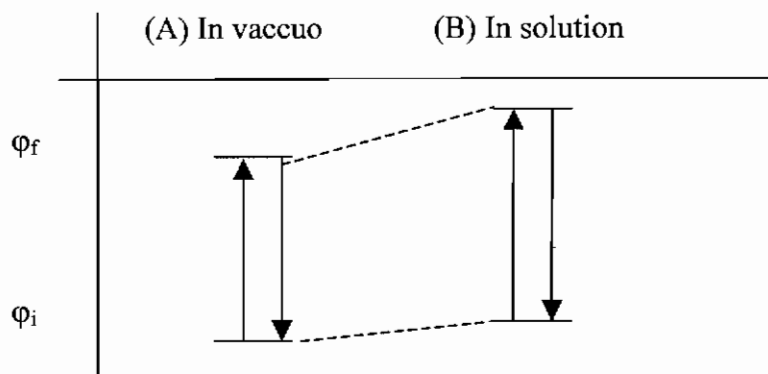


Figure 3.2.1. Schematic illustration of Solvatochromism

Solvatochromic shift results from the difference of solvation energies between the electronic states involved in the observable absorption or emission transition. In solution, it would be presumed the amount of solvent molecules interacting is very large and it is, but 90% of the total solvation energy is accounted for in the solvation of the first shell¹. Due to this limited amount of interaction a Quantum mechanical equation, (equation 3.3.2.) has been proposed to describe the interaction between the solute and solvent molecules.

$$H_{ij} = (\phi_j^0 H + H' \phi_i^0) = w_i^0 \delta_{ij} + (\phi_j^0 H' \phi_i^0) \quad \text{Eqn. 3.2.2.}$$

ϕ_i and ϕ_j are the wavefunctions of the solvent and solute molecules. The final results of such an equation are given in terms of macroscopic solvent properties such as, dielectric constant, D , and refractive index, n . Although the results would give the interaction energy if the Hamiltonian operators could, in practice it is difficult to define these wavefunctions for complex systems. Solution expressed in terms of D and n allow the theory to be related to the Onsager model of dielectrics. This is the most popular theory used to interpret solvent shifts. The theory was initially derived as a quantum mechanical treatment such as, McRae's model². It is not possible to consider all the various improvements to these simple models, oversimplified though they are, give a very good account of solvatochromic shifts of polyatomic molecules, with the important exception of hydrogen-bonding effects for which there is no exact theory at this time. The most abundant solvent on the planet is water. Numerous models have been developed, but as of yet no existing model has been able to determine fully the physico-chemical properties of water and an interpretation of its

anomalies. This gives an indication of the complexity of describing the inner structure of a solvent.

The use of the classical model is necessary in order to obtain a correlation with measurable macroscopic properties of the solvent.

A solvent should not be considered a macroscopic continuum characterised only by physical constants such as density, dielectric constant, refractive index, but as a discontinuum, which consists of individual mutually interacting solvent molecules.

To fully understand what effect density, dielectric constant and Polaris ability have at a macro level, one must consider what happens at a microscopic scale.

Even though the equations for the solvation energies are based on Schrödinger's equation, the results are given in terms of macroscopic properties, such as dielectric constant (D) and refractive index (n). The solvation energy, is the energy of interaction between the solute and a solvent as illustrated in equation 3.3.3.

$$E_{solv} = P_m \pi_s \quad \text{Eqn. 3.2.3.}$$

Where

P_m is the polarity of the solute molecule, π_s is the polarity of the solvent.

There are two expressions for the relation of solvation energies, dipole-dipole interaction and ion-dipole interactions. The ion-dipole interaction can be explained using the Born solvation model³ as shown in equation 3.2.4, while the dipole-dipole interaction is the Onsager model³ as shown in equation 3.2.5.

$$E_{SOLV}^{ION} = -\frac{q}{2a} F(D) = ML^2T^{-2} \quad \text{Eqn. 3.2.4.}$$

$$E_{solv}^{dipole} = -\frac{\mu^2}{2a^3} f(D) = ML^2T^{-2} \quad \text{Eqn. 3.2.5.}$$

The above equations are derived from a culmination of the five non-specific interaction such as, multipole - multipole interaction, multipole (solute)-induced dipole (solvent) interactions, solvent multipole-solute induced dipole interaction (stark effect), dispersion interactions and finally interaction between the transition dipole moment of the solute molecule and polarisable solvent. As ions are not being dealt with the Born approximation can be ignored. The molecular properties dipole moment and polarisability can be related to the dielectric

constant D, and refractive index, n, through variations of the Debye as shown in equation 3.2.6. and Clausius-Mosotti equations⁴ shown in equation 3.2.7.

$$\varphi(D) = \frac{D-1}{D+2} = \frac{4N\delta\pi}{3M} \left(\alpha_s + \frac{\mu_s^2}{k_b T} \right) \quad \text{Eqn. 3.2.6:}$$

$$\varphi(n^2) = \frac{n^2 - 1}{n^2 + 2} = \frac{4N\delta\pi}{3M} \alpha_s \quad \text{Eqn. 3.2.7:}$$

Where

n is the refractive index

M is the molecular weight

δ is the density

$(4\pi a^3/3)$ is the molecular volume of solvent

α is assumed to be equal to a^3 , for a spherical conductor.

μ is permanent dipole moment

3.3. Onsager Field Model

The Onsager Field model⁵ is the most widely used model for microscopic field investigation. The model approximates a neutral molecule to a sphere of isotropic polarisability, (α) with a centralised dipole moment, (μ). The dipole produces an electric field, which has an inverse third power dependant on distance r. This has two effects on the surrounding molecules. Firstly, there will be a change in the induction polarisation. Secondly a change in orientation polarisation. In the case of induction polarisation the dipole field induces instantaneous dipoles in the polarisable solvent molecules, as shown in equation 3.3.1.

$$\mu_{is} = \mu_m \alpha_s r^3 \quad \text{Eqn. 3.3.1.}$$

If the term μ_m represents the dipole moment of the solute molecule then the energy of solvation can be written in terms of the refractive index as shown in equation 3.3.2

$$E_{solv} = -\frac{\mu_M^2}{a_M^3} f(n^2) \quad \text{Eqn. 3.3.2.}$$

Where a_M is the radius of the cavity. The orientation polarisation of the solvent dipoles processes a solvation energy as expressed in equation 3.3.3:

$$E_{solv} = -\frac{\mu_M^2}{2_M^3} [f(D - f(n^2))] \quad \text{Eqn. 3.3.3.}$$

It is therefore necessary to separate the solvent's polarisability and the dipole orientation, the former only being able to respond instantly to the change of the solute's dipole moment and polarisability. The reorientation of the solvent dipoles is much slower, of the order of 10^{-10} s in low viscosity liquids. It is therefore necessary to separate these two solvent responses from change in the solutes electric field and this is done by splitting the solvent polarity functions into two terms, one related only to the electronic polarisability, α , through the refractive index n , i.e. $f(n)$ in the case of absorption, where there is no molecular movement. The dipole orientation is represented in the Onsager term and subsequent equations through the dielectric constant, D , representative of fluorescence i.e. $[f(D)-f(n^2)]$ in the Onsager equation. The validity of this splitting confirmed by observations of solvatochromic shifts and is a result of the Debye and Clausius-Mosotti equations.

The Onsager reaction field model is a somewhat crude model for charting the interaction between dipoles. It includes a series of what can be considered crude approximations. One such approximation involves the cavity radius being taken as completely spherical, which in the case of a real molecule/solvent interaction is too simplistic. Secondly, the idea of point dipoles is unrealistic. More generally, charge distribution is continually fluctuating thus varying from an ideal state. However the simple fact is that with all the assumptions made in the Onsager and subsequent equations, they work. They are the closest approximation for field theory that exist in modern science.

3.4 Onsager examples:

Various research has been carried out on solvent effects and some notable papers in this area include McRae,² Lippert⁶, Abe⁷ and Bakhshiev⁸. However, the non-

trivial aspect of the area is highlighted when one looks at the variety of interactions between a solute and solvent. Notably these include (i) dispersion forces, (ii) dipole-induced – dipole interactions, (iii) dipole-dipole interactions (iv) higher multipole interactions, (v) specific associations such as hydrogen bonding and (vi) solvent cage strains. Fortunately the Onsager model, through various assumptions, has made the treatment of some of the above interactions more complex. Most absorption bands show some solvent dependence and in a few cases this solvent dependence can be quite large. Table 3.4.1. illustrates the results of experimental work done on the solvent dependence of 4 – nitoraniline⁵. The data was analysed using Onsager's⁵ model of dielectrics.

| Solvent | $f(D)$ | $\phi(D)$ | $\nu_{\max} (\text{cm}^{-1})$ | $F(n^2)$ |
|----------------------|--------|-----------|-------------------------------|----------|
| Cyclohexane | .405 | .254 | 30800 | .405 |
| Carbon tetrachloride | .450 | .292 | 30100 | .430 |
| Benzene | .455 | .298 | 29000 | .455 |
| Diethyl ether | .670 | .526 | 28500 | .357 |
| Chloroform | .718 | .595 | 28600 | .421 |
| Acetone | .93 | .865 | 27300 | .360 |
| Ethanol | .94 | .886 | 26800 | .362 |
| Ethylene glycol | .96 | .324 | 26100 | .411 |
| Water | .98 | .969 | 26450 | .341 |
| Dimethylformamide | .96 | .924 | 26300 | .409 |

Table 3.4.1. illustrates the solvent dependence of the absorption maximum for 4 – nitoraniline in various solvents.

This data illustrates that the only property of the solvent, showing a reasonable degree of correlation with the transition energy, is the static dielectric constant D (equation 3.4.1.). This is illustrated by the approximately linear behaviour observed in Figure 3.4.1. From the slope one can calculate parameters such as μ_M if the simple assumptions about a_m are valid.

$$f(D) = \frac{2(D-1)}{(2D+1)} \quad \text{Eqn. 3.4.1.}$$

The $f(D)$ correlation is the most generally applied for polar solute molecules in solvent of varying dielectric constants. For non-polar molecules this is replaced by a $f(n^2)^9$ correlation as shown in equation 3.4.2.

$$f(n^2) = \frac{2(n^2-1)}{(2n^2+1)} \quad \text{Eqn. 3.4.2.}$$

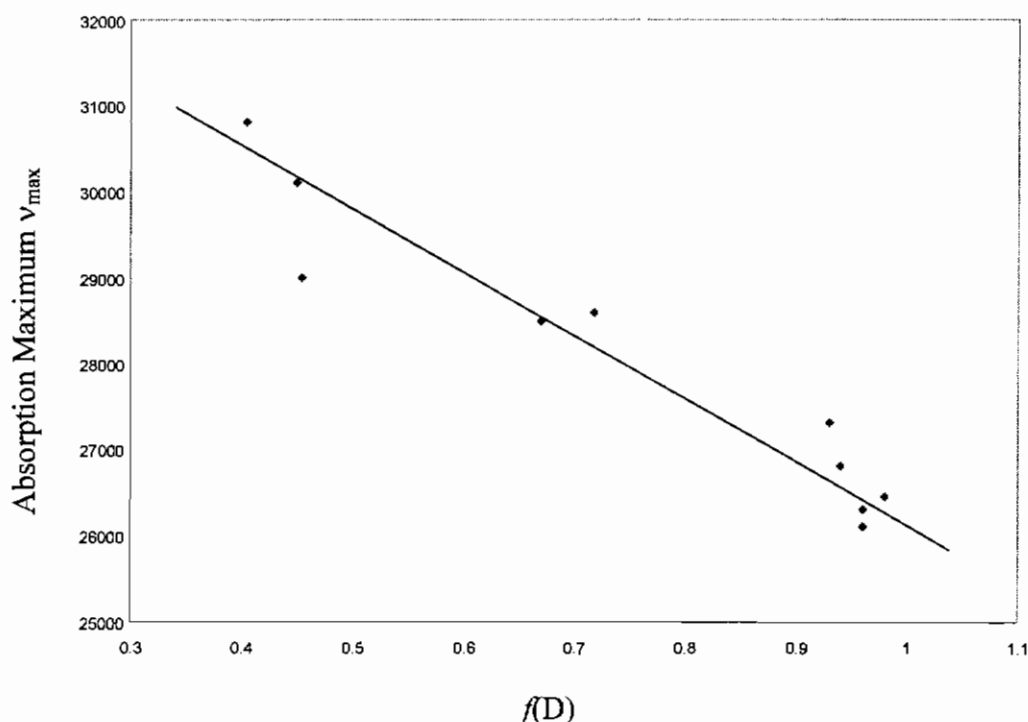


Figure 3.4.1 shows correlation between the absorption maximum and $F(D)$ for 4-nitroaniline.

The example of interest for this work is a non-polar – non-polar interaction. The purpose of looking at various solvents, is to gain an insight into the effects of the vibrational structure of different media on the molecular properties. This effect is not normally considered within the electronic picture of solvatochromism. It is anticipated that variations between solute - solvent interaction will be small, and thus have minimal impact on the photophysical transition energies. Figure 3.4.2. shows the UV-vis spectra for the PmPV trimer in both Benzene and Tetrahydrofuran (THF) illustrates this. As the spectra show there is no substantial difference between the

spectral positioning of the absorbance. Neither is there a substantial difference in the maximum absorbance.

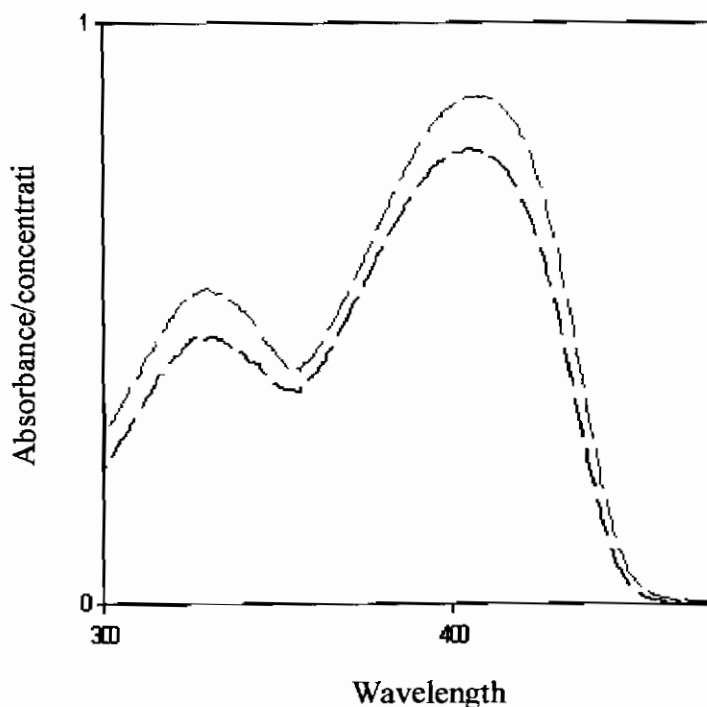


Figure 3.4.2. UV-vis spectra for the PmPV trimer in both Benzene (red) and THF (Black).

The fluorescence spectrum on the other-hand shows differences for the PmPV in various solvents, as shown in Figure 3.4.3. Again, the spectral positioning is relatively independent of solvent, but the relative efficiency is seen to vary significantly from solvent to solvent. Such an effect is not predicted by consideration of the electronic environment of the solute molecule. In this work it will be demonstrated that the dependence of the fluorescent yield on the solvent environment can be correlated to the degree of vibrational coupling, which enhances the nonradiative decay, reducing the radiative yield in accordance with equation 2.9.23

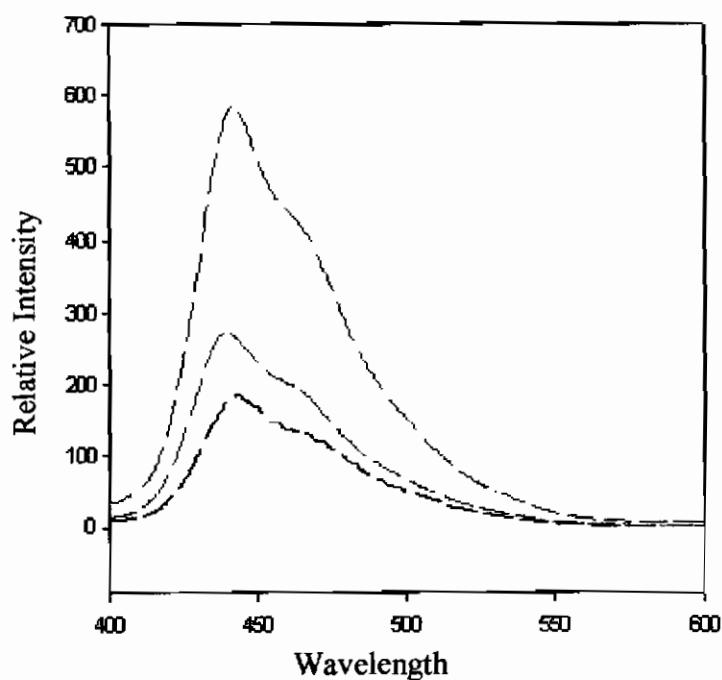


Figure 3.4.3. Fluorescence spectra for the PmPV trimer in various solvents.

3.5 Summary

The choice of solvent is a very important factor when looking at molecules in solution. The variation in polarity and refractive index can have large effects on the optical properties. The solvatochromic shift is discussed in terms of solvation energies and relating the Schrödinger equation to microscopic properties of the medium such as dielectric constant and refractive index. The relationship between that of solvation energies, dipole-dipole interaction and ion-dipole interaction is developed through the Born and Onsager equations. The relationship between the dipole moment and polarisability with dielectric constant and refractive index is explained through the Clausius-Mosotti equation. All these relationships combine to give the Onsager reaction field theory, which is the most used theory in explaining solvent-solute interactions.

In exploring coupling on environment it is important to consider whether the environment is having a significant effect on the molecule and so a solvatochromic study is needed.

Solvent choice is very important to keep the solvatochromic effect to a minimum. It will be shown later that despite the small change in solvatochromic shift, this cannot be used to explain the dramatic change in fluorescence intensity.

The UV-vis and Fluorescence spectra for PmPV are shown. The absorption spectra for the trimer in two different solvents are nearly the same illustrating the fact that the absorption coefficient is the same. This means that the same number of electrons are in the excited state, whereas the fluorescence spectra changes dramatically from solvent to solvent accounting for the decline in fluorescent intensity. Both the environmental effect and explanations surrounding it and the results of the solvatochromic study are discussed in successive chapters.

3.6. References

- 1: Suppan P. and Ghoneim N; Solvatochromism; Royal Society of Chemistry Information Services (1997).
- 2: ^{MC}Rae E.G. *Jour. Phys Chem*, **61**, 562 (1957.).
- 3: Physical Chemistry; Atkins, P. W; 3rd ed; Oxford : Oxford University Press, (1986).
- 4: Onsager L; *Jour. Am. Chem. Soc*; **58**; 1486-1493; (1936).
- 5: Suppan P; *Chem. Phys. Lett. A*; 3125-3133; (1968).
- 6: Lippert E; *Z. Elektrochem*; **61**; 962; (1957).
- 7: Abe T; *Bull. Chem. Soc. Japan*, **38**; 1314; (1965).
- 8: Bakhshiev N.G; *Optics and Spectroscopy*; **10**; 379; (1961).
- 9: West W; Geddes A.L; *Jour. Phys. Chem*; **68**; 837; (1964).
- 10: Birks J.B; *Organic Molecular Photophysics*; Wiley; (1973).

Chapter 4 *Materials*

| | |
|--|----|
| 4.1 Materials and Experimental | 65 |
| 4.1.2 Synthesis | 66 |
| 4.2 Electronic Spectroscopy: | 71 |
| 4.2.1 Introduction: | 71 |
| 4.2.2 Instrumentation: | 72 |
| 4.2.3 Experimental: | 74 |
| 4.3 Fluorescence Spectrometer: | 75 |
| 4.3.1 Introduction: | 75 |
| 4.3.2 Instrumentation: | 76 |
| 4.3.3 Experimental: | 77 |
| 4.4 I.R. Spectroscopy: | 78 |
| 4.4.1. Introduction: | 78 |
| 4.4.2. Instrumentation ¹⁸ : | 78 |
| 4.4.3 Experimental: | 79 |
| 4.5 Raman Spectroscopy: | 81 |
| 4.5.1 Introduction: | 81 |
| 4.5.2. Instrumental: | 82 |
| 4.5.3. Experimental: | 82 |
| 4.7. Summary: | 85 |
| 4.8. References: | 86 |

4.1 Materials and Experimental

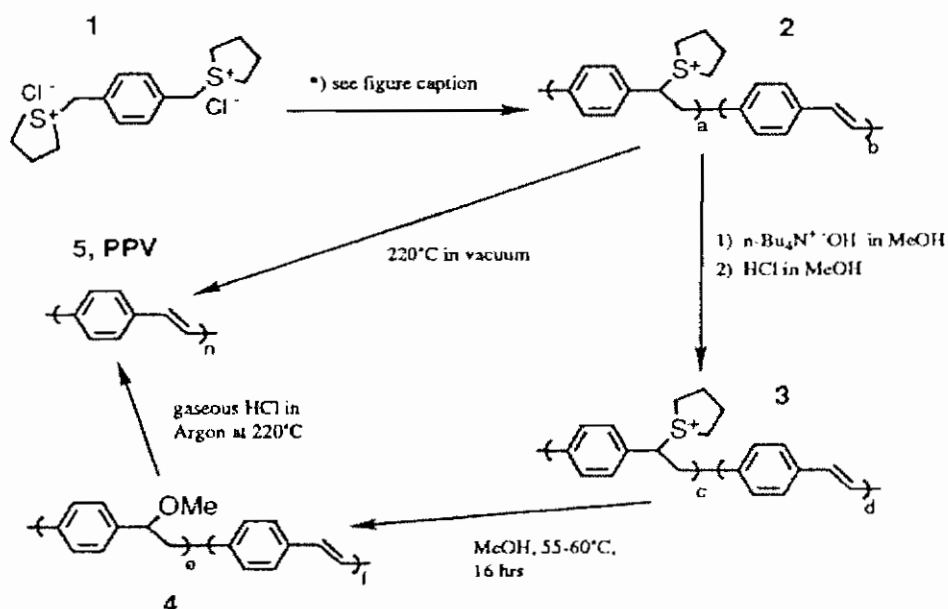
There exists a vast array of π conjugated polymers and small organic molecules, which show potential for application in the development of optoelectronic devices. Figure 2.1.11 shows that for conjugated systems the energy difference between the π and π^* bands can be controlled by variation of the molecular structure. This ability to control the energy difference between π and π^* allows one to tailor the molecular properties and renders this class of materials potentially very useful for both optical and electronic purposes. Polyacetylene was the first conjugated polymer to be studied extensively. Since its discovery¹ in the 1950's, numerous studies have been carried out both in synthesis and opto-electronic characterisation. Its promising electrical properties and the prospect of cheap polymeric devices led to many proposed device applications². It has remained one of the most widely studied materials and while it was originally viewed as a wide band semiconductor³ it became the basis for models of electron-phonon coupled quasiparticles in conjugated polymers, as discussed in section 2.9⁴. While polyacetylene generated great interest because of its electronic properties, interest in application of its optical properties was limited due to its negligible fluorescent yield and photoinstability⁵.

Other conjugated systems studied were the more rigid molecules such as laser dyes⁵. These show good optical properties, and in particular very high fluorescent yields in solution. As dye molecules are small, however, films tend to be of poor optical quality. These dye molecules often crystallise which is unfavourable for the formation of homogeneous films. Focus turned to marrying the mechanical and electronic properties of polymers with the optical properties of smaller dye-like molecules. The observation of electroluminescence in poly-(phenylene-vinylene) or PPV in 1989 led to an explosion of the field of polymeric optoelectronic devices⁶.

Although devices based on organic materials are competitive with those based on inorganics, the efficiency of material in solid is much less than that of isolated molecules. Much is still misunderstood and thus there is much room for optimisation. In this work a PPV based polymer and model oligomer are chosen to explore the influence of environment and conformation on the photophysical properties.

4.1.2 Synthesis

Standard PPV is synthesised through the route shown in Figure 4.1⁷. For device applications, high quality thin films of the precursor **2** can be fabricated. The PPV is generated by either of the two mechanisms indicated, the latter being favoured as the product has higher fluorescence quantum yield⁶. Typically it has a molecular weight of 102 g, with an absorption maximum of ~440 nm (3.6eV). It exhibits a bright fluorescence with maximum at 520 nm (2.25eV) with typical efficiencies of



30%.

Figure 4.1.1, illustrates chemical synthesis route to standard and improved PPV. Step (1), polymerisation with NaOH or $n\text{-Bu}_4\text{N}^+\text{OH}$ in H_2O or MeOH, respectively; Step (2), neutralisation with HCL in H_2O for NaOH or HCL in MeOH for $n\text{-Bu}_4\text{N}^+\text{OH}$, Step (3) dialysis in H_2O for NaOH or in MeOH for $n\text{-Bu}_4\text{N}^+\text{OH}$.

Following the initial breakthroughs in the field⁶, further progress was hindered by the insolubility of the final product. No systematic route towards improvement in luminescence efficiency was obvious, and backbone modification to yield tunability of the optical properties was not possible. The former was of particular interest for device efficiency, whereas the latter was desirable for applications to multicolour display technologies.

The easiest way to achieve solubility in PPV based conjugated polymers is to utilise long flexible side chain groups on the phenyl groups. This is frequently achieved by disubstitution of dialkoxy groups at opposite sides of the phenyl ring. All positions on the ring are sp^2 hybridised and substitution of the hydrogen by an alkoxy group should maintain the π conjugated electronic properties of the backbone, while rendering the polymer soluble. Introduction of these bulky sidegroups can, however, introduce torsion into the backbone, representing an effective reduction in backbone conjugation and a reduction of the optical bandgap⁴. Irregular or random substitution can add to such steric effects. These effects are undesirable when they introduce random variations in effective conjugation and thus optical properties, but in the case, for example, of poly alkyl thiophenes have been employed to regulate backbone conformation⁸.

Alkyl or alkoxy groups can be employed to improve solubility but can also influence the optical properties. Introduction of electron withdrawing or donating groups is a more precise route towards tuning the optical properties^{9,10}. Commonly employed examples of such groups in PPV are MEH_PPV and cyano groups⁶ through which the absorption can be tuned from 400nm – 600nm and the emission from 400nm – 600nm.

Another technique employed to achieve variation in electronic structure of the backbone¹¹ is the introduction of *meta* or *ortho* linkages. This introduces an effective reduction in the conjugation of the molecule, with the result of a shift to the blue region of the spectrum. It may also be expected that the geometry of the backbone reduces the distances over which vibrations or phonons can propagate. Consequently, relaxation processes are less likely to be non-radiative and the luminescence yield should be enhanced. The break in conjugation can also cause a change in the conformation of the molecule in a solvent. This change can cause the molecule either to coil more tightly or fan out in the solvent¹².

Tunability of the electronic and optical properties still remains an extraordinary challenge for material science⁶. When investigating materials for semiconductor devices, there exists certain fundamental considerations, which must be taken account of, such as band gap, energy of valence and conduction bands etc. Unfortunately, it is not yet possible to predict whether a polymer will have the desired properties after substitution. Several reasons are responsible for this. Firstly it is rarely

possible to vary only one property of the material. Modifying structure most often leads to conformational changes. Secondly, the number of possible permutations makes it difficult to generalise rules for molecules. Thirdly is the fact that synthesising such compounds is far from simple, mostly generating low yields.

Sidechain and backbone alteration have been extensively studied¹³. One of the driving forces behind choice of material for this study was high efficiency in the blue region of the spectrum. The discovery of poly(m-phenylenevinylene-co-2,5-dioctyloxy-p-phenylene) or PmPV in Figure 4.1.2. shows promise in this respect¹⁴. This is the material utilised in this project and the synthesis route is illustrated in Figure 4.1.3.

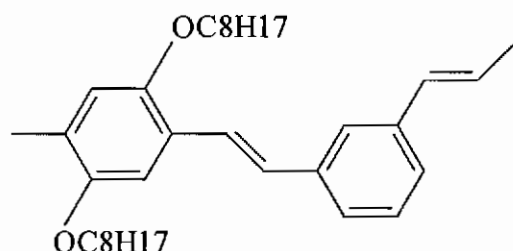


Figure 4.1.2 illustrates the repeating unit of PmPV-co-DoctPV.

In addition to the aforementioned properties, PmPV is also currently topical due to its usage as a host material for single and multiwall carbon nanotubes.¹²

In preparing PmPV, the alkoxy side groups are introduced by alkylation of hydroquinone using methods of Johnson and Rose.¹⁵ The resulting 1,4-di-n-octyloxybenzene is then reacted with paraformaldehyde and potassium bromide in acetic acid and sulphuric acid to give 1,4-bis (2,5-dialkoxy) benzylbromide, which is then reacted with triphenylphosphine in dry toluene to give the phosphonium salt¹⁸. This salt can then be used to in a Wittig reaction in either dry toluene or dry DMF to give either the polymers WTOLPmPV or DMFPmPV (average molecular weight, 14900 and ~ 500,000 (g/mol) respectively)

The study of polymers with very large numbers of repeating units can be very complicated as the intrinsic electronic and photophysical properties can be masked by morphological and conformational effects. The fundamental photophysics can often be elucidated through a study of model compounds. In particular, it is of interest to establish whether in terms of the photophysics the polymeric systems behave as extended 1-D semiconductors or more like smaller dye molecules as discussed in

Chapter 2. These model compounds are usually small and easier to study, thereby making it easier to rationalise photophysical processes in the compound. The main model compound utilised in this project is 2,5-dioctoxy-p-distyrylbenzene. This compound is synthesised in similar fashion to that of the polymer PmPV, although there are slight changes¹² in the final stages, involving reaction conditions shown in Figure 4.1.4. Throughout the remainder of this text, this material will be referred to as the trimer.

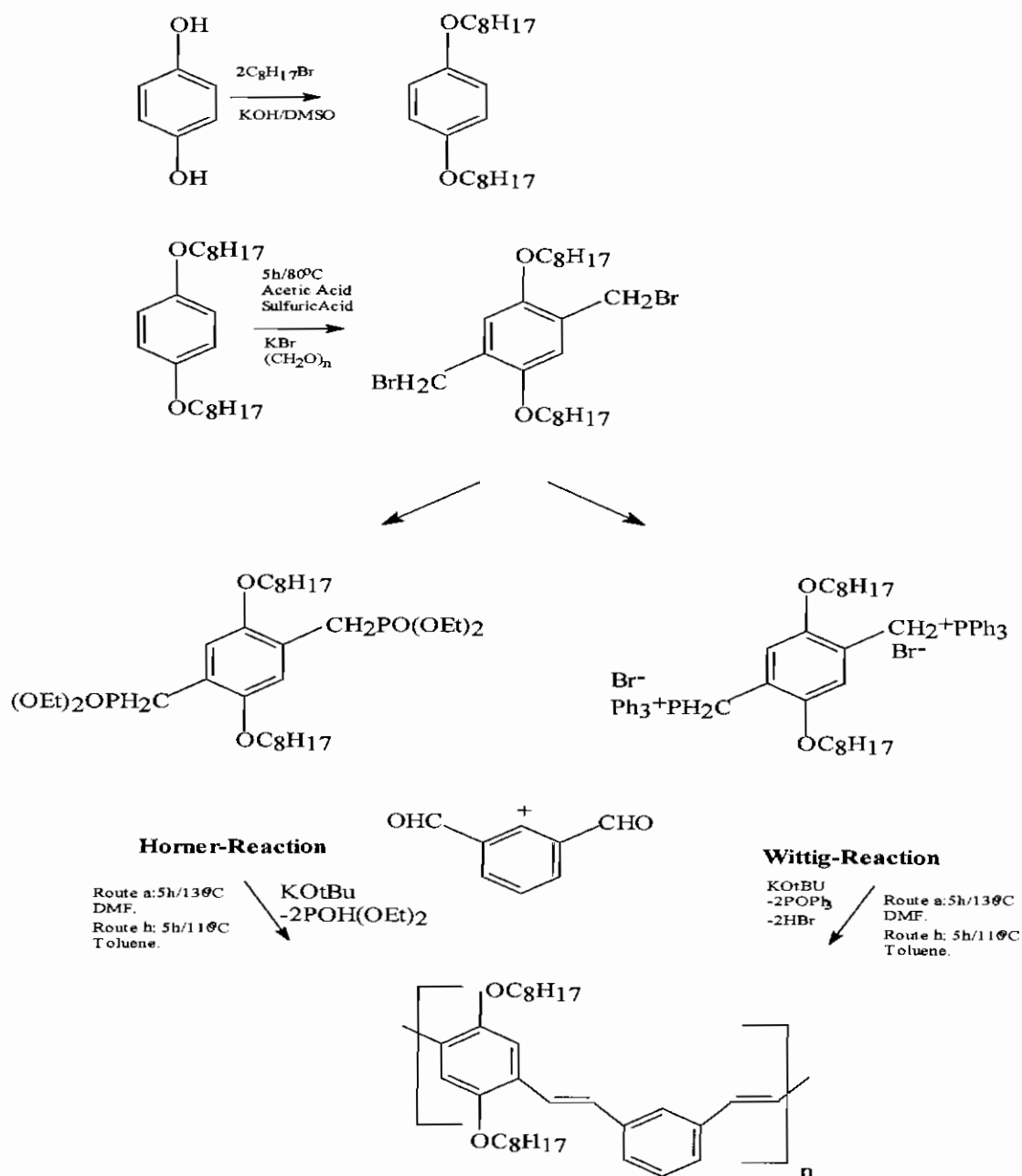


Figure 4.1.3. illustrate the reaction scheme for the synthesis for the polymer PmPV.

The Williamson reaction of hydroquinone (compound I) with two equivalents of octyl bromide yields 1,4-dioctoxybenzene (II). The Bromomethylation of (compound II) using paraformaldehyde and potassium bromide yields 1,4-bis(bromomethyl)-2,5-dioctoxybenzene (III), while the reaction of (III) with two equivalents of triphenylphosphine gives the bis-phosphonium salt (IV) (Whittig intermediate), (III) can also give the bis-phosphonate ester (V) (Horner – Wadsworth - Emmons intermediate). Through the Arbuzov reaction with triethyl phosphite, reaction of either (IV), (V) with benzaldehyde in the presence of potassium tert-butoxide give 2,5-dioctoxy-p-distyrylbenzene (VI).

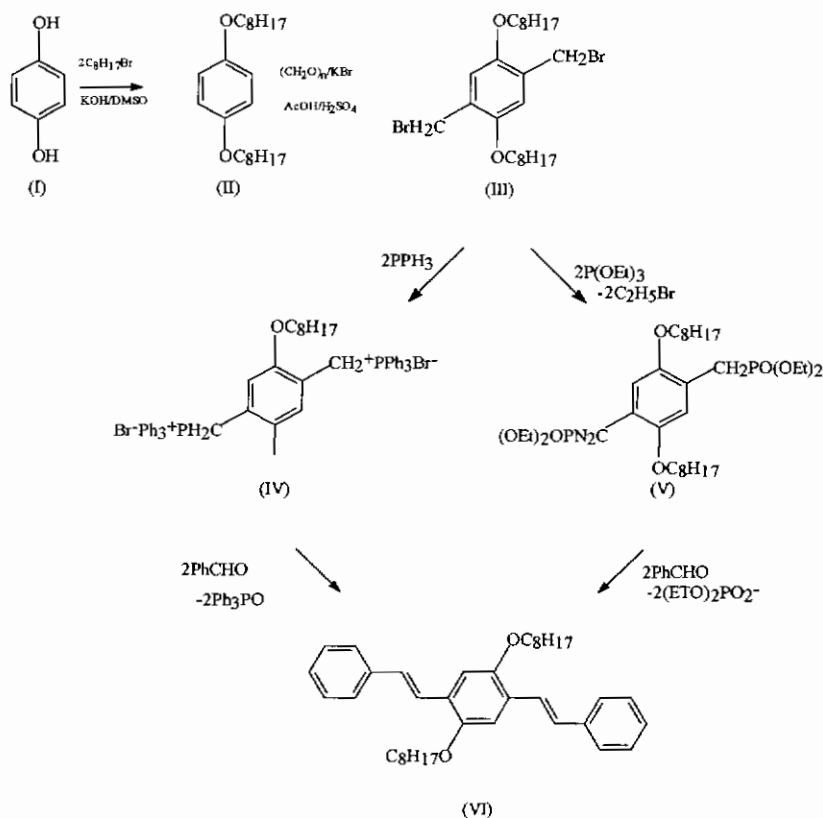


Figure 4.1.4. illustrates the synthetic scheme for the preparation for 2,5-dioctoxy-p-distyrylbenzene.

4.2 Electronic Spectroscopy:

4.2.1 Introduction:

As outlined in Chapter 2, UV-vis spectroscopy is the measurement of the wavelength and intensity of absorption of near-ultraviolet and visible light by a

sample. Ultraviolet and visible light possesses enough energy to promote outer electrons to higher energy levels. Transmission is measured as a ratio of intensity of sample to intensity of reference beams. The UV-vis spectra have broad features that are of limited use for sample identification but are very useful for quantitative measurements of $\pi - \pi^*$ transitions. The concentration of an analyte in solution can be determined by measuring the absorbance at some wavelength and applying the Beer-Lambert Law, equation 2.1.5. An alternative format of the Beer-Lambert law, which is usually employed in spectroscopy states:

$$-\log_{10} T = A = \epsilon lc \quad \text{Eqn. 4.2.1.}$$

where A is absorbance

ϵ is the molar absorptivity with units of $\text{l mol}^{-1} \text{cm}^{-1}$

l is the path length of the sample - that is, the path length of the cuvette in which the sample is contained.

c is the concentration of the compound in solution, expressed in mol l^{-1}

The above form of the equation applies to solutions in which the molecules are noninteracting and effectively isolated. In many systems, interactions leading for example to dimerisation, aggregation, formation of excimers or exciplexes can cause a deviation from this ideal behaviour. Monitoring the absorbance as a function of concentration is therefore a valuable probe of these interactions.

4.2.2 Instrumentation:

In UV-vis absorption the light source is usually a hydrogen or deuterium lamp. The wavelengths of these broadband light sources are selected with a wavelength separator such as a prism or grating monochromator. Spectra are obtained by scanning the wavelength separator and quantitative measurements can be made from a spectrum or at a single wavelength. A typical set-up for a UV-vis spectrometer is shown in Figure 4.2.1¹⁶.

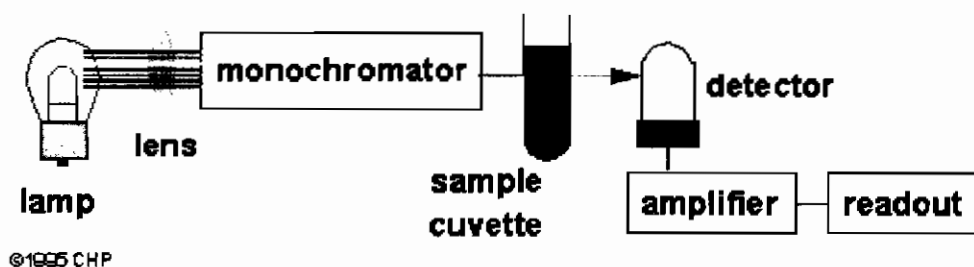


Figure 4.2.1 illustrates the set-up for UV-vis spectrometer.

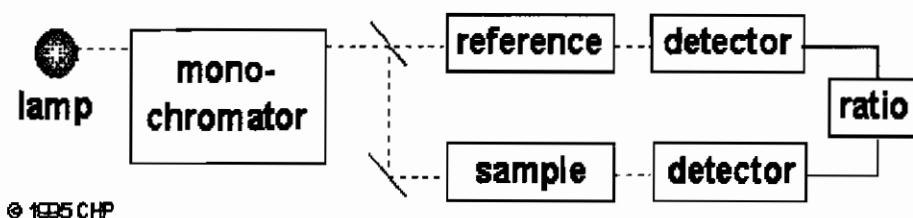


Figure 4.2.2. illustrates the schematic of double-beam spectrometer.

The UV-vis spectrometer used in gathering the spectra was a Shimadzu UV-2101PC Absorption Spectrophotometer¹⁶.

The Shimadzu UV-2101PC is a double beam as shown in Figure 4.2.2¹⁶, direct ratio photometric measuring system using a dynode feedback method. This type of spectrometer utilises equation 2.1.6, in determining a direct ratio of light in to light out. In normal operation, absorbance spectra are recorded in terms of equation 4.2.1. It has a photometric range of -4 to ~5 in Absorbance, 0 to ~999.9% in Transmittance. It employs a 50W halogen lamp and a Deuterium lamp. Spectra are dispersed by a Czerny-Turner monochromator with a high performance blazed holographic grating, and detected by an R-928 photomultiplier. The instrument has a range of 190nm to 900nm.

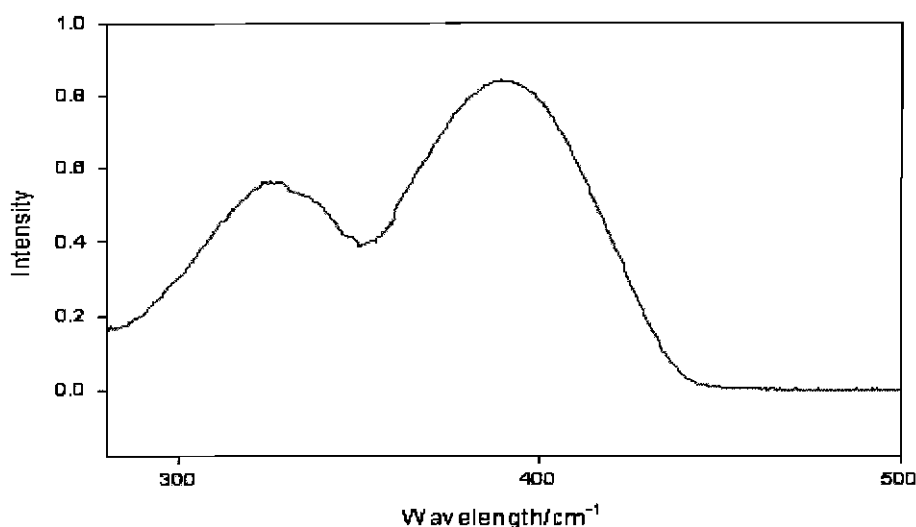


Figure 4.2.3. Typical UV-vis spectra for the trimer.

4.2.3 Experimental:

The UV-vis spectra for both the trimer and WTOLPmPV were taken using quartz cuvettes with the material dissolved in a solvent near to infinite dilution. (10^{-6} mol) Figure 4.2.3. illustrates UV-vis absorption spectra for the trimer in toluene solution. There are absorption maxima at 380nm (3.25eV) and 330nm (3.8eV). The broadness of the spectrum highlights the unresolved nature of the spectra showing no fine structure and is indicative of the superposition of many electronic and vibronic states as described in section 2.1. This suggests that as the conjugation increases the distance between the π and π^* decreases and the spectra becomes unresolved as the individual states broaden into a band. Figure 4.2.4 illustrates, for comparison, the spectrum of WTOLPmPV in toluene. It is similar in character but the maximum is shifted to \sim 405nm (3.2eV). The positioning of the long wavelength absorption with respect to that of the trimer is indicative of a longer effective conjugation length in the polymer. The spectrum is, however, slightly blue shifted in comparison with similar para-phenylenevinylene co-polymers where the maxima occurs at 440nm (2.8eV). This is a direct indication of the effect of the *meta* linkage¹⁷. The shift in comparison to the trimer is small however, indicating that the photo excitation is relatively localised, conjugation does not extend over the polymer chain. Thus the polymer may be better represented by a molecular model.

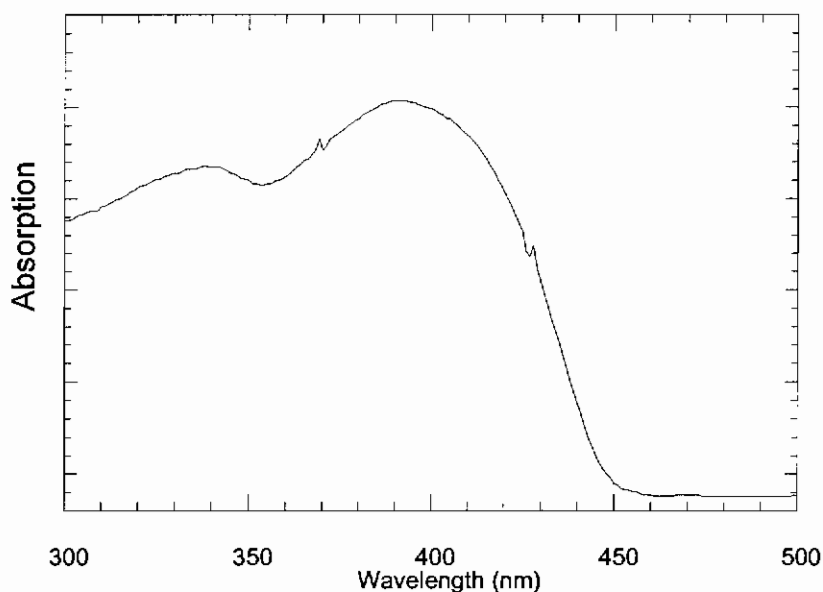


Figure 4.2.4: Absorption spectrum of WTOLPmPV in toluene

4.3 Fluorescence Spectrometer:

4.3.1 Introduction:

Fluorescence spectroscopy, as outlined in section 2.4, monitors the radiative relaxation of excited states. The spectrum is Stokes shifted and a mirror image of the UV-vis spectrum. Further probe of the $\pi - \pi^*$ transition and quantum yield is a measure of competition between radiative and non-radiative processes. Quantitative measurements are difficult but, between two samples, which are measured under the same experimental conditions semi-quantitative comparisons can be made. Thus assessment of relative efficiency of differing compounds or compounds in differing environments is possible.

4.3.2 Instrumentation:

The fluorimeter utilised in this project is the Perkin Elmer LS50B Luminescence Spectrometer in Figure 4.3.1¹⁷. The LS50B is a computer controlled ratioing luminescence spectrometer with the capability of measuring fluorescence or phosphorescence, as well as a range of other processes including electro-, chemi- and bio-luminescence. Excitation is provided by a pulsed Xenon discharge lamp, of pulse width at half peak height of <10msec and pulse power 20kW. The source is monochromated using a Monk- Gillieson type monochromator and can be scanned over the range 200-800nm. The luminescence is passed through a similar monochromator, which can be scanned over the range 200-900nm, and is detected using a gated photomultiplier. Synchronous scanning is available with constant wavelength or frequency difference. Sensitivity is specified as a signal to noise ratio of 500:1 rms using the Raman band of water with the excitation at 350nm and 10nm excitation and emission bandpass. The excitation slits (2.5-15nm) and the emission slits (2.5-20nm) can be varied and selected in 0.1nm increments. In the phosphorescence mode, delay and gate times can be varied with a minimum total period of 13.0msec.

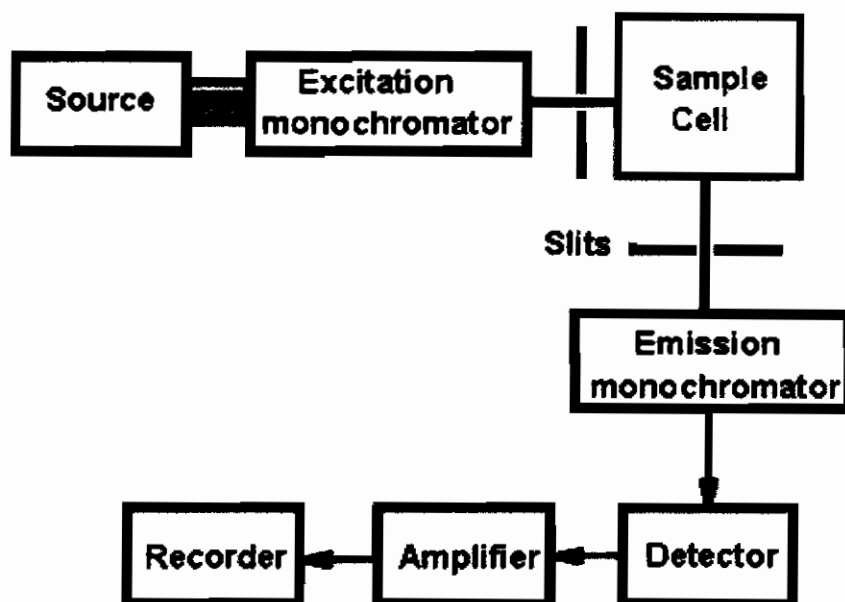


Figure 4.3.1 illustrates the schematic a typical fluorimeter¹⁹.

4.3.3 Experimental:

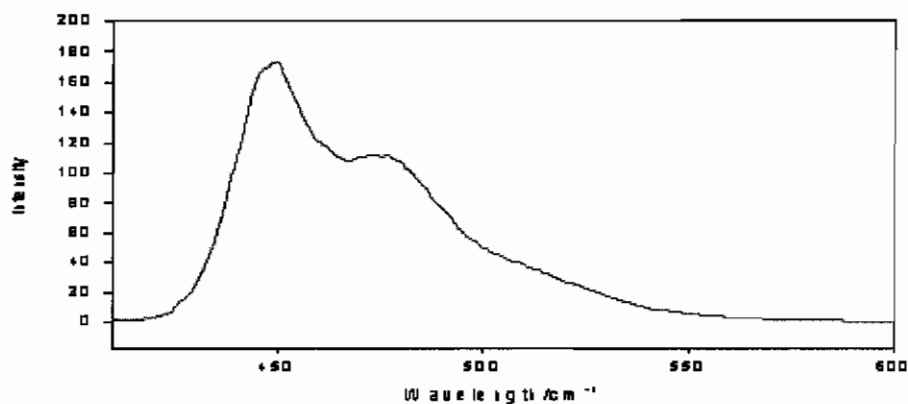


Figure 4.3.2. Typical Fluorescence spectrum for the trimer.

The spectrum shows two reasonably resolved features at 440nm (2.8eV) and 485nm (2.54eV) and a broader shoulder at 510nm (2.42eV). It is a typical vibronic progression of molecular species with a separation of ~ 0.2 eV. The profile is independent of excitation wavelength over the range of the absorption spectrum. This indicates the two bands in the absorption spectrum represent transitions to the first and second excited singlet states. The single emission profile is compliance with Kasha's rule (section 2.2).

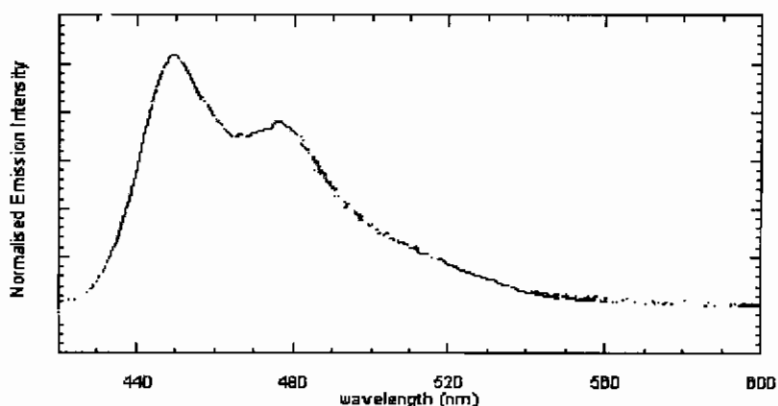


Figure 4.3.3 Typical fluorescence spectrum for the WTOLPmPV polymer.

The fluorescence spectrum of WTOLPmPV is illustrated in Figure 4.3.3. Similarly to the case of the absorption spectra, it is essentially the same in character to that of the trimer. It is red shifted, with maximum at 450nm (2.74eV) which is indicative of a greater degree of conjugation, but is not as red as typical para-phenylenevinylene copolymers, which have maxima at ~ 475nm (2.6eV), as a result of the presence of the *meta* linkage.

4.4 I.R. Spectroscopy:

4.4.1. Introduction:

As outlined in section 2.5, vibrational spectroscopy provides useful information on the structure of molecules. The molecules will absorb radiation if the radiation is the same as the natural frequency of the molecule. The frequencies depend on a variety of factors, one such being the strength of the bond between the atoms and the molecular weight of the atoms as described in equation 2.6.1. I.R. absorption is an electric dipole transition and so is governed by the same rules as UV-vis spectroscopy. Frequently strong I.R. modes are asymmetric in character. Raman on the other is a scattering process, which depends on changes in molecular polarisability, as the molecule vibrates. Such changes are often strongest for symmetric modes. I.R. and Raman are often mutually exclusive and thus are complimentary techniques. Due to the difference in selection rules, in conjugated materials I.R. is predominantly a probe of the sidechains, while Raman principally probes the backbone.

4.4.2. Instrumentation¹⁸:

The Mattson Infinity spectrometer is a single-beam, Michelson interferometer based, Fourier transform I.R. spectrometer. It has an operating range in the mid and far infrared, covering 200cm⁻¹ to 5000cm⁻¹ with a resolution of 0.5cm⁻¹. The system is upgradable to a multirange system capable of an extended range from 50cm⁻¹ to 25000cm⁻¹ with a resolution as good as 0.125cm⁻¹ in a dual beam geometry. All optics are contained in a sealed and desiccated chamber which protects from chemical and

atmospheric contamination. All samples were prepared by mixing powder with KBr which was fused to a disc.

4.3.3 Experimental:

Figure 4.3.1. shows a typical spectrum for the trimer. The strong bands at 3500 cm^{-1} and 2900 cm^{-1} are indicative of C-H and O-C-H out of plane stretching respectively. Around 1200 cm^{-1} C-O vibrations can be seen whereas modes in the region between 691 cm^{-1} and 960 cm^{-1} have been assigned to different C-H in plane stretching modes. In addition to these modes associated with the sidechain, those in the region between 800 cm^{-1} to 840 cm^{-1} can be associated with a 1,4, di-substituted phenyl ring. The peaks at approximately 1500 cm^{-1} also derive from the phenyl ring.

Figure 4.3.2. illustrates the I.R. spectrum for the WTOLPmPV polymer. It is similar to that of the trimer. However, the relative intensity of some of the peaks is greater than those in the, trimer especially those around 1600 cm^{-1} . These peaks are associated with Phenyl and Phenylene-vinylene stretches and an increased relative intensity is indicative of a higher degree of conjugation in the polymer, in agreement with the results of UV-vis and fluorescence spectroscopy.

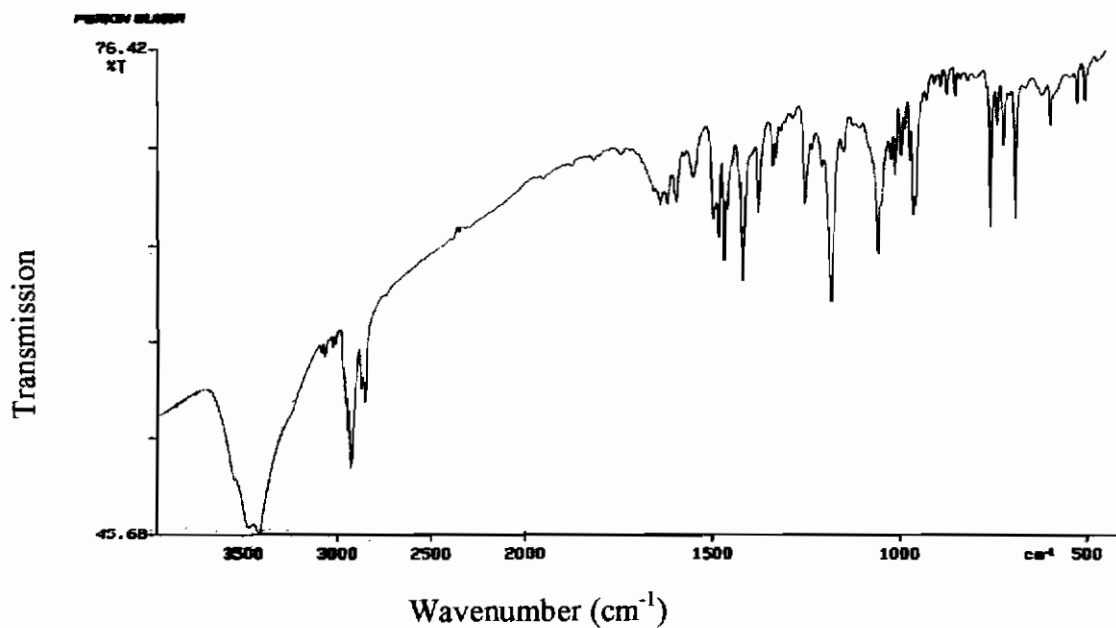


Figure 4.3.1. Typical I.R. Transmission spectrum for the PmPV trimer.

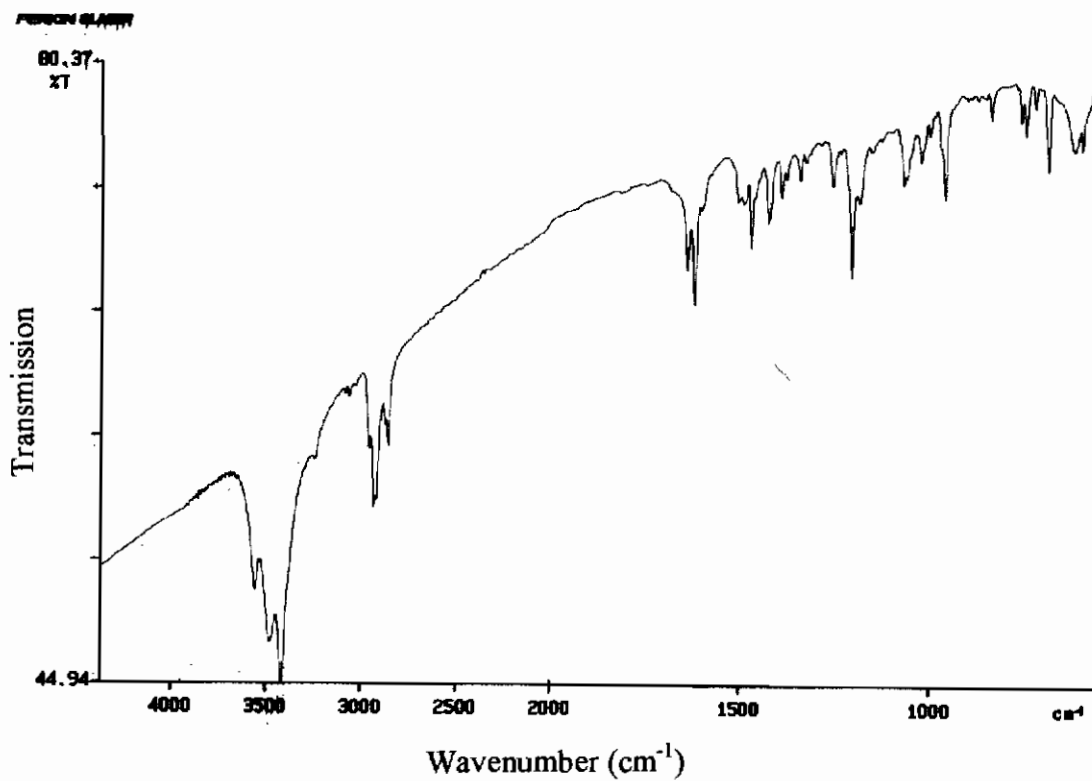


Figure 4.3.2. Typical I.R. transmission spectrum for PmPV polymer.

4.5 Raman Spectroscopy:

4.5.1 Introduction:

In the past Infra - red has been used as the sole tool for routine fingerprinting of materials. However recent development in CCD technology and holographic filters have brought Raman into the realm of the everyday laboratory. Raman microscopes enable rapid measurements of vibrational spectra with minimal sample preparation.

The ease of measurement makes it feasible for use as an in-situ probe of a variety of processes. Vibrational spectroscopy is a measure of the vibronic states of the material and it is these states of a material which are involved in radiationless transitions. Radiationless transitions compete with fluorescence and to reduce them it is important to understand the vibronic structure. In subsequent chapters Raman will be employed as a semi-qualitative measure of radiationless transition rates. In this section it is used as a spectroscopic tool for comparison to I.R.

4.5.2. Instrumental:

The Raman spectrometer utilised in this project is a Instruments S.A. Labram 1B¹⁸. The Labram system is a confocal Raman imaging microscope system. Both Helium-Neon (632.8nm, 11mW) and Argon ion (514.5nm, 50mW) are available as sources. Both are polarised, enabling measurement of depolarisation ratios and studies of orientation in materials.

The light is imaged onto a diffraction limited spot (typically 1 micron) via the objective of an Olympus BX40 microscope. The scattered light is collected by the objective in a confocal geometry, and is dispersed onto an air cooled CCD array by one of two interchangeable gratings, 1800 lines/mm or 600lines/nm, allowing the range from 150 cm⁻¹ to 4000 cm⁻¹ to be covered in a single image, or with greater resolution in a combination of images. With the former, a spectral resolution of 1cm⁻¹ per pixel is achievable.

The confocal, microscopic system allows measurement of powdered samples with no further sample preparation, direct measurement of liquids and solutions, as well as thin films.

4.5.3. Experimental:

Figure 4.5.3.1 illustrates a typical Raman spectrum for the PmPV trimer in powder form. The Raman in conjunction with the I.R. are invaluable in determining the make up of the molecule. In complementing each other they give enormous information on the vibrational make up of the molecule, from which, types of bonds and their strengths can be determined. The modes associated with phenyl/vinyl stretches in the region of 1600cm^{-1} dominate the spectrum. The spectra shows an unresolved feature at 1600cm^{-1} . This unresolved region is made up of several peaks dependant on the coupling to the vinylene bond on the backbone (i.e. cis/trans). These distortions in the vinylene through changes in isomerisation will have a direct effect on the relative intensities of these peaks. This is discussed in more detail in chapter 7. The region around 1100cm^{-1} shows several small bands, centred around 1140cm^{-1} . These features are assigned to external cycle vibrations of the chain, which to a large extent are determined by the length of the oligomer.

Figure 4.5.3.2 illustrates a typical Raman spectra for the polymer WTOLPmPV, similar bands can be highlighted as in the trimer. The region around 1600cm^{-1} is similar in complexity and, as will be shown in subsequent chapters, is a fingerprint of the backbone conformation. The similarity of the structures, both in infrared and Raman affirm that the trimer should act as a good model system for the polymer.

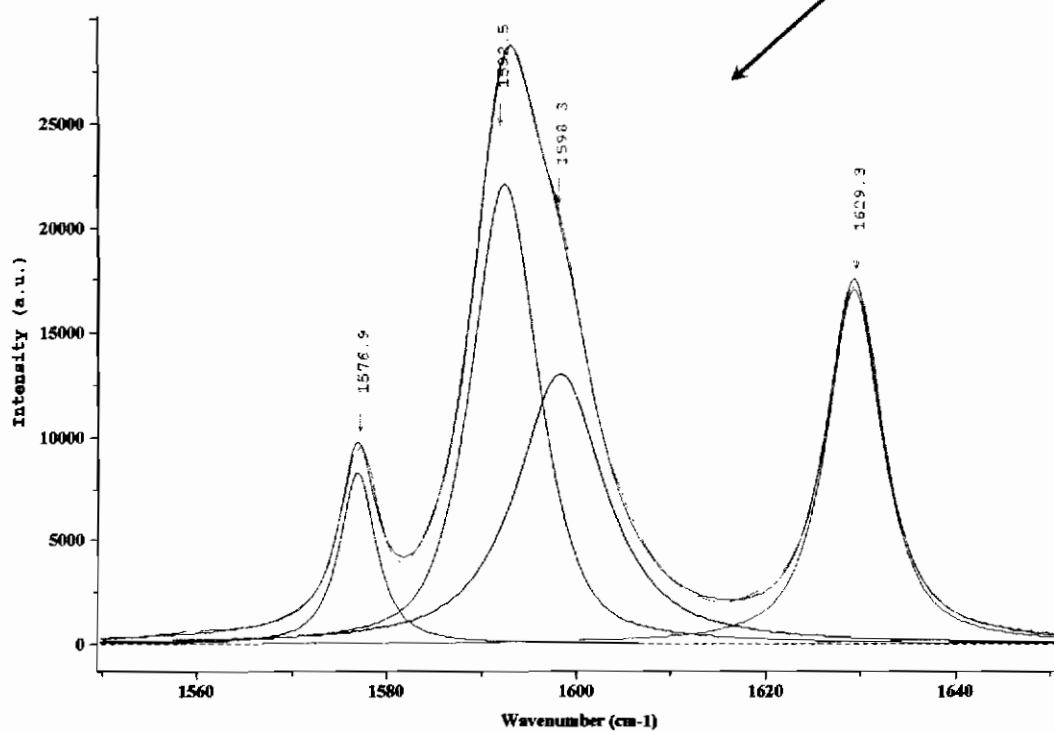
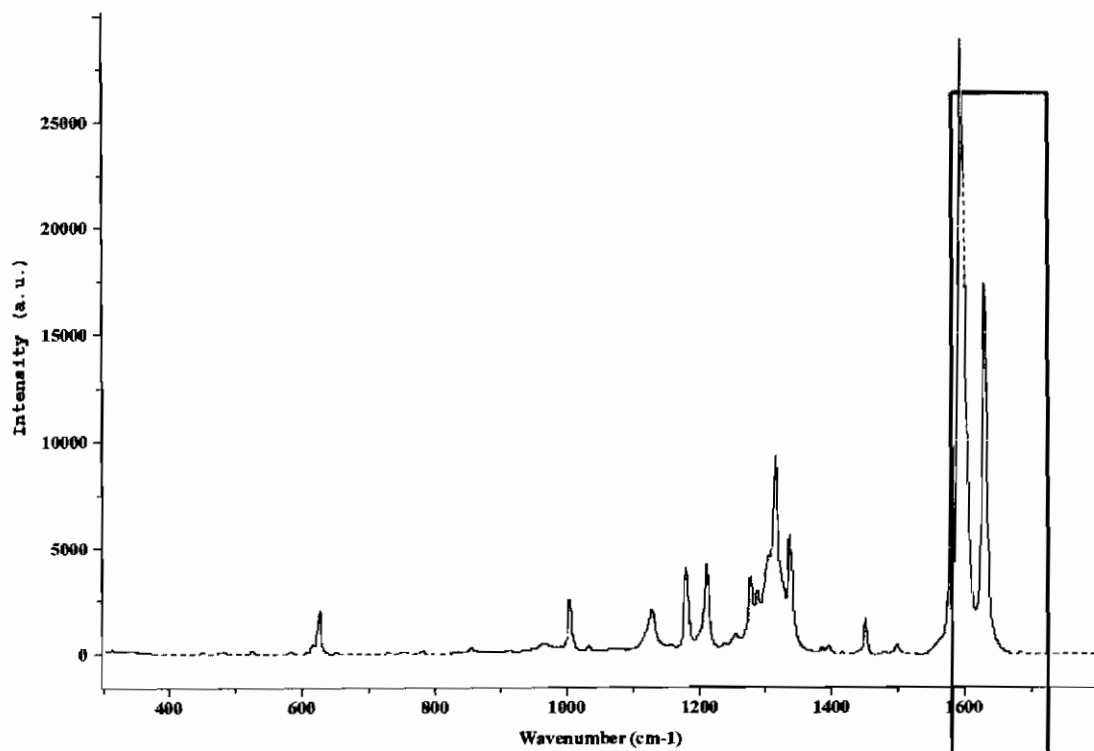


Figure 4.5.3.1 Typical Raman spectra for PmPV trimer showing inset of area of interest 1600cm⁻¹

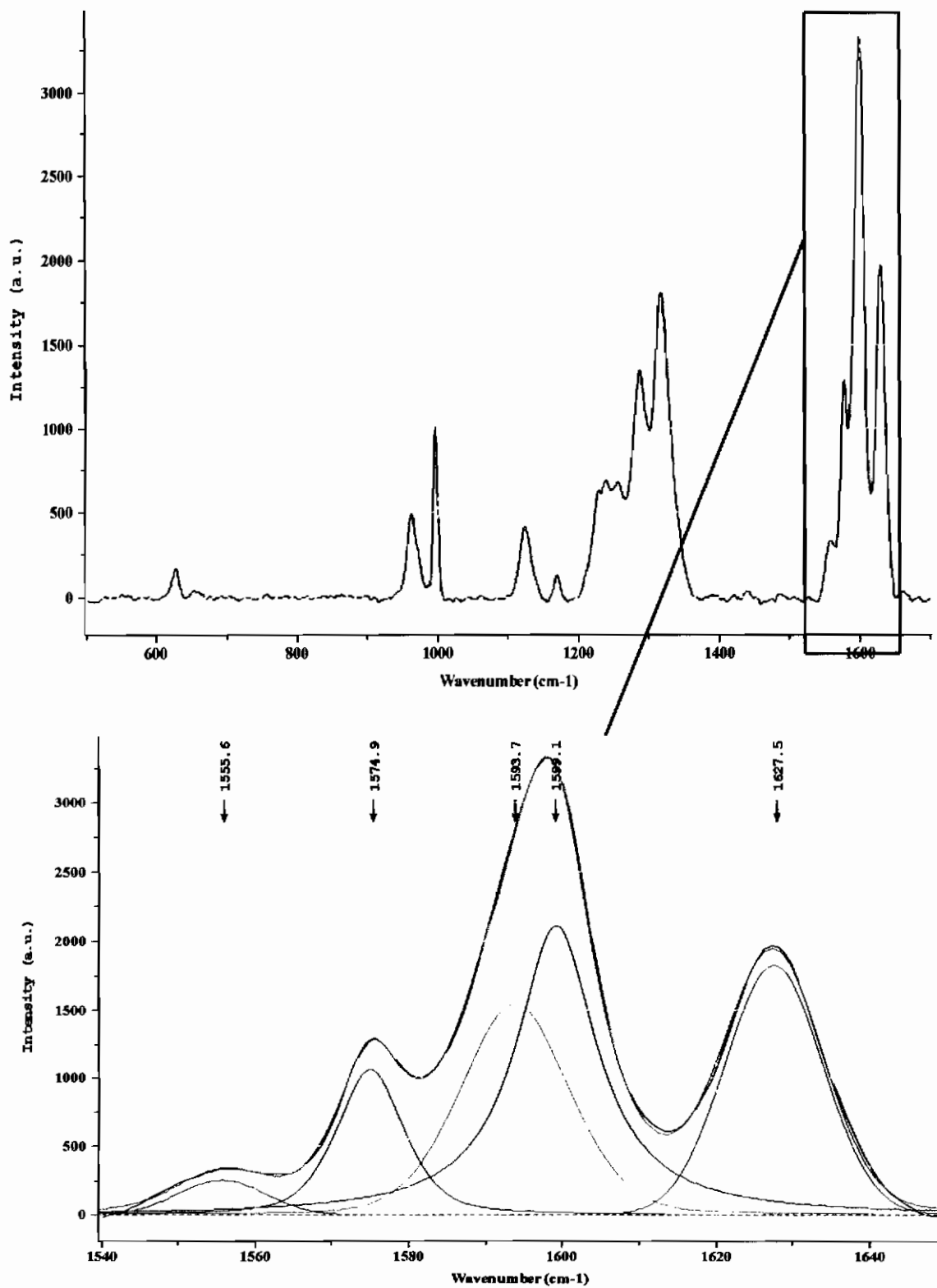


Figure 4.5.3.2 Raman spectrum for WTOLPmPV, showing inset of area of interest 1600cm^{-1}

4.7. Summary:

The materials which are being used in this project have been discussed and the difficulties associated with measuring them spectroscopically have been introduced relating to synthesis, solubility and low fluorescence yields in the transition from solution to solid phase. The complexity of the polymeric materials forces one to look at so-called *model* compounds. These model compounds allow fundamental spectroscopy to be performed. The spectroscopic investigation allows the establishment of the fundamental photophysics and electronic nature of simpler, yet highly similar compounds. The simplicity of these compounds allows for the characterisation of behaviour, which can be applied to the more complex compound.

The model compound, the trimer, absorbs in the blue region of the UV-vis spectrum and exhibits a small Stokes shift. As expected in a more conjugated system, the Polymer on the other-hand exhibits shifts in both the UV-vis and Fluorescence, the shifts seen are not as large as other PPV derivatives and this would be an expected result due to the presence of the meta linkage. This meta linkage causes disruption to the conjugation of the molecule, something, which is not seen in other PPV systems.

Vibrational spectroscopy also provides a vast quantity of information as has been shown. The two types of vibrational spectroscopy, I.R. and Raman compliment each other and give information on the backbone and sidechains. The I.R. is predominantly used for the elution of the modes associated with the sidechain, whereas Raman will provide in-depth information on the backbone of the molecule. In particular, backbone modes involving para-conjugation will dominate the Raman spectrum.

As the project deals with the optimisation of materials fluorescence, vibrational information is of vital importance. The vibrational information can give vital clues to the origin of non-radiative process, which will be discussed in detail in the next chapter.

4.8. References:

- 1: Natta G. Mazzanti G. Corrandi P. Atti. AccAd. Naz. Lincedi, *Cl. Sci. Fis. Mat. Nat. Rend.* **25**, 3, (1958).
- 2: Pope M; *Electronic Processes in Organic Crystals*, Clarendon Press, Oxford Universities Press 1982.
- 3: Hatano M. Kambara S. *Jour. Poly. Sci.* **51**, 26, (1961).
- 4: McGehee M.D; Miller E.K; Moses D; Heeger A.J; *Twenty Years of Conducting Polymers: From Fundamental Science to Applications.*
- 5: Schäfer F.P. *Dye Lasers*, Thied and Enlarged and Revised Edition
- 6: Greenham N.C., Moratti S.C., Bradley D.D.C., Friend R.H. and Holmes A.B. *Nature*, **365**, (1993).
- 7: Lange F; *et al* Structural influences on luminescence properties of substituted PPP'a and model compounds.
- 8: Goutermann M. *The Porphyrins, Vol II*, Academic press 1978.
- 9: Sheridan A.K., Samuel I.D.W., Bleyer A., Bradley D.D.C., *Syn. Metals*, **101**, 259-260, (1999).
- 10: Lange F., Holnholz D., Leuze M., Ryu H., Hohloch M., Freudenmann R., Hanack M., *Syn Metals*, **101**, 652-653, (1999).
- 11: Vaschetto M.E., Springberg M., *Thermochem, Jour. of Molecular Structure*, **160**, 141-157, (1999).
- 12: Dalton A; PhD Thesis Trinity College 2000.
- 13: Maier S. PhD Thesis, Trinity College Dublin 2000.
- 14: Burns P.L., Kraft A., Baigent D.R., Bradley D.D.C., Brown A.R., Friend R.H., *Jour. Amer. Chem. Soc.* **115**. 10117, (1993).
- 15: Johnstone R.A.W., Rose M.E., *Tetrahedron*, **35** , 2169, (1979).
- 16: <http://www.scimedia.com/chem-ed/spec/Uv-Vis/Uv-Vis.htm> <Accessed Sep 01>
- 17: Miller E.K; Beabec C.J; Neugebauer H; Heeger A; Saricifti N.S; *Chem. Phys. Lett.*, **335**, (2001)
- 18: http://www.focas.dit.ie/core/core_steadystate.html <Accessed Sep 01>
- 19: <http://www.scimedia.com/chem-ed/spec/molec/mol-fluo.htm> <Accessed Sep 01>
- 20: LUPO Project Report, Esprit Basic Research Proj. No.20038:LUPO(1996).

Chapter 5 *Lifetime Measurements*

| | |
|--|-----|
| <i>5.0. Molecular Environment-Vibronic Coupling:</i> | 88 |
| <i>5.1. Introduction:</i> | 88 |
| <i>5.2. Solvatochromism:</i> | 91 |
| <i>5.3. Vibronic coupling:</i> | 93 |
| <i>5.4. Lifetime measurements:</i> | 95 |
| <i>5.5. Instrumental:</i> | 96 |
| <i>5.5 Experimental:</i> | 98 |
| <i>5.6. Summary:</i> | 102 |
| <i>5.7. References:</i> | 103 |

5.0. Molecular Environment-Vibronic Coupling:

5.1. Introduction:

In trying to increase the fluorescence quantum yield of a material, it is important to understand the behaviour of the molecules involved as defined through the Einstein coefficients in Chapter 2, whereby radiative and non-radiative processes are facilitated through competing routes. Radiative processes are determined by the electronic structure as well as transition selection rules. These radiative processes compete with non-radiative processes such as internal conversion and intersystem crossing and the relative contributions determine the luminescence quantum efficiency of the system. Intersystem crossing can, to a large extent, be dictated by the molecular structure and the spin orbit coupling¹. Both intersystem crossing and internal conversion require coupling to the vibronic states of the molecule. The energy must ultimately, however, be coupled to the environment. It may reasonably be suggested that the vibrational structure of the environment would have a significant effect on the rate of coupling between the molecule and the environment and thus would result in a dramatic effect on the non-radiative decay. This concept is illustrated in Figure 5.1.1. It is an environmental effect but is quite distinct from the solvatochromic effects described in Chapter 3, in that the latter is an electronic interaction. S_0 and S_1 refer to the parabolic potential curves with associated vibrational levels. Both the vibrations of the molecule and the environment are quantised. The series of lines on either side of the drawing are indicative of the different vibronic structures of two different environments. One of the environments has vibrational levels, which are of similar energetic separation to those of the molecule, and thus the transfer of energy between them can occur readily. The other series of lines represents a system where the molecule and environmental energy system are substantially mismatched and thus energy transfer between them is inhibited. If a molecular system can be housed in an environment where there can be no transfer of vibrational energy, non-radiative decay should be prohibited and relaxation of the system should be limited to radiative processes. In this chapter this phenomenon is probed.

In Chapter 4 the use of vibrational spectroscopy as a diagnostic and characterisation technique has been described. Following from the discussion above it should also be a valuable tool in the estimation of vibrational coupling between molecules and their

environment and thus the non-radiative yield of the system. A molecule with a strong vibration at 1000cm^{-1} , for example, should couple well with an environment having a vibronic mode at the same frequency. Figure 5.1.2. compares the Raman spectra of toluene and the trimer. It can be seen that in the region of 1600cm^{-1} , both toluene and the trimer exhibit Raman activity, however to differing degrees. Activity in this region is associated with phenyl/vinyl groups, principle contributors to π conjugated systems. One would expect the non-radiative yield of the trimer to be higher in toluene solution than in THF for example and consequently the luminescence to be lower. Figure 5.1.3a shows that the different solvents had little or no change on the absorption spectra (Toulene and THF being solvents shown in Figure 5.1.3. However for the luminescence, as illustrated in Figure 5.1.3b, significant changes in the magnitude were observed. The luminescence yield is clearly weaker in Toluene than in THF, lending support to such a vibrational approach to the photophysics of molecules in solution.

The principle of the use of Raman spectroscopy to optimise radiative processes has been illustrated and will be extended within this chapter to a quantitative comparison between a range of solvents. As outlined in Chapter 3 solvents can have a significant effect on the electronic properties of molecular systems. It is important, therefore, in examining non-radiative processes in different solvent environments, that radiative processes are not significantly influenced through solvatochromic effect as outlined in Chapter 3. Thus a solvatochromatic study of the materials is merited.

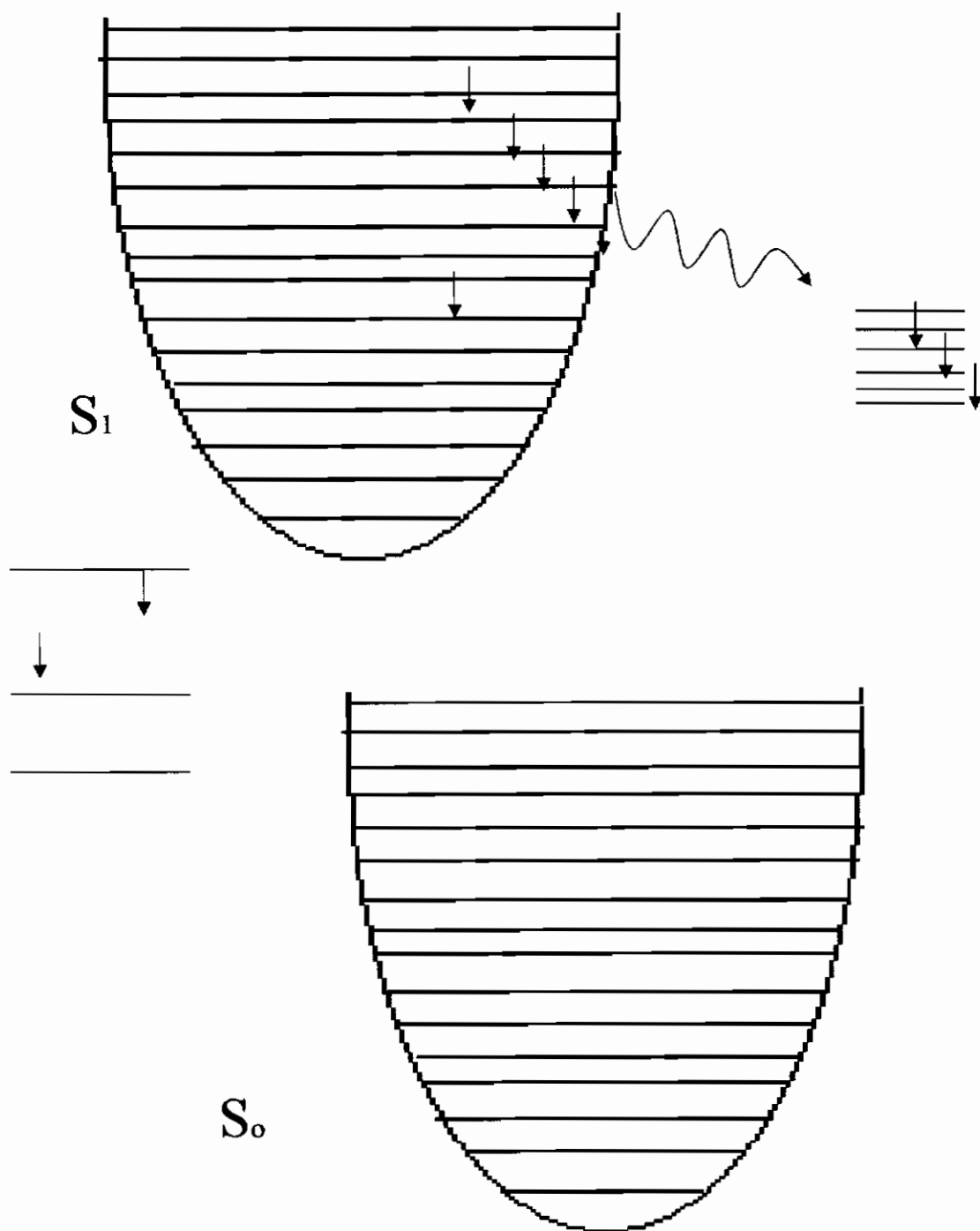


Figure 5.1.1 Schematic illustration of vibrational coupling of an excited molecule with two different environments².

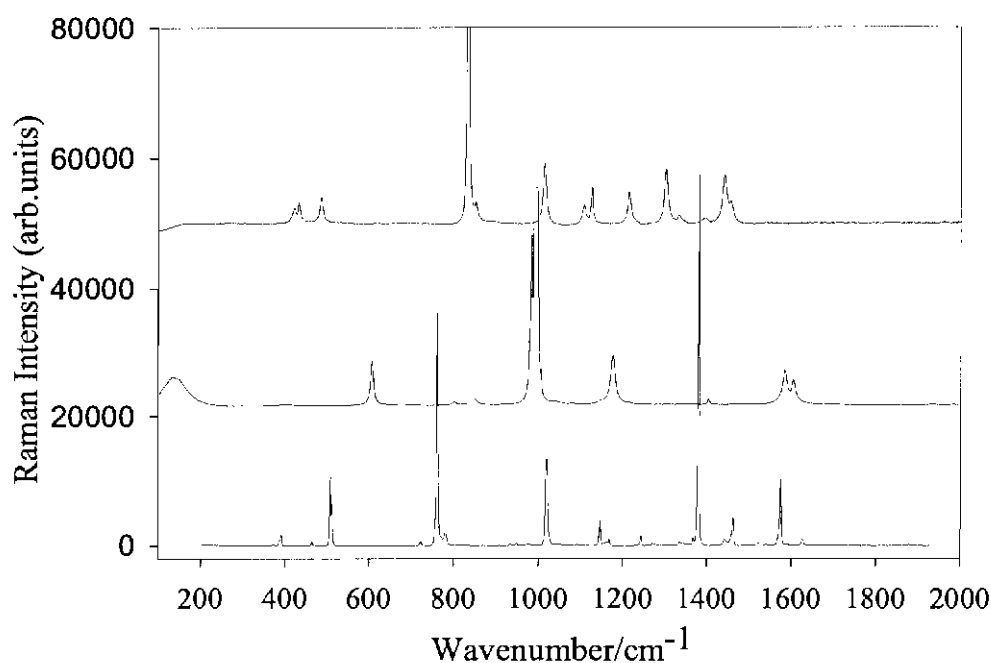


Figure 5.1.2 Comparison of Raman spectra of Toluene (Bottom), Therphenyl, (Middle) and Dioxane (Top).

5.2. Solvatochromism:

The absorption and fluorescence spectra for the trimer shown above were also carried out in a wide variety of solvents such as cyclohexane, hexane, toluene, benzene, THF, ethanol and dioxane. The positioning of the absorption and fluorescence maxima can be read and plotted as a function of the Onsager parameters, as discussed in Chapter 3. Figure 5.2.1. illustrates the shift of the UV-vis spectral maxima for the trimer in the range of solvents. The positioning of the spectral maxima, plotted against the Onsager polarisation function of the solvent, is well behaved.

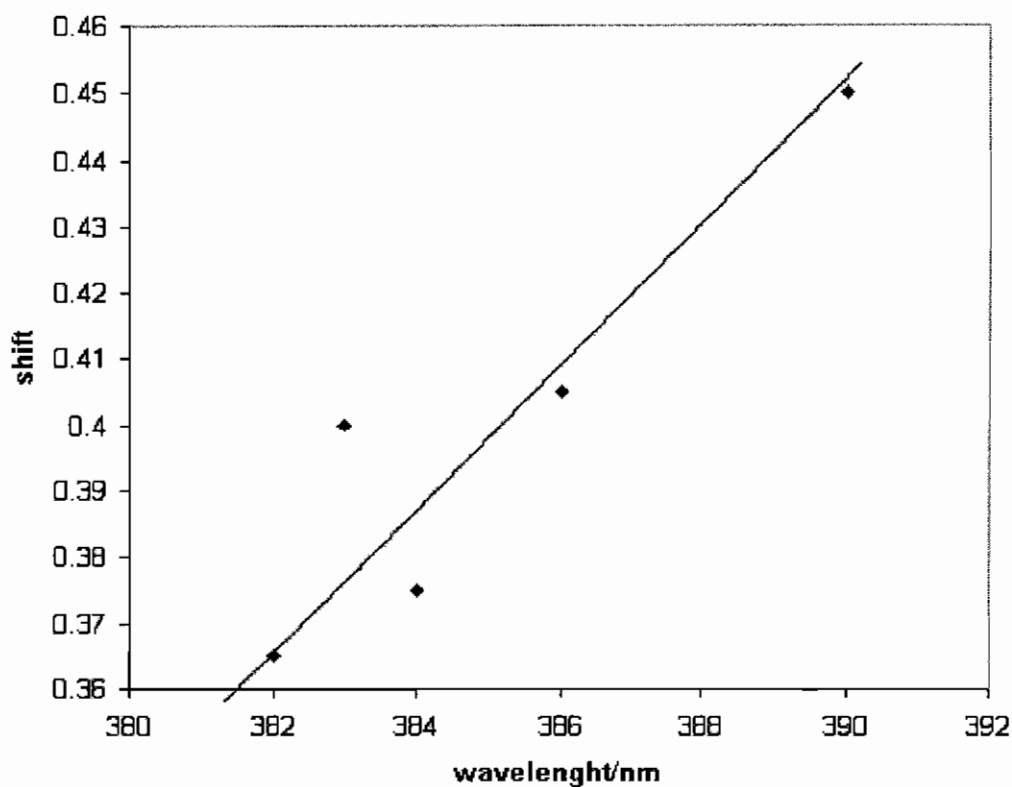


Figure 5.2.1. The solvatochromic shift, the shift of the UV -vis spectra maxima for the trimer in a variety of solvents.

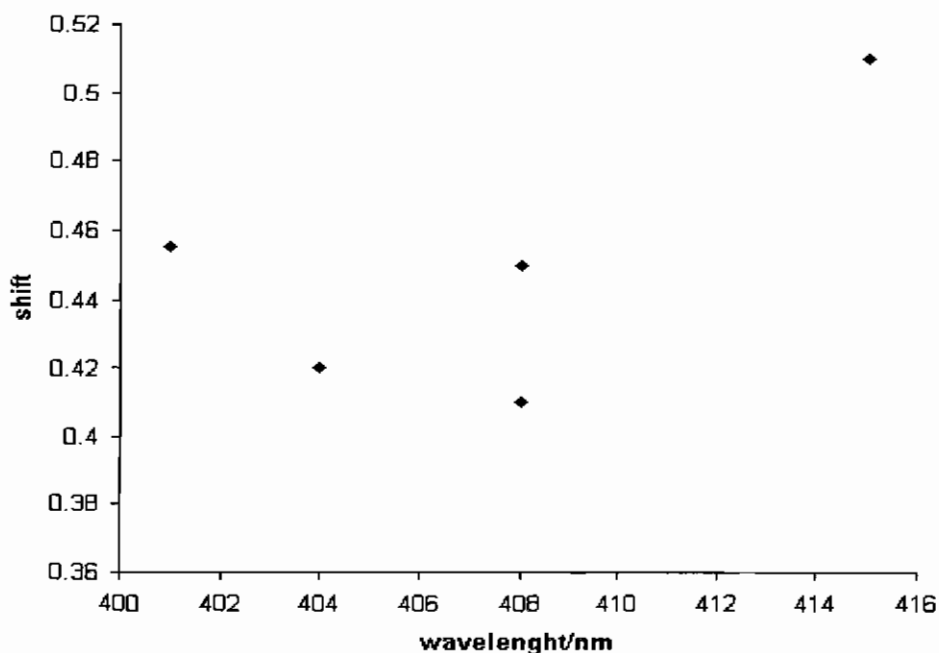


Figure 5.2.2. The solvatochromic shift, the shift of the UV-vis spectra maxima for the polymer in a variety of solvents.

The solvatochromic shift for the luminescence spectra is similarly well behaved, but while the oscillator strength for absorption is, within the accuracy of the

measurement, constant over the range of solvents, there are dramatic variations in the luminescence output. These variations show no correlation to the solvatochromic parameters.

The polymer is not as well behaved as the trimer and shows no discernable correlation for solvatochromic shift. Similarly for the polymer it shows large variation in fluorescence yield. Figure 5.2.2. illustrates that the solvatochromic shift for the polymer does show a similar trend to that of the trimer.

The lack of clear correlation for polymers is discussed and further explored in subsequent chapters.

5.3. Vibronic coupling:

Non-radiative decay through internal conversion is one of the principle competing processes to radiative decay in molecules and in order to undergo this process, the local environment must be capable of absorbing the vibrational quanta of the molecule. It is proposed that the overlap of the vibrational spectra of solute and solvent spectra is a gauge of the efficiency of the internal conversion and therefore the luminescent efficiency. Raman spectra for the solvents were taken keeping conditions constant such that a semiquantitative comparison could be made. For all solvents the overlap of the trimer spectrum with that of the solvent across the entire spectrum (200 - 3500 cm^{-1}) was calculated. In Figure 5.3.1 a plot of the integrated luminescence output versus the overlap of the vibrational spectra for the trimer. There is a clear correlation between the two parameters, illustrating that the highest luminescent output occurs in solvents which have the weakest vibrational coupling to the trimer. The correlation emphasises that efficient light emission in molecules is achievable only by inhibiting vibrational coupling to the local environment. The resulting graph points towards the fact that control of optical properties is intertwined with the vibronic properties of the environment.

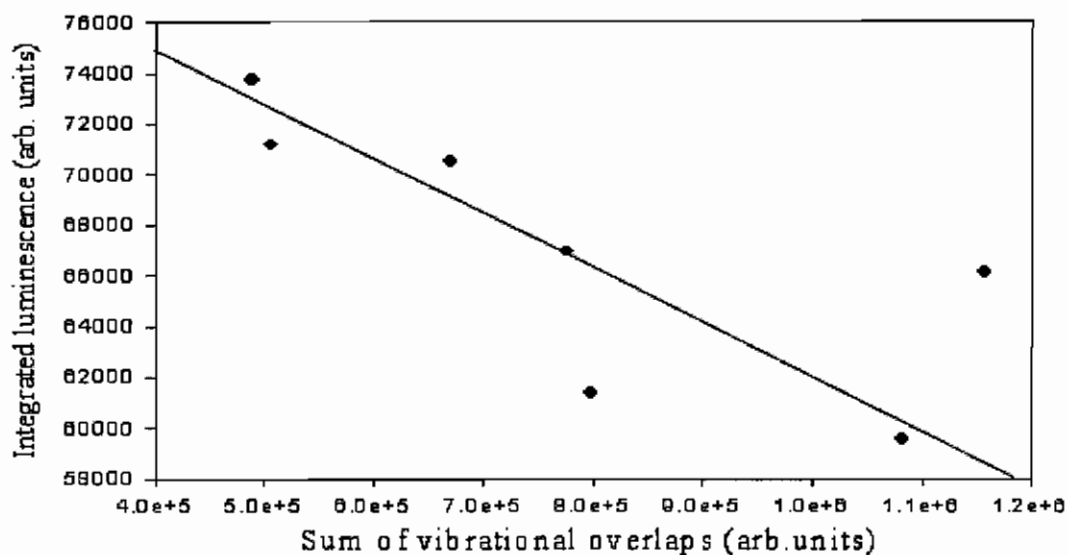


Figure 5.3.1. Plot of the integrated luminescence output versus the overlap of the vibrational spectra for the trimer.

The above result shows that there is some correlation between environmental effects and Integrated Luminescence and Vibrational overlap. However this correlation is not mirrored in the polymer medium as highlighted in Figure 5.3.2. This reflects the integrated luminescence output for the various polymer solutions against the vibrational spectra for the polymer. These Figures support the fact that trimer behaves as a molecule. Although the polymer does possess molecular like photophysics as in the processes are more complex in terms of coupling to the environment.

As in the case for solvatochromic effects, the coupling of the polymer to its environment is clearly more complex than that of the molecule. This more complex behaviour can be further examined by monitoring the kinetics of the photophysics.

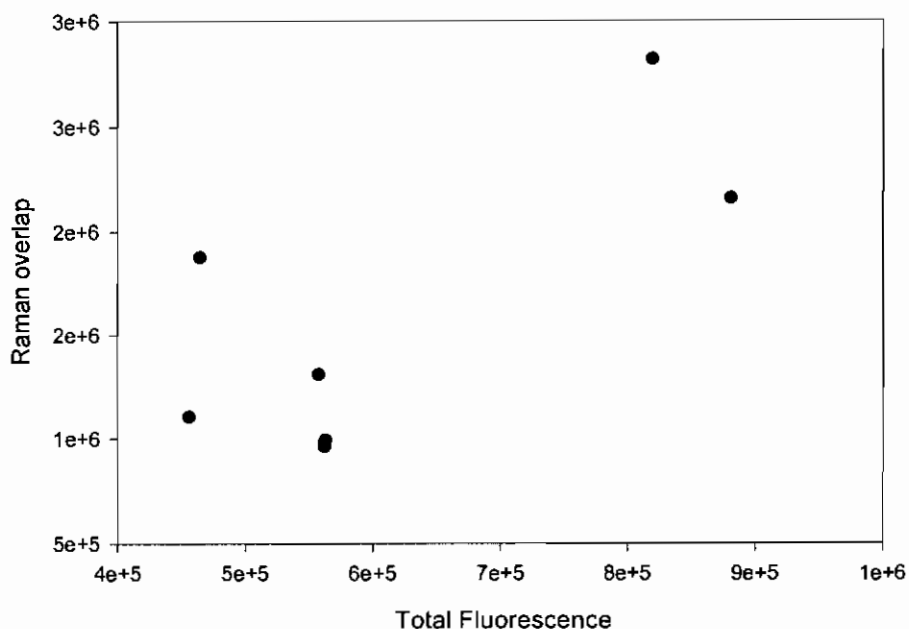


Figure 5.3.2. The solvatochromic shift, the shift of the UV-vis spectra maxima for the polymer in a variety of solvents.

5.4. Lifetime measurements:

In attempting to measure the lifetimes for the fluorescence transitions, similar problems are encountered as in normal fluorescence. Impurity quenching and general environment effects can be problematic. The measurement of fluorescence decay times can be done in various ways. The modulation method, basically involves a sample being excited by a light source, modulated (usually sinusoidal) at between 10 and 50 MHz, and the reliance is placed upon the measurement of the phase angle between detected fluorescence and the exciting light and the amplitude of the modulated signal³. Another technique is pulse-sampling, where a gaseous discharge lamp of a few nanoseconds duration is used to excite the sample and the detected fluorescence is monitored using a photomultiplier for direct display on an oscilloscope. Time-correlated single photon counting, developed in the 1960's is still

the main technique and is constantly being refined even today³. Pico-second or sub-pico-second resolution can be obtained using a streak camera.

5.5. Instrumental:

Figure 5.5.1. illustrates the typical set-up for a single photon counting instrument.

The single photon counting measurement relies on the concept that the probability distribution for emission of a single photon after an excitation event yields the actual intensity against time distribution of all the photons emitted as a result of excitation.

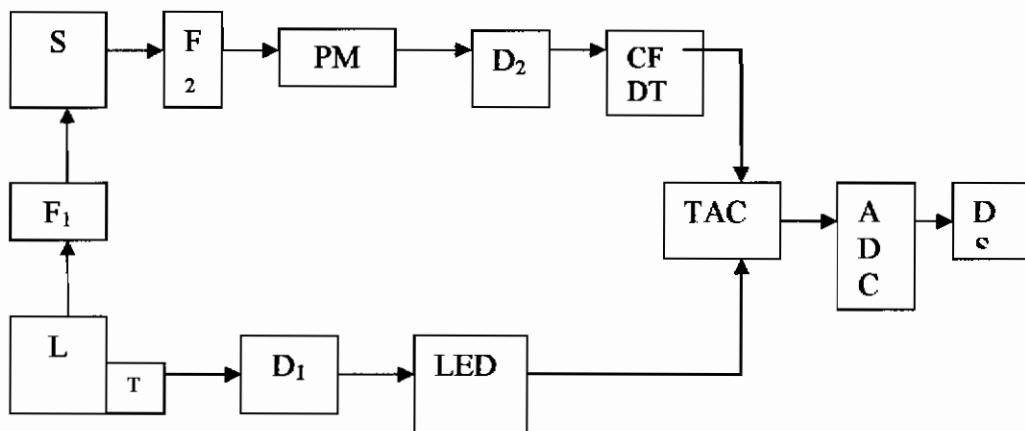


Figure 5.5.1. Illustrates the typical set-up for a single photon counting instrument.

| Optical signal | | Electronic signal. | |
|----------------|--|--------------------|---------------------------------|
| L | Excitation source | T | Trigger |
| S | Sample holder | F1 F2 | Filter or monochromator |
| D1 D2 | Delay lines | LED | Lead Edge timing discriminator |
| CFT D | constant fraction timing discriminator | | |
| TAC | Time-to-amplitude convertor | ADC | anaologue-to-digital convertor. |
| DS | Data storage | | |

By sampling the single photon emission following a large number of excitation flashes, the experiment constructs this probability distribution. This is carried out in the following way. The trigger T, which can be a photomultiplier for example, generates an electrical pulse at the time exactly correlated with the time of generation of an optical pulse. The trigger pulse is routed through a discriminator to the start input of time-to-amplitude converter (TAC) which initiates charging a capacitor. The optical pulse excites the sample, which fluoresces in front of an aperture, which has been adjusted so that one photon is detected for exciting events. The resulting signal from this stops the charging ramp in the TAC. This in turn puts out a pulse, the amplitude of which is proportional to the charge in the capacitor representing a time difference between start and stop pulse. The TAC output pulse is given a numerical value in the analogue-to-digital converter and a count is stored in the data storage device in an address corresponding to that number. Excitation and data storage are repeated in this way until a histogram of number of counts against address number in the storage devices represents the decay curve of the sample. This is usually taken with the time profile of the instrumental response to allow for the deconvolution of the data.

The statistics of single photon counting have been examined in detail by Morton, Pfeffer and Wahl. To gain an accurate decay, the best decay curve must be obtained. The mathematics behind this need to be very well defined to allow deconvolution of the curve. The process of deconvolution is necessary due to the fact that molecules excited by photons at earlier times are decaying while others are being excited by photons in the tail of the excitation pulse. Another important fact to take account of is the instrument response. Standards for measurement of an instrument response function are well known. Colloidal solutions of Ludox®, glycogen (Weber and Teale) scatter light and thus mimic the instantaneous instrumental response. Care must be taken at shorter excitations wavelengths as fluorescence can occur. The system of the National Laboratory for Laser Applications, National University of Ireland - Galway used in this experiment is a slight variation on that described above³. The underlying principle are the same, but the detection system is an uncooled Hamamatsu H5783-01 PMT with a dark count of ~440 cps and an anode response time of ~0.65 ns. The emission wavelength is determined by means of interference filters on every 50nm from 400 to 750 nm. Excitation measurements, cited in future

chapters use a 450nm filter. In theory it should be possible to measure lifetimes down to ~ 200 ps with deconvolution of the laser pulse.

5.6. Experimental:

Lifetime measurements were taken for both the trimer and the PmPV polymer in various solvents at concentration of 10^{-6} . The results reinforce earlier studies, whereby the polymer showed more complex behaviour than the trimer. Figure 5.6.1 illustrates the different lifetime results for the trimer in two different solvents, THF and Benzene, which are off-set for clarity. In these curves a single exponential decay is observed, which over the range of solvents the lifetime is seen to vary from 1.49ns to 1.68ns. According to equation 2.9.26, this variation should be directly correlated with the variation in fluorescence efficiencies. Figure 5.6.2. illustrates this correlation which is well behaved over the range of the solvents. The photophysics of the trimer is in accordance with that of a unimolecular system as described by the Einstein equations in Chapter2.

The results for the range of solvents used can be related to the Raman overlap to show correlation between the lifetime and vibrational structure, as illustrated in Figure 5.6.2. The results for the range of solvents can also be used to show the relationship between Lifetimes versus the Integrated Fluorescence for the trimer as illustrated in Figure 5.6.3.

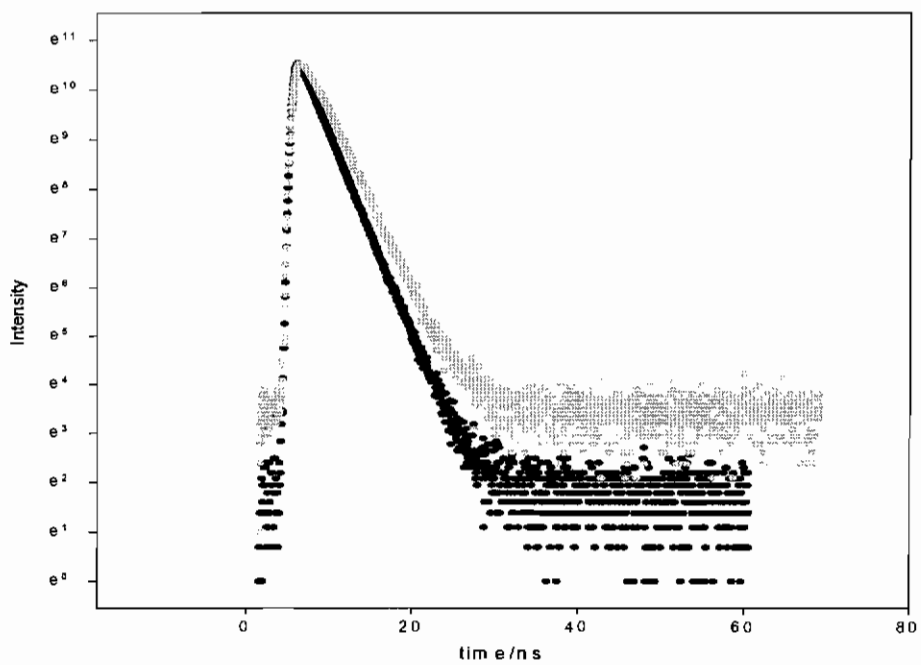


Figure 5.6.1. Lifetime of trimer in various solvents.

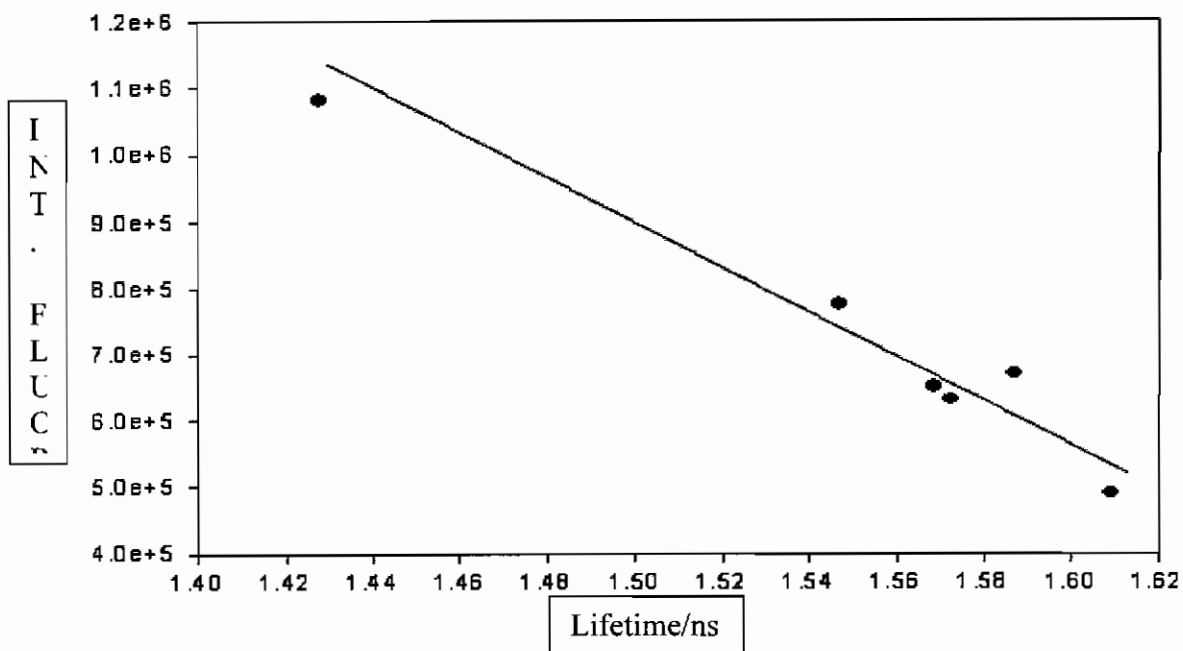


Figure 5.6.2 Plot of Lifetimes versus the Integrated Fluorescence for trimer.

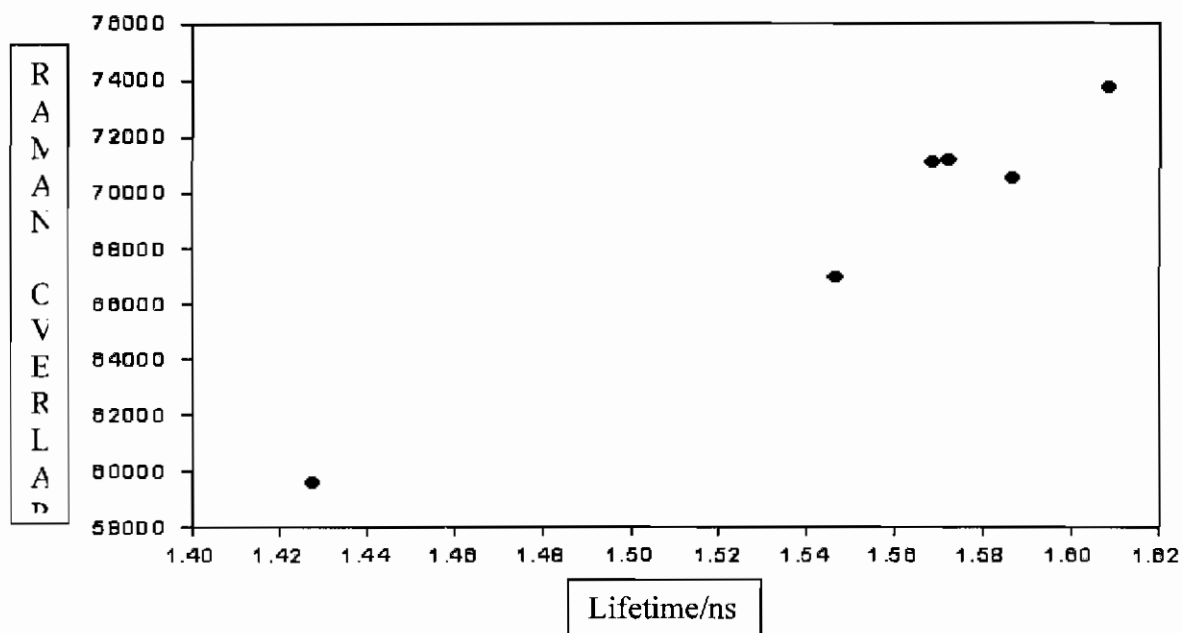


Figure 5.6.3. Plot of Lifetimes versus the summed overlap of Raman Spectra for trimer.

This variation in lifetime and quantum yield is a reflection of differing vibrational coupling to the environment, which can be monitored using vibrational spectroscopy. The correlation between the lifetime and both the Raman spectra and the integrated fluorescence highlights the value of vibrational and, in particular, Raman spectroscopy as a simple and rapid technique for evaluating non-radiative processes in molecular systems. However, in comparison to the lifetime measurements of the trimer the polymer is a much more complicated system. The decay shown in Figure 5.6.4 at concentration 10^{-6} mol/l is not single exponential decay, as can be easily seen by comparing Figures 5.6.4. and 5.6.1. The best fit is to a double exponential with components of 1.5ns and 2.54ns and a smaller artifact of only several picoseconds most probably instrumental. The first component is similar to the trimer and is most likely to be single chain polymer relaxation. The longer component most likely represents a departure from single unimolecular photophysics described in Chapter 2. The relative contributions of the two components vary from solvent to solvent. The origins of this variation and departure from unimolecular photophysics are of key importance to understanding the photophysics of polymer materials and optimising their performance. This unfortunately does not allow for a correlation similar to that shown in Figure 5.2.1 for the polymer.

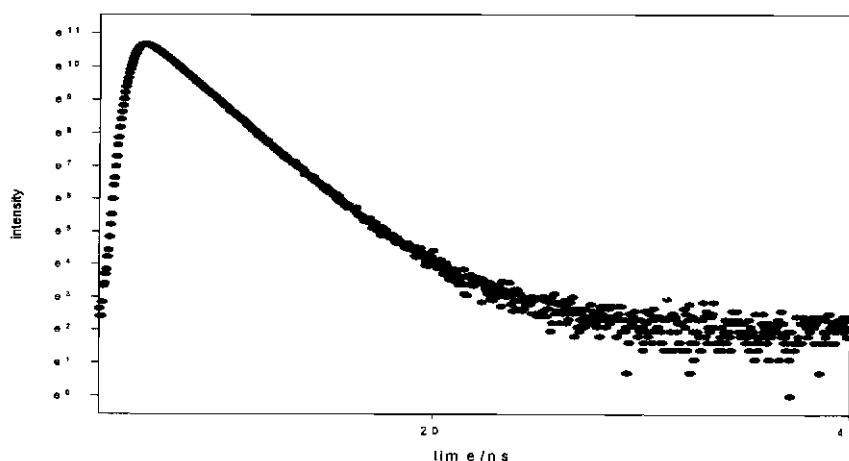


Figure 5.6.4. Lifetime for polymer in a Toluene.

5.7. Summary:

Environmental effects have been shown to be very important in looking at the photophysics of any molecular system. The trimer exhibits in the UV-vis spectra some solvatochromism, but the observed variation in fluorescent yield doesn't correlate with the solvatochromic parameters. Figure 5.1.1. illustrates an additional interaction between the molecules and the environment that can take place, and how by mis-matching the environmental vibrational structure with that of the molecule the photophysics can be controlled. Raman spectroscopy has shown itself to be a highly useful tool in probing the effect of the environment on the photophysics of the materials being studied. The differing solvatochromic effect between the trimer and the polymer highlights the complex coupling between the environment and the polymer, while the trimer is to a greater extent well behaved. In collaboration with the National University of Ireland.-Galway experiments were done to obtain lifetime measurements. These show very good correlation with the Raman overlap. The greater the Raman overlap the shorter the lifetime as the vibrational energy can easily transfer itself from the molecule to the environment. Therefore the higher the integrated fluorescence is the longer the lifetime becomes. The use of Raman as a technique for probing the photophysics of a material has proven itself to be a viable and versatile technique.

5.7 References:

- 1: Gouterman H. The Porphyrins, Vol. III Academic Press (1978).
- 2: Birk J.B; Photophysics of Aromatic Molecules, John Wiley & Sons (1970).
- 3: O'Connor P.D; Time-correlated single photon counting D.V. Academic Press (1984).

Chapter 6

Intermolecular coupling

| | |
|---|-----|
| 6.0 Intermolecular Coupling: | 105 |
| 6.1 Concentration dependent absorption of the PmPV trimer | 105 |
| 6.2 Concentration dependent photoluminescence of the PmPV trimer | 107 |
| 6.3 Concentration dependent absorption of the PmPV polymer | 108 |
| 6.4 Concentration dependent photoluminescence of the PmPV polymer: | 112 |
| 6.5 Concentration dependent Photoluminescence lifetime measurements | 115 |
| 6.6 Summary: | 116 |
| 6.7 Reference..... | 117 |

6.0 Intermolecular Coupling:

In chapter 5 the coupling of the electronic states of a molecule to its environment via the vibronic modes and its effect on the photophysics of the system was explored. Realistically, potential applications of these polymeric systems rely on optimised performance in the condensed phase, in which the environment can not be arbitrarily tailored. It has already been seen that the polymer, both in terms of electronic and vibronic coupling does not behave as a simple molecular system suggesting some morphological effects. It is important therefore to examine the degree of intermolecular coupling and the effects on the photophysics. In soluble systems this is facilitated by examining the spectroscopic properties of the material as a function of concentration. Any departure from the Beer-Lambert law indicates a departure from single molecular behaviour.

6.1 Concentration dependent absorption of the PmPV trimer

The PmPV trimer was dissolved, sonicated and degassed in toluene, yielding various concentrations ranging from 3×10^{-3} M to 3×10^{-6} M. The lower end is assumed to be approaching infinite dilution. Figure 6.1.1. shows the UV-vis spectrum as a function of concentration. All spectra show peaks at approximately 395nm (3.2eV) and 325nm (3.8eV), as discussed in Chapter 4. The shape of the spectra shows no significant change or distortion in going from high concentration to low concentration. However, the absorbance does not increase linearly with concentration. This is clearly indicated in Figure 6.1.2, in which the absorbance at the maximum at 395nm is plotted as a function of concentration. Initially the absorbance increases quasi-linearly, but at concentrations as low as 3×10^{-4} M a clear departure from linearity is observed. Such a hypsochromic shift is commonly observed in molecular species, particularly those with planar chromophores and is commonly attributable to aggregation¹. The pronounced effect on the spectroscopic properties is the route of the difficulties in realising device applications in the solid state.

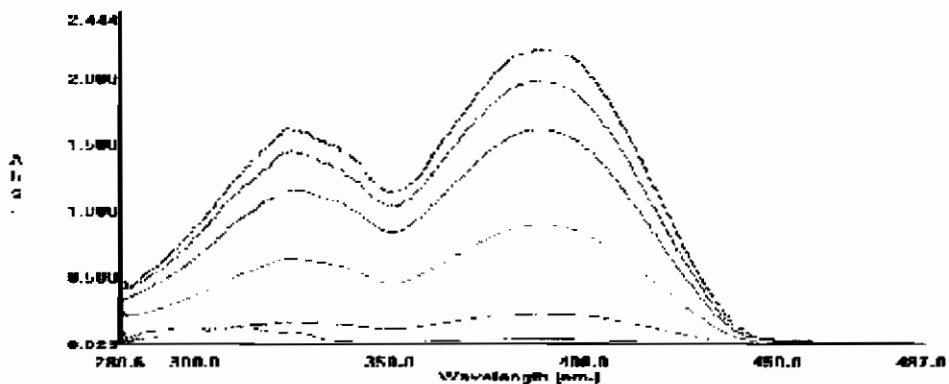


Figure 6.1.1. Plot of the UV-vis absorption of the trimer as a function of concentration from $3 \times 10^{-6} \text{ M}$ to $3 \times 10^{-3} \text{ M}$ in toluene solution.

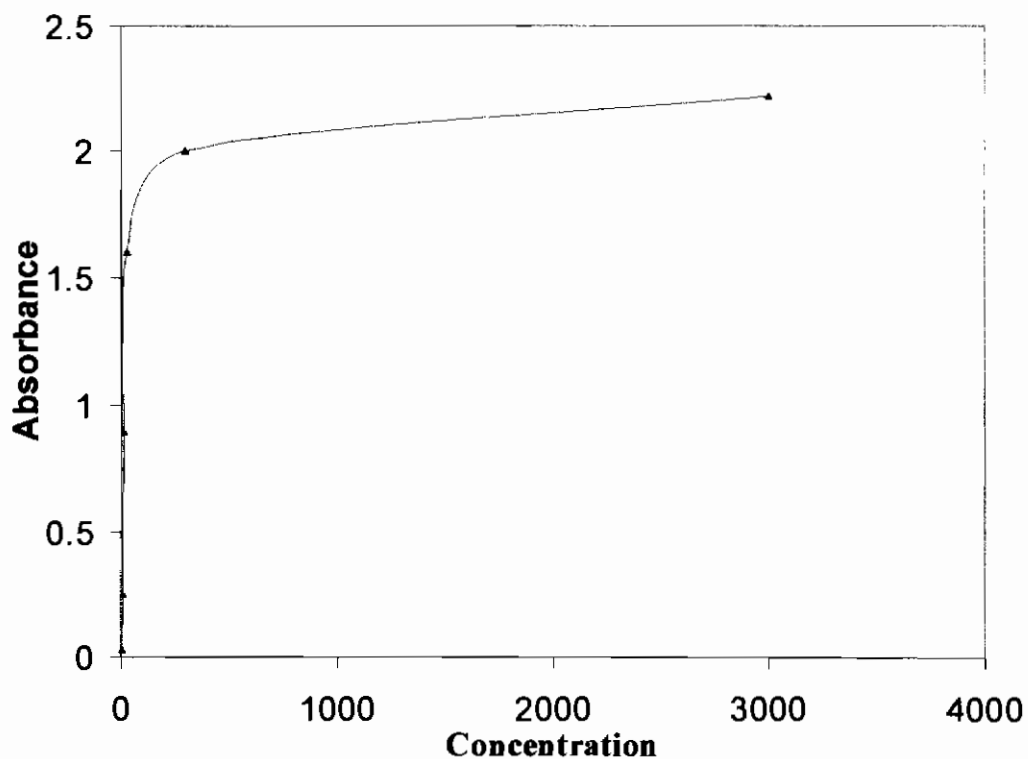


Figure 6.1.2 Plot of Absorbance of the Trimer versus Concentration, ($\times 10^{-6} \text{ M}$)

6.2 Concentration dependent photoluminescence of the PmPV trimer

The departure from the Beer-Lambert law of the absorbance of the PmPV trimer as a function of concentration is further pronounced in the photoluminescence of the solutions. Figure 6.2.1. shows the fluorescence of the trimer in toluene solution as a function of concentration in the range 3×10^{-6} M to 3×10^{-3} M. For ease of comparison, the spectra are arbitrarily normalised at 500nm. The fluorescence spectrum has a maximum at 440nm at the lowest concentration, 3×10^{-6} M. As the concentration increases the spectrum appears to shift to the red and at the maximum concentration of 3×10^{-3} M a new feature at 525nm has emerged. This emission is a further clear departure from unimolecular photophysics and is attributable to an intermolecular species with a weak, redshifted emission². The apparent red shift of the intramolecular emission can be the result of reabsorption in the solution, but the strong concentration dependence suggests that a further concentration dependent absorption of an intermolecular species, to the red of the principle molecular absorption, emerges³.

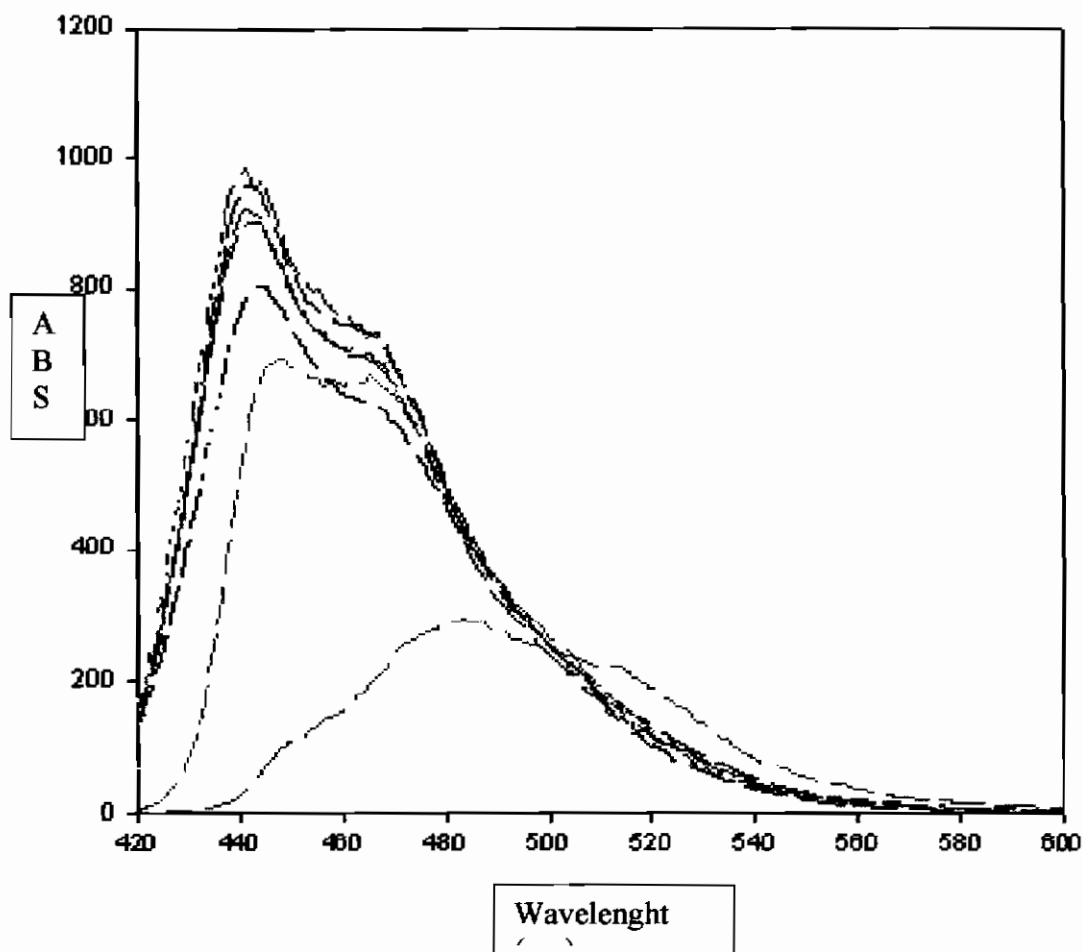


Figure 6.2.1. illustrates the concentration effect on the fluorescence spectra of the PmPV trimer.

6.3 Concentration dependent absorption of the PmPV polymer

In terms of solvatochromatic effects and vibrational coupling, the trimer is well behaved at low concentrations, exhibiting photophysics of a unimolecular system. With increasing concentration, however, a clear departure from this behaviour to one characteristic of aggregation phenomena is observed. Even at low concentrations, the polymer in solution does not exhibit simple unimolecular photophysical behaviour, as is evident in the decay of the photoluminescence (Chapter 5). This departure from unimolecular behaviour is most likely an aggregation phenomenon and should be pronounced with increasing concentration. Figure 6.3.1 illustrates the absorption spectra for the polymer produced via the Wittig synthetic route with toluene. The WTolPmPV powder was dissolved in a variety of concentrations in toluene. At the

lowest concentration, 1×10^{-5} M, peaks at 325nm and 395nm are observed. As is the case with the trimer, no new features appear with increasing concentration, although comparison of the spectra at 1×10^{-5} M and 5×10^{-4} M suggest that there is a red shifting of the maximum with concentration. The absorbance of the solutions is far from linear as a function of concentration, as shown in Figure 6.3.2 for the case of the absorption maximum at 395nm. The absorbance increases approximately linearly until $\sim 1 \times 10^{-4}$ M at which point it suddenly decreases until the final concentration of 5×10^{-4} M. The departure from linearity, as is the case with the trimer, is indicative of an aggregation effect, but as expected it is much more pronounced in the polymer. It should be noted, however that any new intermolecular species does not exhibit a strong, discernable absorbance.

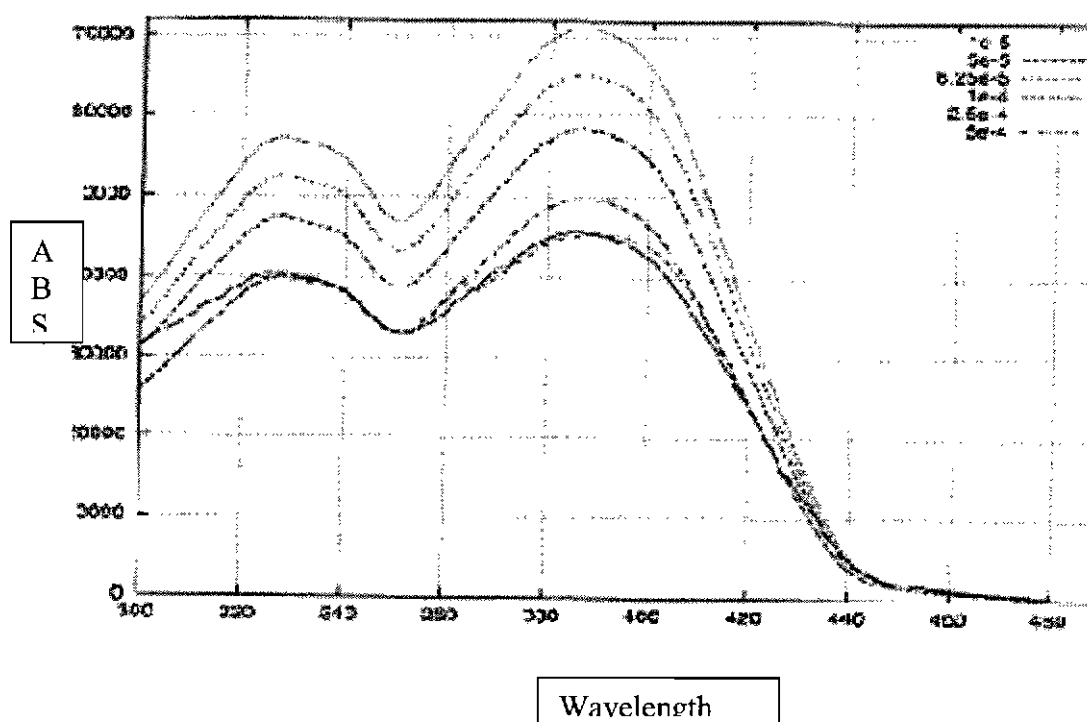


Figure 6.3.1. illustrates the spectra for the WTolPmPV in a variety of concentrations in toluene.

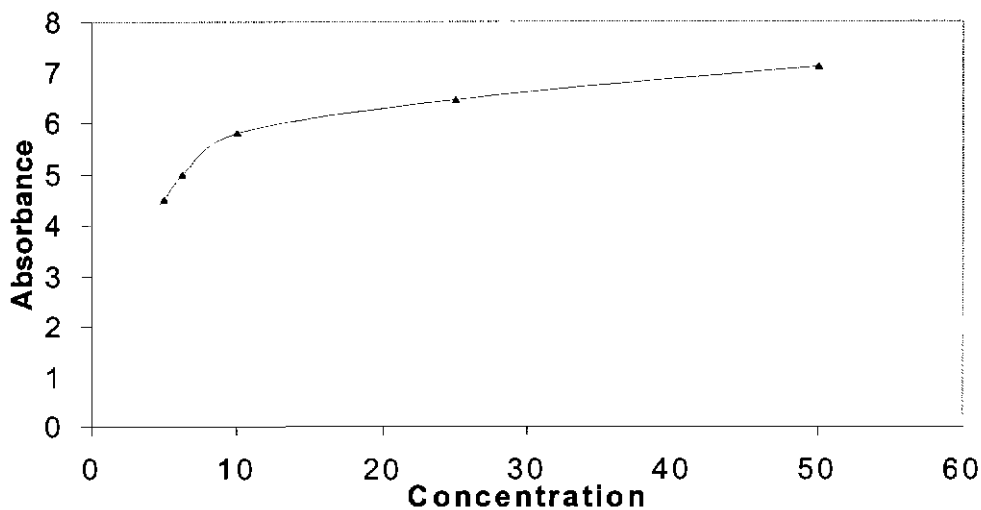


Figure 6.3.2 Plot of Absorbance of the WtolPmPV Polymer versus Concentration, (x10⁻⁵M)

To confirm that the behaviour of the WTolPmPV polymer is universal, the polymer produced via the Horner-Emmons-Wadsworth route in toluene (HtolPmPV) was monitored in a similar fashion. Figure 6.3.3. illustrates the absorption spectra of the HTolPmPV in a variety of concentrations in toluene. As shown in Figure 6.3.4, although the absorbance of the maximum at ~395nm increases initially with concentration, a maximum is reached at approximately 1×10^{-4} M, whereupon an abrupt decrease in absorbance is observed. The absence of a red shift might however suggest that the intermolecular interaction is less pronounced in the HtolPmPV solutions.

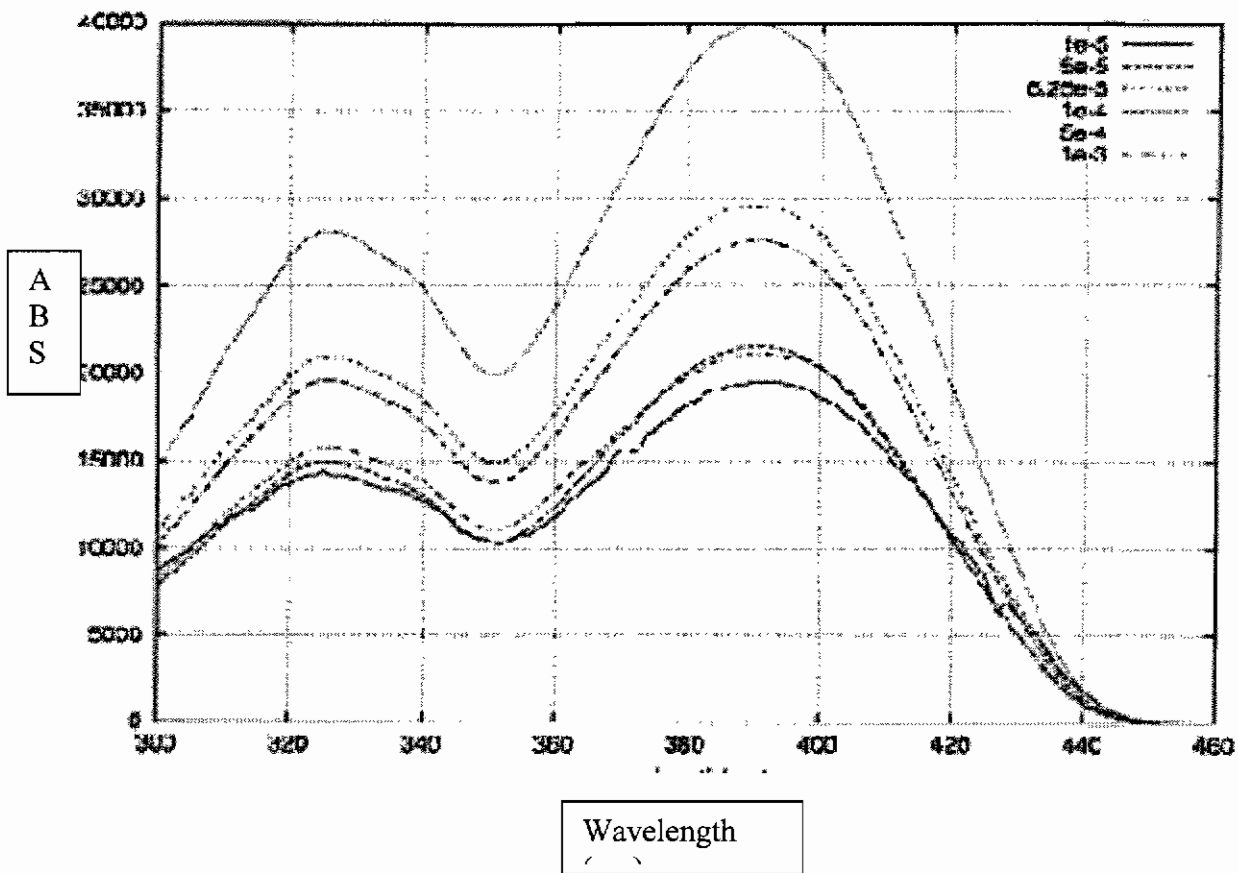


Figure 6.3.3.illustrates the absorption spectra for the Horner-Emmons-Wadsworth synthetic route with toluene.

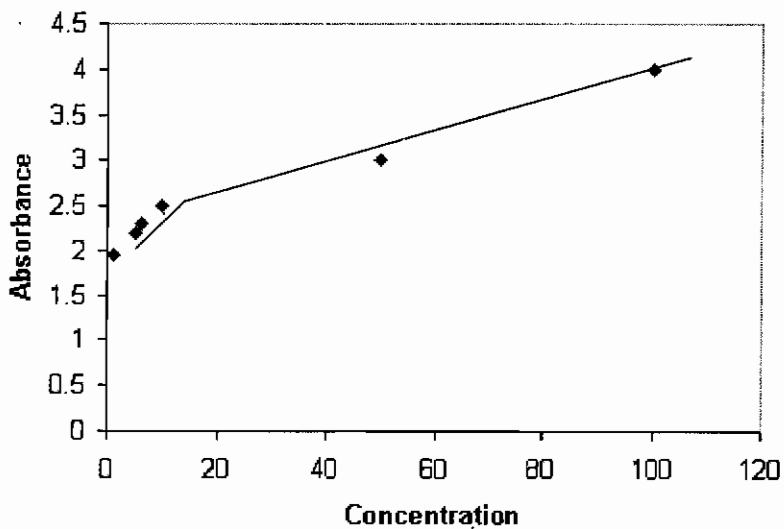


Figure 6.3.4. Plot of Absorbance of the Horner-Emmons-Wadsworth synthetic route with toluene., ($\times 10^{-5}M$) versus Concentration,

6.4 Concentration dependent photoluminescence of the PmPV polymer:

Figure 6.4.1. illustrates the emission spectra for the WTolPmPV polymer. The spectra for the various concentrations can be seen. At the lowest concentration, “absolute dilution”, 10^{-5} the main peak is at 440nm. When the concentration is increased the spectrum appears to move to longer wavelengths. The initial shoulder at 475nm is eroded leaving a broader, less structured spectrum, at a concentration of 1×10^{-3} M. In addition to the apparent red shifting, a new feature centred at 525nm appears. As is the case with the trimer, this would seem to be the result of concentration induced aggregation, which also results in a decrease in the absorption. This behaviour is also observable in solutions of the HtolPmPV polymer, as shown in Figure 6.4.2. It is notable, however, that the feature centred at 525nm is less pronounced than that in WTolPmPV emission spectra.

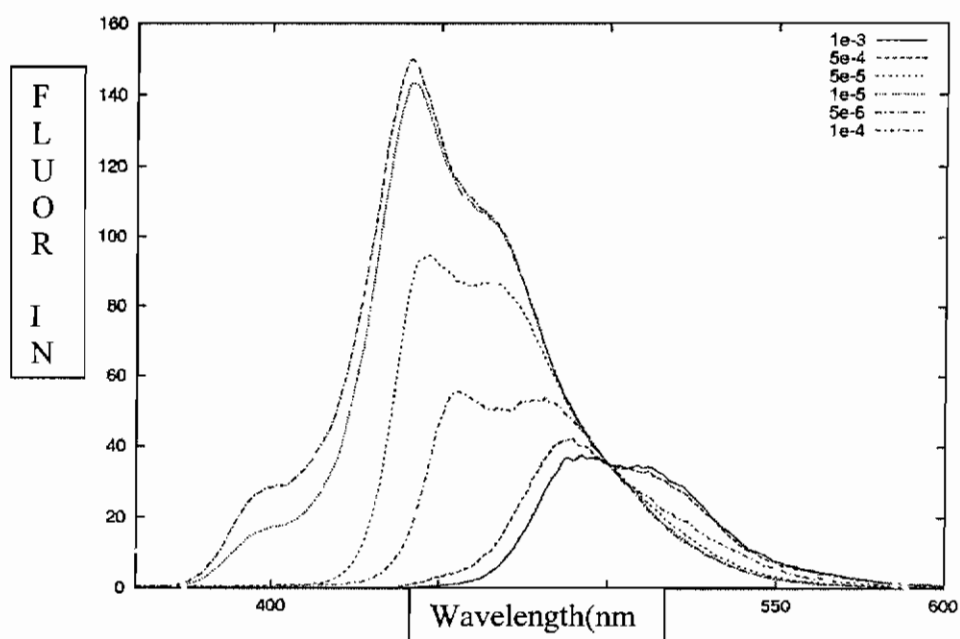


Figure 6.4.1. illustrates the emission spectra for the WTolPmPV in various concentrations in toluene solution.

As in the case of the trimer solutions, the new feature at ~ 525 nm can be attributed to the emission of new, intermolecular species formed at higher concentrations. The decrease in emission on the blue side of the spectrum can be attributed to a combination of reabsorption by the solution with increasing

concentration and possibly the emergence of a weak red-shifted intermolecular absorption, although there is none discernable in the absorption spectra. The fact that no new species is seen in the absorption, but is evident in the emission spectra raises the possibility that the new species is an excimer.

In order for an excimer to form, a ground state molecule must become excited and then comes into close enough proximity with a non-excited to bond and form an excimer. The absorption spectrometer scans from higher wavelength to lower. The excimer is a larger oscillator than the individual atoms and so absorbs at higher wavelengths. The spectrometer scans through the wavelength at which the excimer absorbs, is inconclusive. The excimers can only be formed when the molecular excitation wavelength has been reached.

In emission studies the sample is continuously excited at a wavelength it is known to absorb at, exciting the molecule and leading to excimer formation with increasing probability at higher concentrations. This being the case, excimers would be evident in the emission spectra. The fact that the new emission feature is red shifted with respect to the low concentration peaks, is broad and featureless, is characteristic of excimer emission.

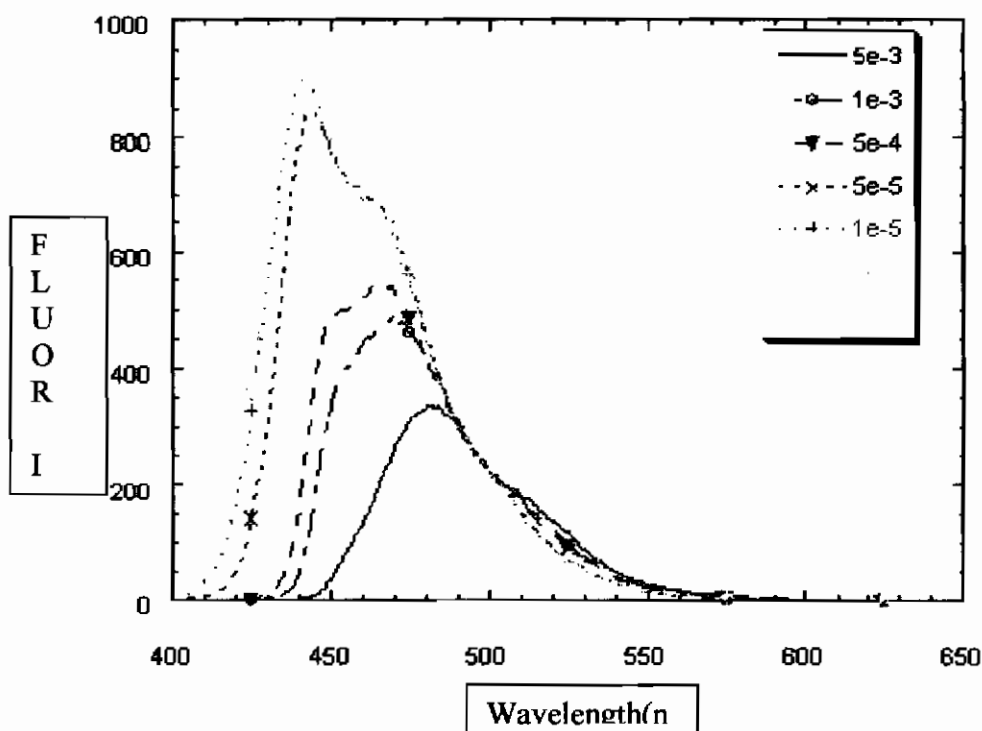


Figure 6.3.2. illustrates the emission spectra for the Horner-Emmons-Wadsworth reaction.

6.5 Concentration dependent Photoluminescence lifetime measurements

The complexity of the polymer system is highlighted in the luminescence decay curve shown in Figure 6.5.1. Compared with the trimer decay shown in Figure 6.5.2, which is single exponential and largely independent of concentration, the polymer is substantially more complex.

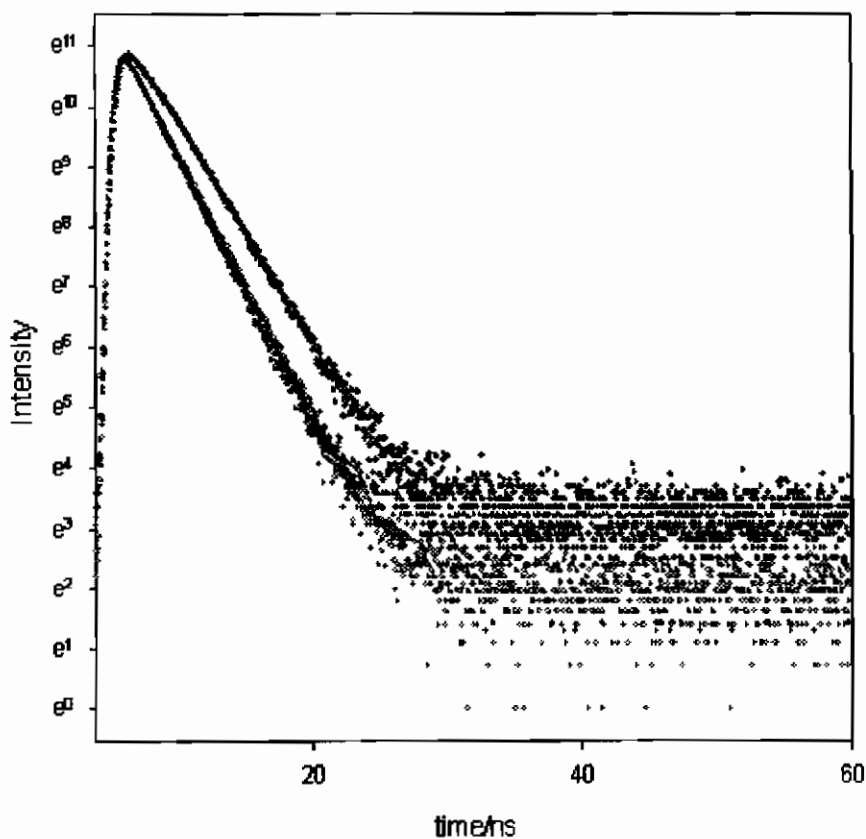


Figure 6.5.1. illustrates the decay curve for the trimer molecule in various concentrations in toluene at absolute dilution.

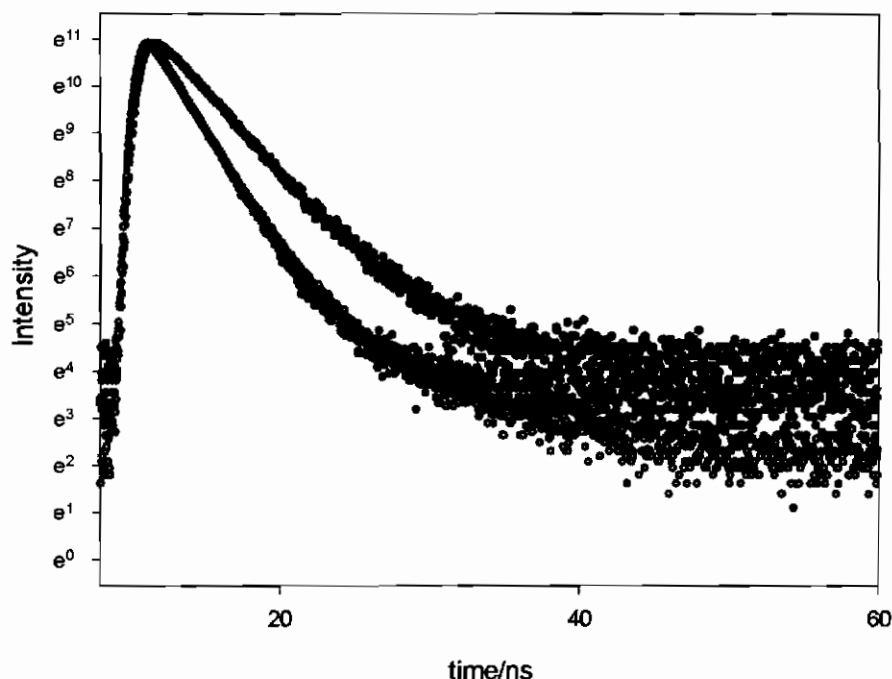


Figure 6.5.2. illustrates the decay curve for the WtolPmPV polymer in various concentrations in toluene at absolute dilution.

Figure 6.5.2 shows the decay of the WtolPmPV polymer in toluene solutions of varying concentrations. At concentrations of 3×10^{-5} M (red curve) the decay is almost single exponential with a deconvoluted lifetime of 1.85ns, similar to the trimer. At concentrations of 3×10^{-4} M, (green curve), where clear indications of aggregation are apparent in both the absorption and emission spectra, a second, long lived component emerges. Further increase in concentration to 3×10^{-3} M (black curve) results in a further increase in the long lived component and a lengthening of the shorter lived, molecular-like component.

This behaviour is further evidence of an aggregation phenomenon producing a longer lived, red shifted emission. These aggregates allow for the inter-molecular interaction of the many molecules. This will quench the fluorescence intensity as it allows for the transfer of energy internally and decreases quantum efficiency.

6.6 Summary:

Concentration dependent studies of the trimer show hypsochromic shifts in both the absorption and emission spectra, characteristic of molecular aggregation. This behaviour is more pronounced in the polymer solutions and clearly reduces the photoluminescence efficiency and potential of the material. There is clear evidence of the evolution of new species in solutions of higher concentrations. Whether the species is indeed an excimer or a ground state aggregate is immaterial in terms of material performance, as a significant departure from unimolecular behaviour occurs with increasing concentration. Tailoring and design of optical and electronic properties at a molecular level is futile if these properties are not maintained in the condensed state. Furthermore, the simple rate equation models and indeed the vibrational approach to optimising photoluminescence quantum efficiencies fall down in aggregated materials. A significant observation, however is that the HtolPmPV solutions aggregate significantly less than those of the WtolPmPV, although the materials are chemically identical, and there appears to be no significant difference in chain length⁴. The origins of this difference will be further explored in the following chapter.

6.7 Reference

- 1: PhD Thesis, Byrne H.J; Trinity College Dublin, (1989).
- 2: Rumbles G; De Souza M; Samuel I.D.W; Holmes A.B. *Synthetic Metals* **101**, 631-632 (1999).
- 3: PhD Thesis, Dalton A; Trinity College Dublin, (2000).
- 4: PhD Thesis, Maier S; Trinity College Dublin, (2000).

Chapter 7

Isomerism

| | |
|--|-----|
| 7.0 Isomerism:..... | 119 |
| 7.1 Isomerism an Introduction: | 119 |
| 7.2. Isomerisation of Stilbenes:..... | 121 |
| 7.3. Vibrational Spectra: | 122 |
| 7.4 Isomerism of PmPV trimer. | 124 |
| 7.5. Raman Spectroscopy of Trimer: | 127 |
| 7.6 Isomerism of the polymer: | 130 |
| 7.7.Molecular Modelling: | 132 |
| 7.8 Summary | 133 |
| 7.9 References..... | 135 |

7 Isomerism:

7.1 Isomerism an Introduction:

In the previous chapters the trimer has been shown to obey classical photophysics at low concentrations, whereas the polymer does not. Moreover, the polymer made by two different methods appears to behave differently. This deviation is most evident at higher concentrations and thus may be attributed to differences in the aggregation of the two materials. A possible source of differences between the methods could be different degrees of isomerisation in the polymers.

The term “isomerism” refers to the relationship that exists between two or more different chemical compounds that have the same molecular formula, but different configurations (spatial arrangements).¹ In its simplest form the different configurations are referred to as Cis/Trans or similarly *e/z* ((*entwieden* (Trans)/*zusammen* (Cis)) depending on the terminology being used. Figure 7.1.1, illustrates the different configurations for butane, Cis defining the orientation when the substituents, such as –CH on Butane in Figure 7.1.1 are on the same side and Trans when the substituents are on opposite sides.

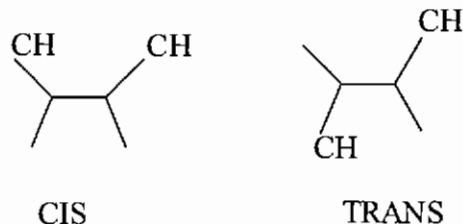


Figure 7.1.1. The different Cis/Trans configurations for Butane.

The level of isomerism is potentially very important when looking at the optical and electroluminescent properties of both the polymer of PmPV and trimer of PmPV. The different degrees of aggregation can effect packing and in effect change the coupling between molecules in the solid. The illustrations of the synthetic route of both the polymer shown in Figure 4.3 and the route of the trimer shown in Figure 4.4, shows how complex the mechanism can be. The synthesis of the polymer and trimer can utilise two different techniques, the Wittig reaction and the Horner-Wadsworth-Emmons reaction with two different solvents, Toulene and DMF and varying

temperature. The effect of a variation of synthetic route is highlighted in the different properties of polymers made by two different routes (as discussed in chapter 4). In this chapter it is proposed that the resultant variation in the properties may be attributed to the different Cis/Trans ratio in the sample. The ratio can depend on reaction conditions such as temperature, environment and solvent effects.

7.2. Isomerisation of Stilbenes:

In an attempt to comprehend the effects and signatures of isomeric mixtures, a model system was studied in which the Cis/Trans ratio could be varied with a high degree of accuracy. The system chosen was the stilbene or stilbenoid compound. Figure 7.2.1 illustrates the Cis and Trans form of the stilbene, which can be purchased nearly 100% pure from Aldrich. The high degree of accuracy in the make up of the stilbene, allows for a complete study of the Cis/Trans spectroscopic signatures.

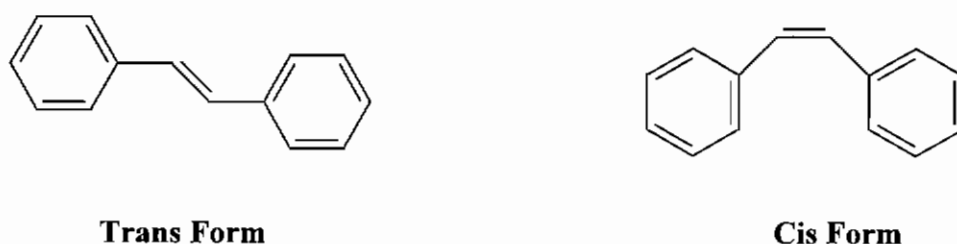


Figure 7.2.1 Trans and Cis form of the stilbenoid complex.

The Cis-Trans isomerisation of the stilbene has been documented for the past 80 years.³ X-ray structural analysis of crystalline Trans stilbene shows that the molecule is almost planar⁴, is of symmetry group C_{2h} and has a twist angle of 32° for the phenyl group.⁵ Electron diffraction studies also show that the Cis form of stilbene possesses a propeller type structure, again C_2 symmetry and a twist angle⁶ of $43.^\circ$ The most important aspect of the stilbenoid complex is the fact that stilbene can form oligostyrylarene complexes such as illustrated in Figure7.2.2

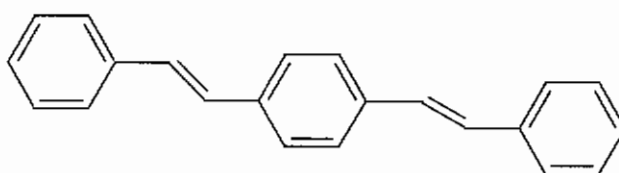


Figure 7.2.2 illustrates an oligomer of Trans stilbene.

This Trans oligomer looks extremely similar to the PmPV trimer, except it is missing the disubstituted octoxy groups. The fact that the stilbene exhibits extremely similar structural properties makes it a very important tool in characterising what is happening in the PmPV trimer and polymer.

7.3. Vibrational Spectra:

Vibrational spectra give very useful information on the isomerism ratios in compounds, which can be demonstrated in the case of stilbene. Figure 7.3.1, illustrates the Raman spectrum for a mixture of 60/40 Trans/Cis stilbene. A full characterisation of different ratios was performed to demonstrate the changes in the vibrational spectrum associated with the variation with Cis/Trans ratio. The area of interest is the 1600 cm^{-1} region as shown in Figure 7.3.2. It contains two peaks of importance, and variation in the ratios enables the 1629 cm^{-1} (black arrows) peak to be associated with the Cis-vinylene and the 1639 cm^{-1} (red arrows) with Trans-vinylene modes. Figure 7.3.3. illustrates the relative variation of the intensities of the Cis and Trans peaks in this region.

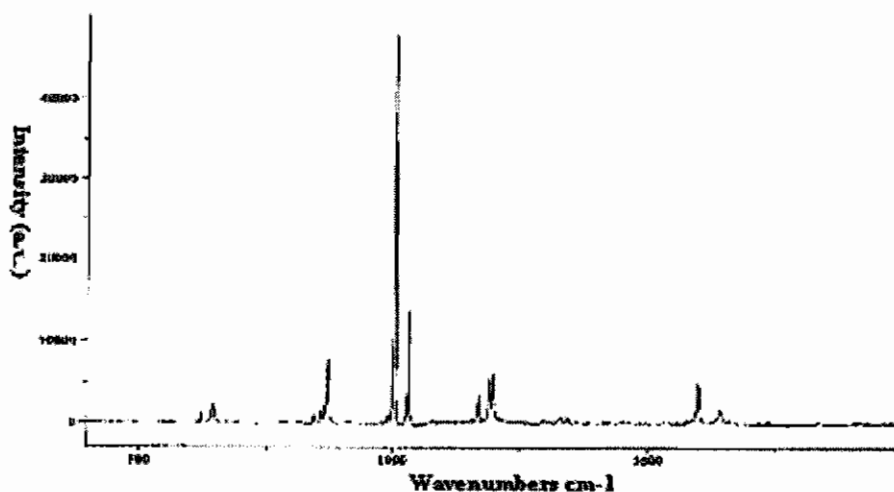


Figure 7.3.1.illustrates the Raman spectra for a mixture of 60/40 Trans/Cis stilbene.

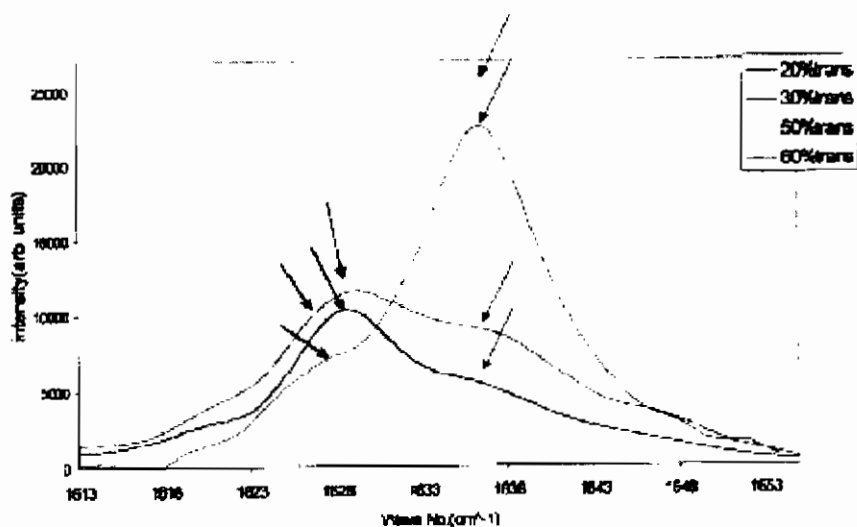


Figure 7.3.2. The relative relationship between the Cis (Black) and Trans (Red) peaks in this region.

A linear relationship in relative concentration of Cis/Trans is observed. The ratio of these peaks is a direct measure of the Cis/Trans ratio in stilbenes. It should be noted that a 1:1 Cis/Trans ratio does not result in a relative intensity of 1, implying that the Raman scattering cross-sections of the two isomeric structures is not identical.

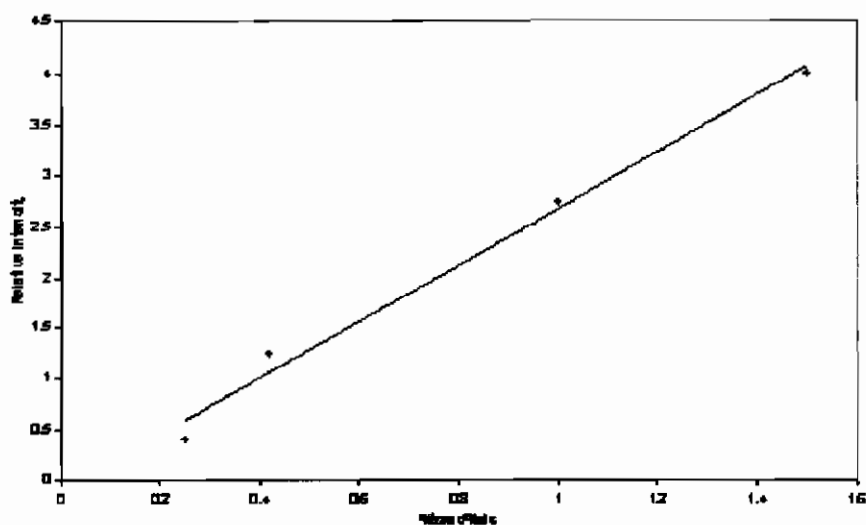


Figure 7.3.3. A graph of relative Raman max intensities versus % Trans/Cis.

The importance of vibrational spectroscopy in determining isomer ratio is re-enforced by I.R. studies. Figure 7.3.4. shows the I.R. spectrum for 80% Cis/Trans ratio in stilbenes. Again there is one specific area to be observed is the region 600cm^{-1} - 1000cm^{-1} . Peaks in this region are CH out of plane stretching modes. The Cis (red arrow) and Trans (blue arrow) peaks occur at 690 cm^{-1} and 960 cm^{-1} respectively, again as determined by varying the Cis/Trans ratio. When the results are graphically displayed a linear relationship is observed as in Figure 7.3.5.

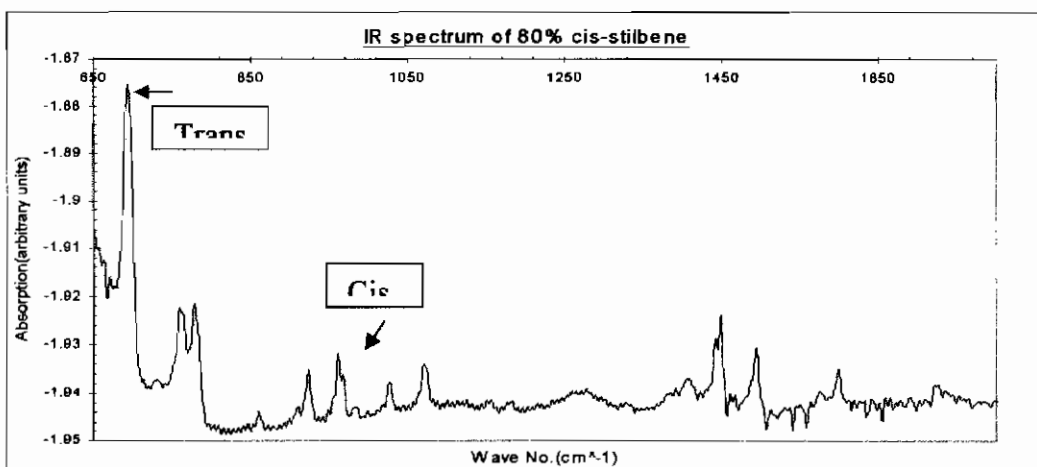


Figure 7.3.4. The IR spectrum for 80% Cis/Trans ratio.

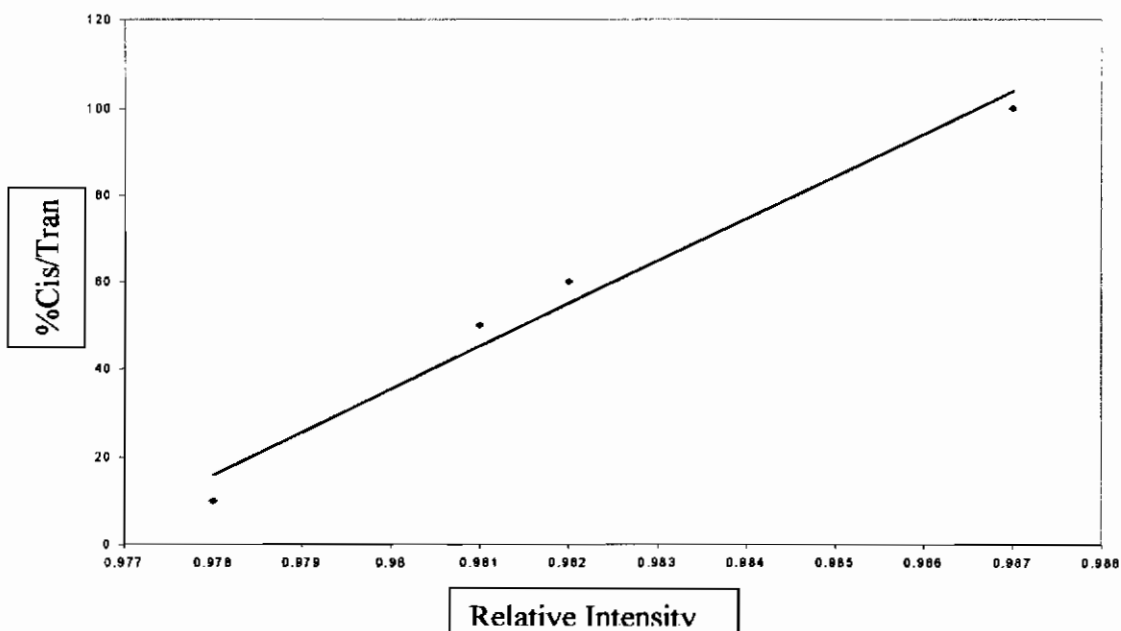


Figure 7.3.5. Graphical display for the relationship between relative intensity of the IR peaks against relative %Cis/Trans stilbene.

The stilbene complex offers a good ideal molecule for comparison with the PmPV trimer and indeed the polymer for identifying signatures of isomerisation and its effect on the optical properties. In this sense, it is worth noting that stilbene itself exhibits significant concentration dependencies of the optical properties, indicative of aggregation, as evidenced, for example, in the concentration dependence of the Trans isomer fluorescence in toluene solution as in Figure 7.3.6. This fluorescence spectrum of the Trans trimer can be compared with that of the trimer in Figure 6.2.1. They both have similar over-riding features, however the stilbene does show broader fluorescence in the 400 – 450nm range. Effects of Cis-Trans on packing can be readily observed, as Cis is liquid at room temperature whereas Trans is a polycrystalline solid.

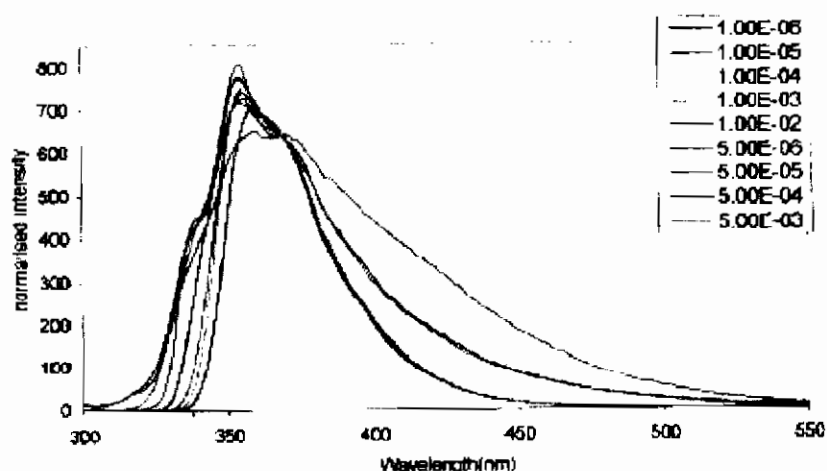


Figure 7.3.6 Concentration dependence of fluorescence spectra for the Trans stilbene form.

7.4 Isomerism of PmPV trimer.

The stilbene offers an interesting look at the effects of variations in the Cis/Trans ratio of molecules. In particular, it may be seen that vibrational spectroscopy can be used as a quantitative tool to determine isomerisation ratios in random admixtures. It should be noted, however, that the Raman scattering cross section of the Cis mode at 1629cm^{-1} is not the same as that of the Trans mode at

1639 cm^{-1} . Similarly the absorption of the Cis mode in the I.R. is not equal to that of the Trans mode. A quantitative relationship may be derived, given the spectra of a series of known isomer mixtures. For many materials, however, this is not easily attainable, and an alternative calibration method should be employed. In the case of the trimer, NMR spectroscopy serves this function.

Figure 7.4.1. illustrates the Cis, Trans 2,5-dioctoxy-p-distyrylbenzene form. The proton NMR (Nuclear Magnetic Resonance) spectrum of the compound can easily be modelled and the constituents of the compound can be determined⁴. Table 7.4.1. gives an indication of the assignment and strength of the bonds. The value, δ (ppm) is a position in the field depending on how the magnetic field causes it to distort, similar to wavenumbers in Raman. Multiplicity, refers to the type of peak seen for example, a single peak or two unresolved peaks which will give a doublet. Cis and Trans peaks are identified thus in a sample and the ratio between them can be determined, as the strength of the signal is independent of whether the proton is in a Cis or Trans configuration.

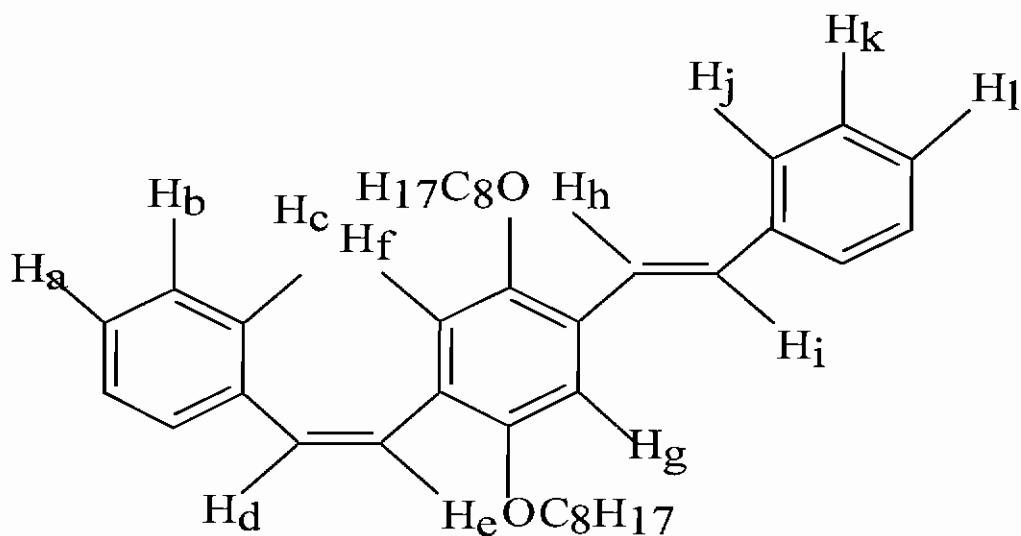


Figure 7.4.1. illustrates the Cis, Trans 2,5-dioctoxy-p-distyrylbenzene form

| δ (ppm) | Multiplicity | J(Hz) | Assignment | Cis/Trans |
|----------------|----------------|-----------|---------------------------------|-----------|
| 7.5728, 7.5553 | Doublet | 7.0 | H _c , H _j | - |
| 7.5327, 7.4926 | Doublet | 16.56 | H _l | Trans |
| 7.5039, 7.4926 | Doublet | 16.56 | H _d | Cis |
| 7.3884 | Double Doublet | 7.56/8.0 | H _b , H _k | - |
| 7.2781 | Double Doublet | 7.56/7.52 | H _a , H _i | - |
| 7.1162, 7.1852 | Doublet | 16.56 | H _h | - |
| 7.1589 | Singlet | - | H _g | - |
| 7.1162, 7.0748 | Doublet | 16.56 | H _e | - |
| 7.0861 | Singlet | - | H _f | - |

Table 7.4.1. NMR spectra for Cis, Trans 2,5-dioctoxy-p-distyrylbenzene, indicating strength and position and assignment of peaks.

The 2,5-dioctoxy-p-distyrylbenzene was synthesised through both the Wittig and Horner-Wadsworth-Emmons reactions as discussed in Chapter 4 utilising toluene and DMF for each yielding four independent compounds. Depending on which reaction was used the product in solid form varied from a yellowish colour to orange. This variation in colour is an indication of different degrees of aggregation. An indication of the extent of isomerisation is to look at the ratio of H_l to H_d. Table 7.4.1 shows the resultant intensities for the case of the Wittig DMF product. Integration of the vinyl signals showed a Trans/Cis ratio of 5:1 in favour of Trans bonding. The percentage Cis is therefore 16.7%⁷.

7.5. Raman Spectroscopy of Trimer:

The Raman modes at 1639 cm^{-1} and 1629 cm^{-1} have been assigned to Trans and Cis vinylene bonds in stilbene. As shown in Figure 7.5.1((a) Htol and (b) WDMF), the trimer shows similar modes, albeit downshifted to $\sim 1600\text{ cm}^{-1}$ and $\sim 1590\text{ cm}^{-1}$ respectively. The ratio of these peaks is shown in Table 7.5.1 for the compounds made by the different routes in different solvents

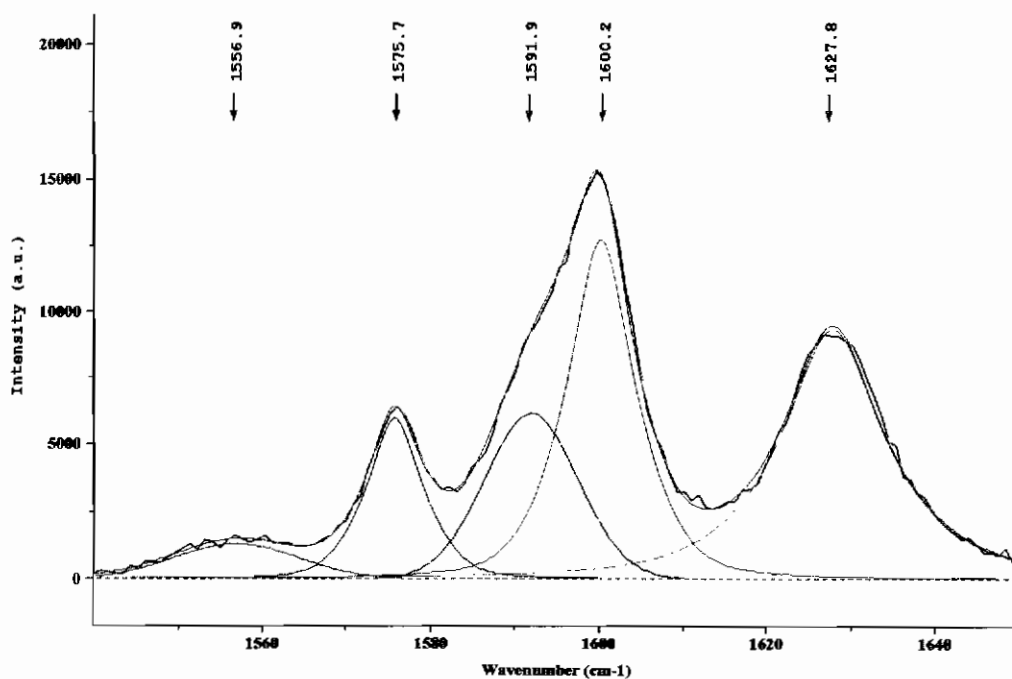


Figure 7.5.1(a) An enlarged view of the 1600cm^{-1} region of Raman spectrum of the Wittig DMF trimer.

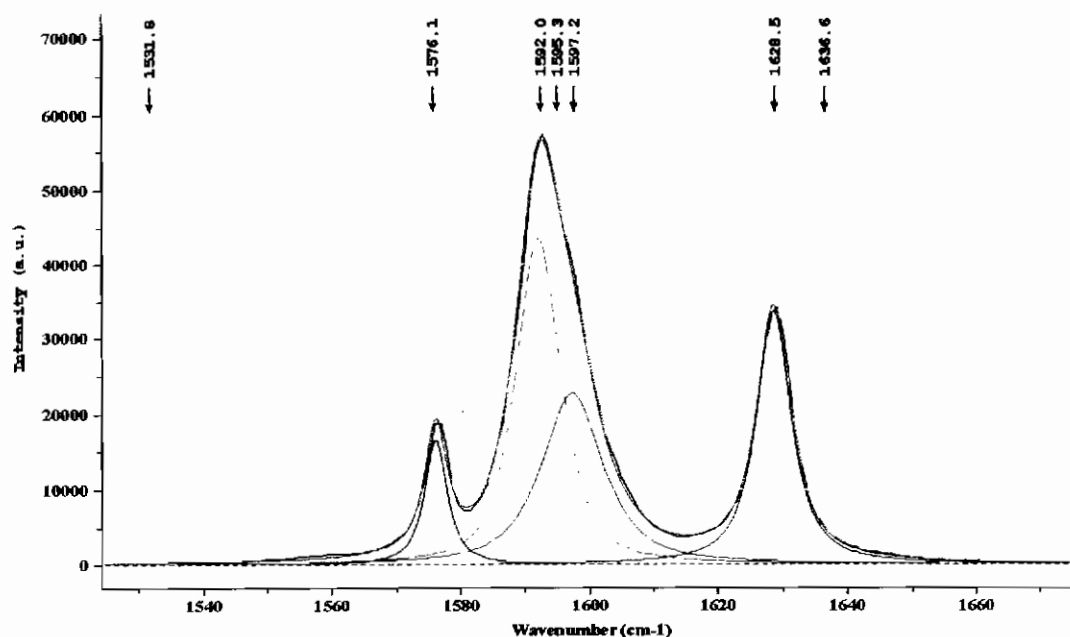


Figure 7.5.1(b) An enlarged view of the 1600cm⁻¹ region of Raman spectrum of the Wittig-Toluene trimer.

The NMR Result of section 7.4 gives a known % Cis value of 16.7% for the Wittig DMF trimer. The Raman spectra yield a different ratio of Cis/Trans to the NMR. This is a result of differing Raman scattering cross-sections of the different isomers. A weighting correction factor can be introduced to account for this. This factor is found to be 0.43 for the Wittig DMF trimer. Thus equation 7.5.1 can be employed to determine the %Cis for the other trimers.

$$\%Cis = \frac{0.43R_{Cis}}{0.43R_{Cis} + R_{Tran}} \quad \text{Eqn. 7.5.1.}$$

The above results show that by varying the preparation method the resultant Cis/Trans ratio can be controlled. If this trend is continued in the polymer a degree of control over Cis/Trans ratio and thus polymer conformation can be exercised. The potential effect of the Cis and Trans isomerisation on the solid state configuration is discussed in section 7.7.

| Method/solvent | Cis (1592cm ⁻¹) | Trans (1600cm ⁻¹) | %Cis |
|-----------------------------------|--------------------------------|----------------------------------|------|
| Wittig-toluene (Wtol) | 16687.3 | 6154 | 51% |
| Horner-DMF (HDMF) | 22085 | 13007 | 42% |
| Horner-toluene (Htol) | 39411 | 19364 | 46% |
| Wittig-DMF (WDMF) | 6190 | 12550 | 17% |

Table 7.5.1. illustrates Raman intensities and modes at 1592cm⁻¹ and 1600cm⁻¹ and Cis Trans ratio for various trimer products.

7.6 Isomerism of the polymer:

In small molecules NMR can be used to give precise isomerisation ratios. Thus the relative Raman scattering cross-sections of Cis and Trans can be determined and Raman subsequently used as a rapid screening mechanism. In long chain polymers or macromolecules the NMR spectrum becomes complex and specific contributions are not resolvable. To determine relative Cis/Trans ratios in different polymers the scattering cross-section ratio of 0.43 determined for NMR/Raman spectra of the trimer is used. Although this is an approximation it should be sufficient to give an indication of significant differences in isomerism in different polymer samples.

In Figure 7.6.1 the Raman spectra of the polymers made by three different methods are compared to that of the trimer. By extrapolation from the trimer the peak at $\sim 1600\text{cm}^{-1}$ is associated with Trans, whereas that at 1591cm^{-1} is associated with Cis. Table 7.6.1. shows ratio of peaks in the polymers made by different methods. Figure 7.6.2 shows expanded area of interest round 1600 cm^{-1} . Utilising the trimer a weighting factor values for Cis/Trans ratios are determined.

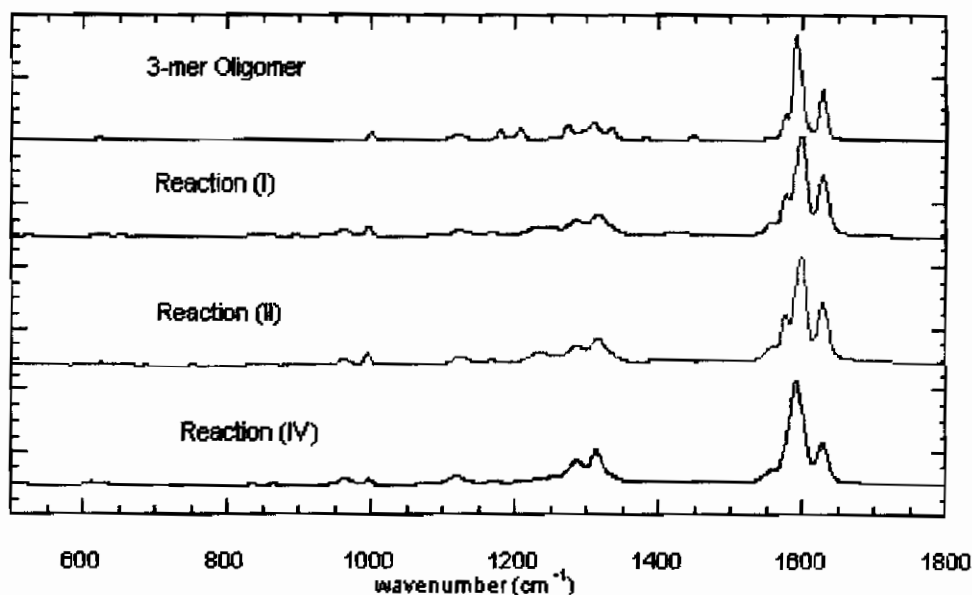


Figure 7.6.1 Comparison of Multiple modes centred at 1600cm^{-1} showing Raman characteristic.

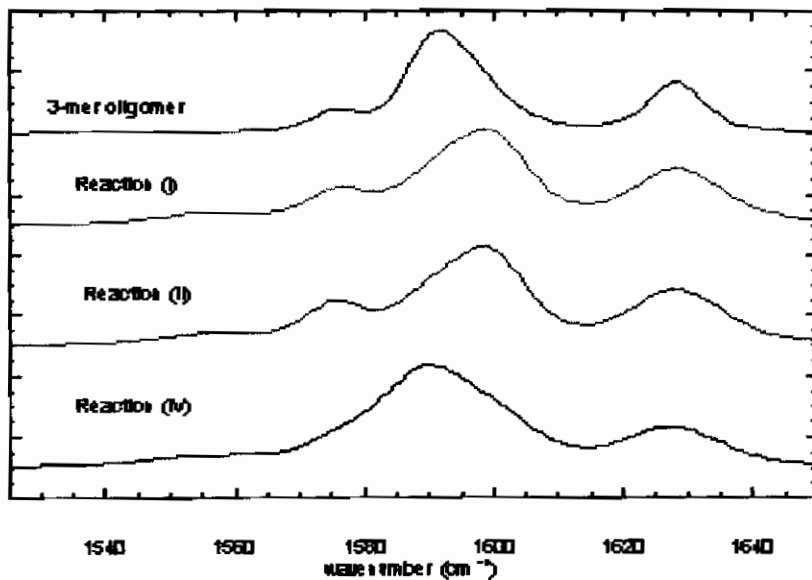


Figure 7.6.2 Expanded view of Raman active area 1600cm^{-1} .

| Reaction | Cis (1592cm^{-1}) | Trans (1600cm^{-1}) | %Cis |
|--------------------------|---------------------------------|-----------------------------------|------|
| Reaction (I) (HDMF) | 43056 | 91195 | 16% |
| Reaction (II) (HTOL) | 6173 | 12700 | 17% |
| Reaction (III) (WDMF) | 22018 | 110090 | 8% |
| Reaction (IV) (WTOL) | 30680 | 10569 | 55% |

Table 7.6.1, Tabulated centred peaks fitted to Lorentzian and Gaussian functions.

In the case of the polymer, that prepared by the Wittig route in Toluene has substantially higher Cis content than the other materials. Again the Wittig DMF polymer has the lowest %Cis. The dramatically different degree of isomerisation may therefore indeed be a source of the differing optical properties at high concentrations outlined in chapters 5 and 6.

7.7.Molecular Modelling:

As has been shown in the preceding sections, the differing Cis/Trans ratios have a profound effect on the properties of the molecule. This reason for this effect becomes evident, when one utilises a molecular model of the Cis and Trans form of the polymer. Figure 7.7.1 shows the different coiling for pure Cis and Trans of a 14 repeating unit section of the polymer, modelled using the package Hyperchem⁸. Although there are no sidechains included within the model, it highlights the complexity of coiling, when mixtures of Cis/Trans are considered. In the all Trans form, the chain is tightly coiled, with a coil diameter of $\sim 20\text{\AA}$. It is prone to intra molecular interactions but the π -backbone is relatively shielded from interaction with other chains. The all Cis form, on the other hand, is loosely coiled and somewhat more irregular. The π -backbone is exposed and is more open to inter molecular interactions. The variation in the properties develops as the Cis/Trans ratio changes, the ratio having a direct effect on the degree of coiling of the polymer. The effect on the coiling will subsequently have an effect on the way in which the molecule interacts with its environment. It should be expected that the open Cis coil will result in a large perturbation to the π -system when packed in the solid state, whereas in the tightly coiled Trans form, the interaction of the π -system is limited and therefore the effects of aggregation is limited. Control of the Cis-Trans ratio in the polymer backbone may therefore be recognised as a significant design parameter.

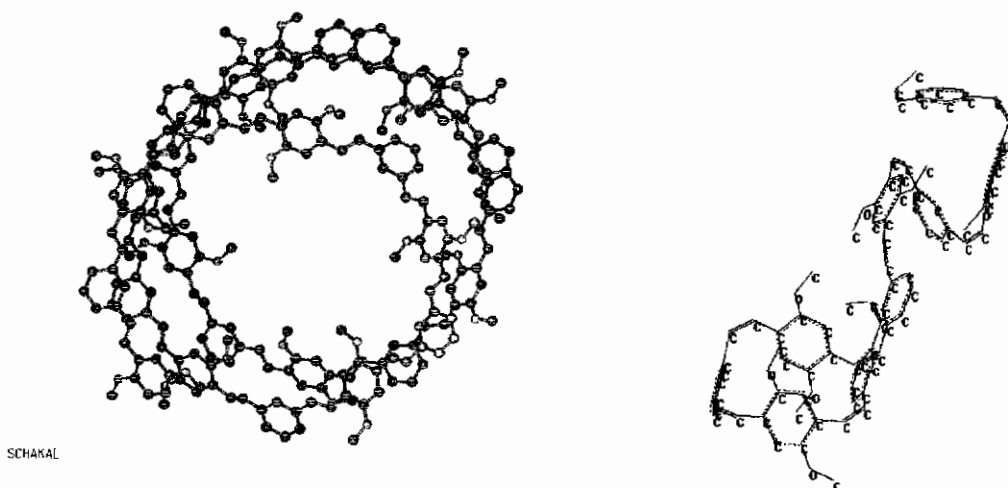


Figure 7.7.1. Illustrates the different coiling forms the PmPV polymer².

7.8 Summary

Chapter 7 looks at the isomerism and the effects that it can have on the optical properties of the molecule. In an attempt to better understand the effects, an “ideal” and intensely studied material, stilbene is examined.

Stilbenes have been around for almost 80 years and have been extensively investigated, in both pure Cis and Trans forms. This makes them ideal for this type of study. As they can be purchased in almost 100% pure form, ratios of Cis and Trans can be easily made. Vibrational and electronic studies of different ratios of stilbene were investigated as a model of the type of interactions involved. This study enabled an identification of the Raman signatures of the Cis and Trans isomers. These signatures were thus identifiable in the Raman spectra of the trimers, and comparison of to NMR enabled the determination of the relative Raman scattering cross-sections. The correction factor determined for the trimer was employed for the Raman of the polymers made by the different routes, and the comparison clearly indicated that the Wittig toluene polymer had a substantially higher Cis content than the others. Thus isomerisation a clear candidate for the source of the differences between the polymers as is supported by the molecular modelling. The results suggest that the Wittig – DMF, (WDMF), would be the ideal compound to use, as it has the lowest Cis/Trans ratio.

In the development of any future material the problems associated with isomerism have been shown to be very detrimental to the optical properties of the molecule. Extensive study of new materials would need to be undertaken to ensure optimum performance for optical applications.

The most graphical example of isomerism is shown in the Hyperchem© modelling of the molecule. The different coiling effects from Cis and Trans forms are extremely different and have been shown to interact differently with their environments.

7.9 References

- 1: <http://www.ndif.org/Terms/isomerism.html>
- 2: Shirakawa Ikeada; *Jour. Poly. Sci.* **12**. 21-28 (1974).
- 3: Stormer, R. *Ber. Dtsch. Chem. Ges.*, **42**, 4865-4871, (1909).
- 4: Hoekstra A; Meertens P; Vos A; *Acy. Crystallog. Sect. B.* **31**. 2813-2817, (1975).
- 5: Traetteberg M; Frantsen E. B; Mijhoff F. C; Hoekstra. A; *Jour. Mol. Strut.* **26**, 57-68 (1975).
- 6: Hyperchem Modelling Program.
- 7: Bradley D; 4th Year project, Diploma in Applied Science(DIT).
- 8: Dalton A; PhD Thesis, Submitted 2000, Trinity College Dublin.

Chapter 8

Conclusion

8.0 Conclusion:

In this thesis, the importance of environment and the control of the environmental effects within PmPV have been discussed. The investigation centred on the PmPV-Trimer and Polymeric PmPV. The presence of the meta-linkages at alternate phenyl bonds causes an interruption of the conjugation causing a blue shift in the optical properties of the dilute solution. In concentrated solution the luminescence quantum efficiency decreases and absorption and emission are shifted to lower energies.

In order to control these effect four different reaction methods, various solvents are used to reproduce the material. Temperature variation of the reaction mechanism is also varied in an attempt to control products.

In chapter 3, an investigation of the solvent effect on the absorption and fluorescent spectra is undertaken. The results show that the variation in the solvatochromic shift as small as it is, cannot be used to explain the dramatic change in fluorescence intensity.

In chapter 4, the model compound, PmPV trimer is investigated and the meta-linkage disrupted effect to the conjugation of the molecules, something, which is not seen in the PPV systems.

Vibrational spectroscopy also provides a vast quantity of information through the two types of vibrational spectroscopy, I.R, and Raman compliment each other and give information on the backbone and sidechains. The I.R, is predominantly used for the elution of the modes associated with the sidechain, whereas Raman will provide in-depth information on the backbone of the molecule. In particular, backbone modes involving para-conjugation will dominate the Raman spectrum.

Environmental effects have been shown to be very important in looking at the photophysics of any molecular system, in chapter 5.

Raman spectroscopy has shown itself to be a highly useful tool in probing the effect of the environment on the photophysics of the materials being studied. The differing solvatochromic effect between the trimer and the polymer highlights the complex coupling between the environment and the polymer, while the trimer is to a greater extent well behaved. In collaboration with the National University of Ireland-

Galway experiments were done to obtain lifetime measurements. These show very good correlation with the Raman overlap. The greater the Raman overlap the shorter the lifetime as the vibrational energy can easily transfer itself from the molecule to the environment. The higher the integrated fluorescence is the longer the lifetime becomes. However, when the polymer is examined, an exceptional more complex system is encountered. Raman overlap does not correlate simply with the fluorescent yield or lifetime. The fluorescent decay shows that even at moderate concentrations the photophysics is not unimolecular.

In chapter 6, concentration dependent studies of the trimer show hypsochromic shifts in both the absorption and emission spectra, characteristic of molecular aggregation. This behaviour is more pronounced in the polymer solutions and clearly reduces the photoluminescence efficiency and potential of the material. There is clear evidence of the evolution of new species in solutions of higher concentrations. Whether the species is indeed an excimer or a ground state aggregate is immaterial in terms of material performance, as a significant departure from unimolecular behaviour occurs with increasing concentration. Tailoring and design of optical and electronic properties at a molecular level is futile if these properties are not maintained in the condensed state. Furthermore, the simple rate equation models and indeed the vibrational approach to optimising photoluminescence quantum efficiencies fall down in aggregated materials. A significant observation, however is that the HTolPmPV solutions aggregate significantly less than those of the WTolPmPV, although the materials are chemically identical, and there appears to be no significant difference in chain length

In chapter 7, the Cis/Trans interaction is investigated utilising an ideal compound, Stilbene's. The variation of the cis/trans linkage and its effect can be shown in the relationship of the %trans/cis and the increase in the relative intensity from the resultant compound. From experimental results it has been shown that the geometry of all trans polymer has a diameter of 20 Å, in comparison to all cis which has an irregular structure as is clearly evident from the hyper-chem models shown.

It is concluded that the isomerisation changes hugely affect the way in which both the trimer and the polymer will interact with their environments. It has been prove that the environmental effect has a profound effect on the optical properties. The differing spectra

and the variation in modes are indicative of differing ratios of cis/trans and the solvation effects.

By the sum of it's parts this thesis has shown that the environmental parameters have a profound effect on the optoelectronic properties of a compound. The introduction of the "*meta*" linkage causes disruption in the backbone and a shift towards the Blue region of the spectra. The meta linkage, also introduced the concept of isomerisation. The reaction conditions have been shown to have a significant effect on the isomerism of the molecule in comparison to an "Ideal" compound, Stilbene.

Concentration effects have been shown to have a significant effect, in varying concentrations, the formation of new species has been shown. Aggregation and it's effects are shown in the lifetime measurements.

All of the above would suggest there are a variety of interactions, which if you can control them, you can limit their interaction.

A number of parameters which are variable and which are potentially controllable have been identified. The prospect is for the development of design principles to control intermolecular interaction towards material optimisation.